SCALING THEORY OF PERCOLATION CLUSTERS

D. STAUFFER

Institut für Theoretische Physik, Universität zu Köln, 5000 Köln 41, W. Germany

NORTH-HOLLAND PUBLISHING COMPANY - AMSTERDAM

PHYSICS REPORTS (Review Section of Physics Letters) 54, No. 1 (1979) 1–74. NORTH-HOLLAND PUBLISHING COMPANY

SCALING THEORY OF PERCOLATION CLUSTERS

D. STAUFFER

Institut für Theoretische Physik, Universität zu Köln, 5000 Köln 41, W. Germany

Received December 1978

Contents:

Abstracts:

For beginners: This review tries to explain percolation through the cluster properties; it can also be used as an introduction to critical phenomena at other phase transitions for readers not familiar with scaling theory. In percolation each site of a periodic lattice is randomly occupied with probability p or empty with probability $1-p$. An s-cluster is a group of s occupied sites connected by nearest-neighbor distances; the number of empty nearest neighbors of cluster sites is the perimeter t. For p above p_c also one infinite cluster percolates through the lattice. How do the properties of s-clusters depend on s, and how do they feel the influence of the phase transition at $p = p_c$?

The answers to these questions are given by various methods (in particular computer simulations) and are interpreted by the so-called scaling theory of phase transitions. The results presented here suggest a qualitative difference of cluster structures above and below p_c: Above p_c some cluster properties suggest the existence of a cluster surface varying as $s^{2/3}$ in three dimensions, but below p_c these "surface" contributions are proportional to s. We suggest therefore that very large clusters above p_c (but not at and below p_c) behave like large clusters of Swiss cheese: Inspite of many internal holes the overall cluster shape is roughly spherical, similar to raindrops.

For experts: Scaling theory suggests for large clusters near the percolation threshold p_c that the average cluster numbers n_s vary as $s^{-\tau}f(z)$, with $z \equiv (p-p_c)s^{\sigma}$. Analogously the average cluster perimeter is $t_s = s \cdot (1-p)/p + s^{\sigma} \cdot \psi_1(z)$, the average cluster radius R_s varies as $s^{\sigma\nu} \cdot R_1(z)$, and the density profile $D_s(r)$, which depends also on the distance r from the cluster center, varies as $s^{-1/\delta} \cdot \tilde{D}_1(rs^{-\sigma\nu}, z)$. These assumptions relate the seven critical exponents α, β, γ, δ, ν, σ, τ in d dimensions through the well-known five scaling laws $2-\alpha = \gamma + 2\beta = \beta\delta + \beta = d\nu = \beta + 1/\sigma = (\tau-1)/\sigma$, leaving only two exponents as independent variables to be fitted by "experiment" and not predicted by scaling theory. For the lattice "animals", i.e. the number g_{st} of geometrically different cluster configurations, a modified scaling assumption is derived: $g_{st}s^s t^t/(s+t)^{s+t} \propto s^{-\tau-1/2} \cdot f(z)$, with $z \propto (a_c - t/s)s^{\sigma}$ and $a_c = (1-p_c)/p_c$. All these expressions are variants of the general scaling idea for second-order phase transitions that a function $g(x, y)$ of two critical variables takes the homogeneous form $x^c G(x/y^b)$ near the critical point, with two free exponents b and c and a scaling function G of a single variable.

These assumptions, which may be regarded as generalizations of the Fisher droplet model, are tested "experimentally" by Monte Carlo simulation, series expansion, renormalization group technique, and exact inequalities. In particular, detailed Monte Carlo evidence of Hoshen et al. and Leath and Reich is presented for the scaling of cluster numbers in two and three dimensions. If the cluster size s goes to infinity at fixed concentration p, not necessarily close to p_c, three additional exponents ζ, θ, ρ are defined by: cluster numbers $\propto s^{-\theta}\exp(-\text{const} \cdot s^{\zeta})$ and cluster radii $\propto s^{\rho}$. These exponents are different on both sides of the phase transition; for example $\zeta(p < p_c) = 1$ and $\zeta(p > p_c) = 1 - 1/d$ was found from inequalities, series and Monte Carlo data. The behavior of θ and of $\rho(p < p_c)$ remains to be explained by scaling theory.

This article does not cover experimental applications, correlation functions and "classical" (mean field, Bethe lattice, effective medium) theories. For the reader to whom this abstract is too short and the whole article is too long we recommend sections 1 and 3.

1. Introduction

1.1. What is percolation?

What is percolation? Figure 1 gives a first answer: Percolation is a very fashionable field. The number of papers published each year has gone up by a factor of 10 in ten years, due in part to the increased interest in disordered systems generally. The greater part of the pronounced peak in fig. 1 for the percolation publication rate could not be covered in the earlier reviews of Shante and

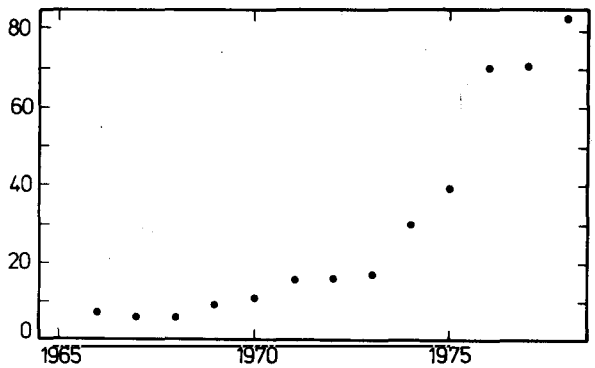

Fig. 1. Variation with time of the number of articles published each year which carry the word percolation, percolating etc. in the title. Tabulated from the Permuterm Subject Index of the Science Citation Index and the Weekly Subject Index of Current Contents, Institute of Scientific Information, Philadelphia, PA, USA. The critical exponent describing this curve has not yet been determined.

Kirkpatrick [1], Essam [2], and Kirkpatrick [3]. Among shorter reviews written since then we mention a more mathematical presentation [4], a simple description of applications [5], and a lecture mainly on random resistor networks [6]. Kirkpatrick [7] recently gave a rather detailed review together with new numerical data. About simultaneously with the present review other reviews are being prepared by Essam [8] and by Pfeuty and Guyon [9], the latter emphasizing applications, which are largely ignored in the present article.

These reviews usually emphasize the "bulk" behavior of the percolation system as a whole. The present article reviews the scaling theory of percolation *clusters*, i.e. it concentrates on the often neglected question of how these "bulk" properties can be explained by clusters, and how the cluster properties depend on the cluster size. Taken together with refs. [7–9] the reader will, we hope, get a balanced view of percolation. (Our list of references is an incomplete and subjective selection of percolation papers.) Instead, if the reader does not have the time to read the present article fully we recommend that he restricts himself to our long introduction and to section 3 only. Then he is informed on those cluster properties which at present seem no more controversial. De Gennes's review [5] is suggested for an elementary introduction into percolation theory and its applications.

What else is percolation? This review tries to show that, besides being fashionable, percolation is also a very simple problem. It is easily defined (see below), and the methods of numerical solution are also easy to understand in principle. In this sense the phase transition behavior of percolation, i.e. the "scaling" properties, can be used as an introduction to more complicated phase transitions and critical phenomena [10, 11]. In order to understand percolation it is not necessary to know what properties a spin has or what a free energy is. In short, one does not have to study physics in order to understand what is going on in this review. Basically, only the concept of probability and the purely geometrical counting of "cluster" configurations is necessary; and usually we do this here on two-dimensional lattices like large chessboards. The most complicated mathematical methods used here (only seldomly) are Taylor expansions, the definition of the Gamma function $\Gamma(x) = \int_0^\infty y^{x-1} e^{-y} dy$ for real argument x, and the related knowledge of $\int_{-\infty}^{\infty} \exp(-y^2) dy = \sqrt{\pi}$. In fact, a simple percolation game, which can be finished during one lecture, has been used repeatedly to give students an active experience of what a critical exponent and a Monte Carlo experiment are [12]. Of course, not everything connected with percolation is simple: So far none of the critical exponents like β etc., which we will discuss later at the end of this introduction, has been calculated rigorously and exactly for two or three dimensions, although for the two-dimensional Ising model of magnetism such exact exponents are known since many years [10, 11]. Our review here will simply try to avoid the complicated problems and concentrate on the simpler concepts.

What is the definition of percolation? Imagine a very large quadratic lattice like a huge chessboard. Assume that every single square on this lattice can be in either one of two states, which we call "occupied" and "empty". Moreover, each square is occupied or empty entirely randomly, independent of whether its neighbors are occupied or empty. Thus the whole problem is defined, for a given lattice type, by a single parameter p, where p is the probability (the same for each square) to be occupied. Fig. 2 shows an example how a 20 by 20 chessboard is slowly filled up from $p = 0.1$ to $p = 0.9$. If our lattice is not a chessboard (square lattice) we call its units the lattice sites; they are either occupied or empty. In the triangular lattice, for example, these units are the dots shown schematically in this diagram; in the simple cubic lattice they are cubes. Numerous such lattices have been studied [1, 2]; the presently widespread belief in "universality" asserts that it does not make much difference which lattice we choose.

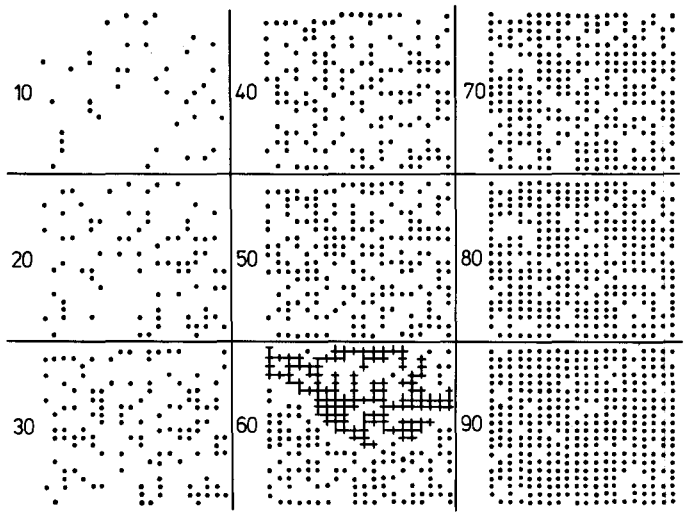

Fig. 2. Examples for percolation on a 20×20 square lattice, for $p = 0.1, 0.2, \ldots 0.9$. Occupied sites are shown as dots, empty sites are not shown. The overlapping crosses at 60 percent probability give the largest "percolating" cluster.

In this percolation problem the occupied sites are either isolated from each other or they form small groups of neighbors. These groups are called clusters:

A cluster is defined as a group of occupied lattice sites connected by nearest-neighbor distances. (1)

In fig. 2 the largest cluster at $p = 0.6$ was symbolized by overlapping crosses +, which distinguish it clearly from the smaller clusters also present there. Isolated sites are regarded as clusters of size unity; and generally we call any cluster consisting of s occupied connected sites an s-cluster.

In a large lattice there will be more clusters than in a small lattice; thus it is convenient to divide the number of clusters by the number of lattice sites in the whole lattice. This ratio is called the number n_s of s-clusters if it is an average over many different distributions of occupied sites among the lattice sites:

n_s is the average number (per lattice site) of s-clusters and depends on concentration p. (2)

Eqs. (1) and (2) define the two most important concepts used in this report, the s-cluster and the number of s-clusters.

If p is close to zero, most occupied sites will be isolated, with only a few pairs and triplets present (fig. 2 with $p = 10\%$). If, on the other hand, p is close to unity then nearly all occupied sites are connected to each other and form one large cluster extending from one end of the lattice to the other (fig. 2 with $p = 90\%$). According to present knowledge [1], in a sufficiently large lattice there is either one or none, but never two or more such "infinite" clusters or "networks". This infinite cluster percolates through the lattice just as water is percolating through wet sand along the network of wet pores. Our examples at $p = 70\%$ and 80% also show that besides this percolating network many finite clusters exist, too. A clear distinction thus exists for large lattices: Either an "infinite" cluster exists, or it does not exist. Therefore it is plausible that for an infinite lattice a sharply defined percolation threshold p_c exists, i.e. a critical point, where for the first time an infinite network percolates through the lattice with finite probability. Thus p_c indicates a phase transition such that:

For p above p_c one percolating network exists;

for p below p_c no percolating network exists. (3)

In this sense percolation is a phase transition [10, 11] which generally can be defined as the phenomenon that a system exhibits a qualitative change at one sharply defined parameter value, if that parameter is changed continuously. Only in an infinite system ("thermodynamic limit") do we observe a true phase transition in this sense. For example, in our finite system of fig. 2, we do not know precisely whether $p = 0.6$ is above or below the percolation threshold p_c; for the large cluster percolates horizontally but not vertically. Such accidental differences between horizontal and vertical directions become less and less probable if the lattice size increases. Thus p_c is defined uniquely in an infinite system. (Of course, even for $p \to 0$ we can produce an infinite cluster by filling merely one row of our lattice with occupied sites. However, such a configuration has an extremely low probability for a large lattice in a truly random distribution of occupied sites. And we require above p_c to have an infinite network in an infinite system with probability one.)

More quantitatively, we call the percolation probability P_∞ the fraction of occupied sites belonging to the infinite percolating network. Then P_∞ vanishes below p_c and is nonzero above p_c; close to p_c we can define a "critical exponent" β by postulating $P_\infty \propto (p - p_c)^\beta$ for p slightly above p_c. The behavior of the infinite network and of large finite clusters, for p very close to p_c, is called the critical behavior of percolation theory; the region of parameters where it applies is called the scaling region.

In general, every lattice site has three choices: It can be empty, with probability $1-p$; it can be part of the infinite network of occupied sites, with probability $p \cdot P_\infty$; or it can be part of one of the many finite clusters including single sites, with probability $p(1-P_\infty)$. Since each s-cluster contains exactly s sites, the probability of any lattice site to belong to an s-cluster is $P_s = s \cdot n_s$ (remember that n_s was defined as the number of s-clusters divided by the total number of lattice sites). The sum of all these probabilities equals unity:

$$1 - p + pP_\infty + \sum_s s \cdot n_s = 1 \tag{4}$$

where Σ_s denotes the sum over all finite cluster sizes, $s = 1, 2, \ldots$. Thus, if we know all the cluster numbers n_s, then we can calculate from eq. (4) the strength P_∞ of the infinite network. We see already here that the cluster numbers n_s are the basic quantities for our discussion.

To study percolation experimentally with simple methods one can flip coins in a classroom experiment [12] to produce easily a probability $p = \frac{1}{2}$ for a site to be occupied. More efficiently, one can ask a computer to do that, and for readers interested in Fortran programming a simple example of such a "Monte Carlo" method is shown in table 1. A computer program similar to the one in table 1 produced the results for fig. 2; our example might be used for teaching Monte Carlo methods since the execution time was smaller than the compilation time. (If computer experts ask for money to make such Monte Carlo computer simulations they in general will not (at least not officially) use that money on the roulette tables of that Mediterranean town in order to produce a series of random numbers needed for percolation. Instead, the computer has built in methods to generate pseudorandom numbers by multiplying large numbers and dropping the leading digits. For the CDC computer used here, this aim is achieved by the function RANF(n) which gives, for arbitrary n, a real number distributed randomly between zero and unity. The program compares this random number with the concentration p to decide whether the lattice site is occupied or empty.)

Table 1
A simple Fortran computer program to produce a percolation example on a 20 × 20 square lattice. The function RANF for this computer produces random numbers distributed evenly between 0 and 1. Empty places are stored as zeros, occupied sites as ones.

```
      DIMENSION IS(2Ø,2Ø)
      P = Ø.6Ø
      N = 1
      DO 1 I = 1,2Ø
      DO 1 J = 1,2Ø
      IS(I,J) = Ø
1     IF(RANF(N).LT.P) IS(I,J) = 1
      DO 2 I = 1,2Ø
2     WRITE(6,3) (IS(I,J),J=1,2Ø)
3     FORMAT (1X,2ØI2)
      STOP
      END
```

Besides such computer experiments, also real experiments can be done to study percolation. Imagine for example that each occupied square on the chessboard is electrically conducting, whereas empty sites are insulators. A current can flow from one conducting square to the other if both squares share one line as common border. This means that an electric current can flow only within one cluster, and not from one cluster to the other. Only if a percolating network is present, i.e. for p above the percolation threshold p_c, has the lattice a nonzero bulk conductivity. In this form the percolation problem is known as the random resistor network; we may also interpret it as oil or water flowing through porous rock or wet sand. By coating candy dragees or plastic bullets from toy guns with copper, the Marseille group [13] studied the conductivity above p_c. Random mixtures of these spheres with equal size but two different colours arrange themselves into a triangular lattice if shaken softly on a flat surface; then clusters and the infinite network can be seen easily. Unfortunately, as quantitative experiments these methods are too complicated [13] for teaching purposes. Earlier simple experiments included the punching of random holes into conducting paper by Last and Thouless [14], and the random cutting of wires in a steel-wire mesh, bought in a local hardware store, by Watson and Leath [15]. But in the present review we will be satisfied with regarding percolation as a mathematically well-defined and simple problem; the difficulties of approximating realistic disordered systems in nature by percolation models and the problems of conducting experiments with real materials are left to other reviews [5, 9].

Readers who insist that everything is explained to them in the language of the spin $\frac{1}{2}$ Ising model for ferromagnets at finite temperature T in a magnetic field H can also be satisfied now; other readers may go ahead to section 1.2. Imagine that in a lattice, magnetic atoms and nonmagnetic atoms are mixed randomly and then cooled down ("quenched") to very low temperatures. Then the magnetic atoms form clusters according to percolation theory, with p = mole fraction of the magnetic spins. Each spin has a magnetic moment μ pointing either up or down. Nearest-neighbor exchange forces force the magnetic moments of neighboring atoms to be parallel since the thermal energy at these low temperatures is too low to break up these exchange bonds. Thus all moments within one cluster are parallel. (We neglect any dipole–dipole interaction between the spins.) The whole cluster therefore acts as if it would be one large isolated ("superparamagnetic") spin. An isolated single spin has in thermal equilibrium a magnetization of $\tanh(\mu H/k_B T)$ in units of the saturation magnetization. Thus for a superparamagnetic cluster the argument of the tanh is replaced simply by $s \cdot \mu H/k_B T$ since its

magnetic moment is $s\mu$. The contribution of clusters to the total magnetization moreover contains a factor s since a large cluster contributes more than a small cluster. Finally, the contribution of all s-clusters is proportional to the cluster numbers n_s. Therefore, the total magnetization contribution from finite clusters is $(1/p) \cdot \Sigma_s s \cdot n_s \tanh(s\mu H/k_B T)$ in units of the saturation magnetization. The infinite network contains the fraction P_∞ of all spins and is oriented either fully up or fully down. Thus the whole equation of state $M = M(p, T, H)$ for the magnetization M (units of the saturation magnetization) is given by

$$M = \pm P_\infty + (1/p) \cdot \sum_s s \cdot n_s \tanh(s\mu H/k_B T)$$

or, with the use of eq. (4):

$$pM = \pm \left(p - \sum_s s \cdot n_s\right) + \sum_s s \cdot n_s \tanh(s\mu H/k_B T). \tag{5}$$

In this way for low enough temperatures the magnetization in this "dilute" ferro-magnet is related directly to the cluster numbers. For p below p_c no infinite network is present, and for $H = 0$ the finite clusters give zero magnetization, corresponding to the paramagnetic state. But for p above p_c the infinite network gives a "spontaneous" magnetization P_∞, i.e. a "remanence" even for zero magnetic field. Eq. (5) looks as if it is a direct experimental realization of the percolation problem; but actually experiments as a function of p are quite difficult [16], and not much information has been gained so far from such experiments on the cluster numbers. The time-dependent behavior of this model [61] is not discussed here. [Experts on metastable systems may notice that the $\pm$ sign in eq. (5) gives above p_c a unique and smooth but nonanalytic continuation of the stable branch, M parallel to H, into the unstable branch, M antiparallel to H. There are no van der Waals loops and no spinodal lines with $\partial M/\partial H = \infty$ in this expression for p above p_c.]

These remarks conclude our qualitative description of percolation; we now turn to the quantitative description of the scaling region by critical exponents.

1.2. Critical exponents

The behavior of systems close to a phase transition [10, 11], also for percolation, is usually described by critical exponents $\alpha, \beta, \gamma, \ldots$ (except for first order phase transitions). For our review we need only the definitions

$$\left[\sum_s n_s(p)\right]_{\text{sing}} \propto |p - p_c|^{2-\alpha} \tag{6a}$$

$$\left[\sum_s s \cdot n_s(p)\right]_{\text{sing}} \propto (p - p_c)^{\beta} \tag{6b}$$

$$\left[\sum_s s^2 n_s(p)\right]_{\text{sing}} \propto |p - p_c|^{-\gamma} \tag{6c}$$

$$\left[\sum_s s \cdot n_s(p) e^{-hs}\right]_{\text{sing}} \propto h^{1/\delta} \tag{6d}$$

$$\xi(p) \propto |p - p_c|^{-\nu}. \tag{6e}$$

All five equations are supposed to be valid only for p near p_c or h near zero. For simplicity we assume that the same exponent describes the behavior above and below p_c, when appropriate. The subscript

sing denotes the leading nonanalytic part of the subscripted quantity and does not necessarily mean that that quantity goes to infinity; for example, if close to p_c a quantity A varies as $A = A_0 + A_1(p-p_c) + A_2(p-p_c)^{1.355} + A_3(p-p_c)^{1.855} + A_4(p-p_c)^2$, then the "singular" (or critical) part A_{sing} is the term $A_2(p-p_c)^{1.355}$, whereas $A_0 + A_1(p-p_c) + A_4(p-p_c)^2$ are denoted as the "analytic background" and $A_3(p-p_c)^{1.855}$ as a "correction to scaling". This review will concentrate on the singular parts only. (According to this definition we have $[\Sigma_s s \cdot n_s]_{sing} \propto P_\infty$ in eq. (6b), since the concentration p which also appears in eq. (4) contributes only to the analytic background etc.) The real number h in eq. (6d) is merely a dummy variable to calculate a sum and approaches zero; the background of that sum is its value at $h = 0$ which is $\Sigma_s s \cdot n_s(p_c) = p_c$, from eq. (4). Finally, ξ is the coherence length (or correlation length, connectivity length) and corresponds to the average radius of a typical percolation cluster, as will be discussed later. We neglect here the possibility that logarithmic factors appear besides powers of $p - p_c$; in six dimensions such factors are important where e.g. $[\Sigma_s s^2 n_s]_{sing} \propto (p_c - p)^{-1} |\log(p_c - p)|^{2/7}$ according to Essam et al. [17]. (Another exponent $\eta \equiv 2 - \gamma/\nu$ is not needed here [18].)

So far eqs. (6) are merely definitions of exponents by various moments of the cluster size distribution n_s. But these definitions are indeed analogous to what is usually defined at other phase transitions where $T_c - T$ replaces $p - p_c$ as the distance from the critical point. In eq. (20) we will see later that $\Sigma_s n_s$ corresponds to a free energy, which at thermal phase transitions is assumed to vary as $(T - T_c)^{2-\alpha}$ in its singular part, in order that the specific heat diverges as $(T - T_c)^{-\alpha}$. Moreover, the percolation probability P_∞ corresponds to the spontaneous magnetization $\propto (T_c - T)^\beta$, similar to our remarks after eq. (5) for dilute ferromagnets. We also see from eq. (5) that the susceptibility $\chi \equiv \partial M / \partial H$ is connected with $\Sigma_s s^2 n_s$, and at thermal phase transitions this susceptibility diverges as $(T - T_c)^{-\gamma}$ as a generalization of the Curie–Weiss law. At the critical temperature $T = T_c$ the magnetization is usually assumed to vary as $H^{1/\delta}$, analogous to eq. (6d); indeed the factor e^{-h} in eq. (6d), basically introduced by Gaunt and Sykes [19], can be interpreted as a "ghost" field (with e^{-h} replaced by $1 - h$), a magical trick avoided in this review but used elsewhere [20–23]. Another interpretation of e^{-h} is given in ref. [24] in connection with semiconductors. Also a coherence length can be defined at thermal phase transitions to describe the decay of correlations over long distances, diverging as $|T - T_c|^{-\nu}$ similar to eq. (6e). Since about ten years this exponent notation is standard for phase transitions and has been adopted consistently in the literature also for percolation. Of course, a reader not familiar with thermal phase transitions may simply overlook the above analogies.

A complete understanding of percolation would require to calculate these exponents exactly and rigorously. This aim has not yet been accomplished, even in general not for other phase transitions. (Ref. [25] gives reasons to hope for an exact result in two dimensions: $\nu = \log(3^{1/2})/\log(\frac{3}{2})$.) The aim of a *scaling theory* as reviewed here, is more modest than complete understanding: We want merely to derive *relations* between critical exponents. And since this review deals mainly with the scaling theory of clusters, we want to understand how the above exponents like β can be calculated from cluster properties and cluster exponents.

For even in the cluster properties some simple power laws are found. Fig. 3 gives Monte Carlo results for the cluster numbers n_s at $p = p_c = \frac{1}{2}$ in the triangular lattice. The data in this double logarithmic plot follow a straight line with slope $-\tau \simeq -2$, i.e. $\log n_s = \text{const} - \tau \cdot \log s$, or $n_s \propto s^{-\tau}$. What relations exist between this new exponent τ and the other critical exponents defined in eq. (6). Does a single exponent like τ suffice to describe the cluster numbers in the scaling region? These are the questions our review tries to answer. Of course, to test these scaling theories we will have to use the numerical methods and results for finding critical exponents, as described in greater detail in

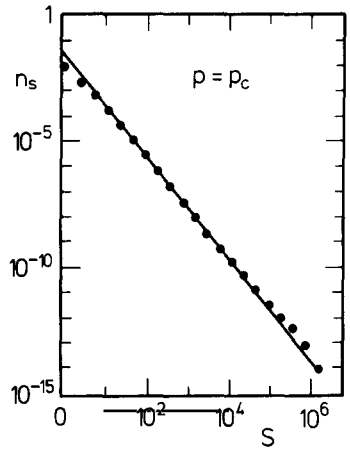

Fig. 3. Computer simulation [26] of cluster numbers in a 4000×4000 triangular lattice at the percolation threshold. The straight line shows $n_s(p_c) \propto s^{-\tau}$, $\tau \simeq 2$.

section 2 and as evident already in this example of fig. 3. After we have explained in section 3.1 the scaling theory of percolation clusters we will list there the present estimates for the exponents and also for the percolation thresholds p_c. We merely mention here that for two dimensions, we have roughly

$$\alpha = -0.7, \quad \beta = 0.14, \quad \gamma = 2.4, \quad \delta = 18, \quad \nu = 1.35,$$

results which are expected according to the universality hypothesis to be valid for (nearly) all two-dimensional percolation problems, independent e.g. of the lattice type. On the other hand, p_c depends on the lattice and equals 0.50 for the triangular and 0.59 for the square lattice.

[One exactly solved problem is percolation on the Bethe lattice, also known as Cayley tree [27–30], where $\alpha = -1$, $\beta = 1$, $\gamma = 1$, $\delta = 2$. We refer to refs. [2, 30] for a discussion of Bethe lattices and restrict ourselves here to the not yet exactly solved cases where the exponents are not integers.]

In this sense the percolation problem can serve as an introduction to the scaling theory of phase transitions and critical phenomena: the critical exponents are defined by mathematically simple expressions in eq. (6); and later in section 3.1 we will derive relations between them [31], using a simple scaling ansatz for the cluster numbers n_s. As promised before one does not have to know concepts like "free energy" of "magnetic moment" to understand the definitions (6), contrary to most other phase transitions [10].

But besides being perhaps the simplest not exactly solved phase transition, percolation theory also serves as an introduction to cluster approximations of collective phenomena. In statistical physics, systems with interactions between the units (molecules, spins, ...) in general cannot be calculated exactly, whereas most systems without interaction are easy to solve. Thus an often-used approximation is the cluster (or droplet) approximation which tries to transform the problem of interacting units into the approximation of non-interacting clusters. For example, to describe the equation of state and the condensation process (nucleation) in a real gas, one may group the gas molecules into clusters of neighboring molecules ("liquid droplets") such that interactions between different groups can be neglected. Interactions within the same group are taken into account either exactly (for very small clusters) or by simple approximations containing only a few free parameters like surface tension etc. If the critical point of a fluid is described [30] by such a "droplet" model, it is

characterized by the appearance of very large clusters leading to critical opalascence in light scattering. Such cluster models exist not only for fluids but also for magnets, polymers, structural transitions, semiconductors. For early references see Domb [32].

To put such cluster models for general phase transitions onto a more rigorous basis one can study simplified models, instead of real water droplets, to look directly at the microscopic clusters and their impact on macroscopic quantities like susceptibility etc. In order to be useful such a model should have five properties:

(i) it can be used in three dimensions
(ii) for every configuration there is an unambigous and unartificial separation of units into clusters
(iii) the definition of clusters according to (ii) is simple enough for computer handling
(iv) at least some macroscopic quantities can be calculated reliably from the cluster properties
(v) the system has a critical point; there and only there large clusters appear.

Some years ago there was reason to hope that the Ising magnet (lattice gas model) fulfilled all the above requirements, since in two dimensions computer simulations [33] agreed well with the Fisher droplet model [31, 34], if a "cluster" is defined as a group of overturned spins connected by nearest-neighbor exchange forces. Unfortunately later work [35] showed that condition (v) is violated in three dimensions. Thus the cluster situation in this Ising model is rather complicated [36], and percolation seems right now to be the only problem where all the above requirements are fulfilled. Thus percolation can be used as a guide to clustering phenomena at other phase transitions. Of course there is no guarantee that other phase transitions will have the same cluster properties as the simple percolation problem; but it seems plausible that a complete understanding of simple clusters (i.e. percolation) is helpful for a better understanding of more complicated clusters (e.g. fluids, magnets). It should be noted, however, that the above difficulties with clusters at other phase transitions arise mainly near the critical point; far below the critical temperature of a fluid, for example, an often experienced example of quite well-defined clusters are raindrops; they are nothing but grown-up stages of those clusters relevant for the liquid-gas phase transition in a supersaturated vapor [37, 38]. The possible similarity of percolation clusters with raindrops will therefore be discussed in detail, see section 4.3.1.

2. Numerical methods

This section describes shortly the main methods used so far to calculate percolation quantities approximately. It is not necessary to read this section in order to understand (we hope) the later scaling theories, where the results of these numerical methods are reported and interpreted.

2.1. Series expansions

The average number n_s of small clusters can be calculated exactly. Take, for example, a pair in the square lattice, i.e. an s-cluster with $s = 2$. It consists of two occupied squares surrounded by six empty neighbor squares. Moreover it can be oriented either horizontally or vertically in the lattice. Thus the average number of pairs is $n_2 = 2p^2(1-p)^6$ since in percolation each of the squares involved is either occupied (with probability p) or empty (with probability $1-p$) entirely independently of the other squares. Generally we denote as the perimeter t the number of empty lattice sites which are nearest neighbors of occupied cluster sites, and as g_{st} the number of geometrically different cluster

configurations of s sites with perimeter t. (The g_{st} are also called the number of "animals"; see section 5; if two configurations are identical apart from a rotation they are counted as different; if they are identical apart from a translation they are counted as the same configuration.) Then we have exactly

$$n_s(p) = \sum_t g_{st} p^s (1-p)^t. \tag{7}$$

The following diagrams show small clusters on a square lattice together with the resulting expressions for n_s; the cluster sites are denoted by dots, the perimeter sites by crosses:

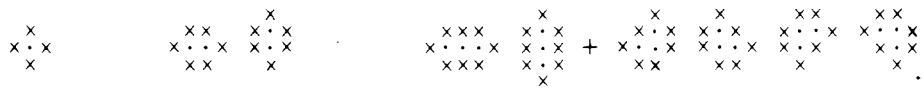

$$n_1 = p(1-p)^4; \quad n_2 = 2p^2(1-p)^6; \quad n_3 = 2p^3(1-p)^8 + 4p^3(1-p)^7.$$

This method of exact cluster counting was already used twenty years ago [39–41]. The above diagrams show that for larger cluster sizes more possibilities and thus more difficulties arise. The exact result for $s = 14$ in the triangular lattice, with $q = 1-p$, is [42]

$$\begin{aligned} n_{14}(p) = p^{14}(&3q^{16} + 168q^{17} + 1524q^{18} + 10029q^{19} + 46119q^{20} + 185220q^{21} + 605766q^{22} + 1730943q^{23} \\ &+ 4287699q^{24} + 9131949q^{25} + 16871550q^{26} + 26571525q^{27} + 35061399q^{28} + 3796541q^{29} \\ &+ 32198928q^{30} + 19012074q^{31} + 5812482q^{32}), \end{aligned}$$

a result which illustrates convincingly that the counting is done best on a computer [43]. Even then the n_s are known only up to $s = s_{max}$, with s_{max} usually of order ten. For example we have $s_{max} = 17$ in the square lattice, $s_{max} = 11$ in the simple cubic lattice, and $s_{max} = 7$ for the hypercubic lattice in arbitrarily large dimensionality [44, 45]. For applications, a table of $n_s(p)$ in two and three dimensions calculated from these polynomials was given in ref. [46].

For the triangular lattice, besides the full range of g_{st} at fixed s up to $s_{max} = 14$, exact g_{st} for fixed t were given in ref. [47] up to $t_{max} = 22$. Duarte [48] analyzed in detail the behavior of averages at constant perimeter t, in particular the deviations from a Gaussian distribution. We will not use this information here since we will look at the distribution of perimeters t at fixed size s instead.

These exact results of Sykes et al. [42, 47] have the advantage that they can be used even far away from p_c where the cluster numbers n_s become very small. That region, for example, is important for nucleation applications [38, 49]. Moreover they give not only the cluster numbers but also the average perimeter t_s of s-clusters: $t_s = \Sigma_t t \cdot g_{st} p^s (1-p)^t / \Sigma_t g_{st} p^s (1-p)^t$. Their main disadvantage is their restriction to small and intermediate cluster sizes s. So far most extrapolations to $s \to \infty$ [46, 50, 51] employed rather simple methods: If a quantity A_s is expected to have a finite limit A_∞ for $s \to \infty$, then A_s is plotted against $1/s$. If one is lucky these data follow a straight line for large s; the intercept ($1/s = 0$) of this line gives A_∞. If instead a clear curvature is seen, one plots A_s against some other power of $1/s$ until the points fit a straight line; again the intercept of that line gives the extrapolated A_∞. Particularly accurate results were given in ref. [52]. Usually the resulting extrapolations are about as accurate as those from Monte Carlo results, as can be seen by comparing the corresponding results of refs. [26, 51] or [53, 52].

Better methods of extrapolation exist to calculate the critical exponents for the various moments of the cluster size distribution, e.g. the exponent γ for $\Sigma_s s^2 n_s \propto (p_c - p)^{-\gamma}$ below p_c, eq. (6c). Instead of first extrapolating for large s the cluster numbers n_s, one deals directly with this sum and expands it into a power series in p by using the exact expressions for $n_s(p)$ and by collecting the appropriate

powers of p arising from $p^s(1-p)^t$ in eq. (7): $\Sigma_s s^2 n_s(p) = \Sigma_k a_k p^k$. Since n_s varies as p^s apart from higher powers in p, exact knowledge of n_s up to $s = s_{max}$ also gives the exact expansion coefficients a_k up to $k = s_{max}$; additional tricks [42] gave a_k for $k = s_{max}+1$ and $s_{max}+2$. These series expansions in powers of p etc. have given this subsection its name; for simplicity we will refer to all results derived from the exact $n_s(p)$ as "series" results even if no power series in p was used. The analysis of such power series in terms of critical exponents is a standard method of phase transition theory and is reviewed in vol. 3 of ref. [11]; usually exponents estimated in this way are more reliable than those estimated by other methods. A rather simple way of series analysis is the "ratio" method: if $\Sigma_k a_k p^k$ is supposed to diverge as $(p_c - p)^{-\gamma}$ and if the ratios a_{k+1}/a_k are plotted against $1/(k+1)$, then the data should follow a straight line for large k, with intercept $1/p_c$ and slope $(\gamma - 1)/p_c$, as the reader can check by himself, employing the Taylor series $f(p) = \Sigma_k [d^k f/dp^k]_{p=0} p^k/k!$ More complicated but usually more accurate are the Padé approximations (particulary when the ratio plots oscillate), where the power series is approximated by the ratio of two polynomials in p [19, 44, 54, 55]. The accuracy sometimes can be increased further by suitable transformations of variables [56]. Practical experience with such series methods has accumulated over many years of experience with other phase transitions [11].

An important difference between percolation and other phase transitions is, however, that no exact expressions so far have been published for the cluster numbers $n_s(T)$ in, say, the Ising model of magnets. Only power series of thermo dynamic quantities like susceptibility etc. as a function of $1/T$ or $\exp(-2\mu H/k_B T)$ have been derived and analyzed, e.g. in ref. [57]. As mentioned above, percolation is the simplest phase transition as far as clusters are concerned.

2.2. *Monte Carlo simulation*

Examples of Monte Carlo computer simulations were already given in the Introduction, figs. 2, 3 and table 1. Similar to series expansions, the quality of the data is limited by the number of computer hours available (and also by limitations in the computer memory). But whereas "series" give exact expressions if s is near 10, Monte Carlo results are available for much larger clusters, $s \sim 10^3$, with finite error bars. (See ref. [58] for a theory of Monte Carlo fluctuations in the cluster numbers.) Therefore it is seldomly necessary to extrapolate Monte Carlo results to $s \to \infty$, since $s = 10^2 \cdots 10^3$ is usually close enough to infinity, if the finite error bars of the computer experiment are taken into account. If possible, a combination in one plot of exact series results for small s and approximate Monte Carlo data for large s gives a good impression of the accuracy and limitations of both approaches. (We refer to Binder's book [59] for reviews of thermal Monte Carlo methods.)

An advantage of percolation compared with other phase transition is that non-equilibrium difficulties do not appear in most percolation studies: If a whole lattice is filled *once* with sites, the resulting clusters can already be used for the statistics of cluster numbers etc. But for thermal phase transitions one first has to simulate perhaps thousands of Monte Carlo steps per site until the system has come close enough to thermal equilibrium in order that the averaging procedure can start.

Our presentation here is restricted to three different methods: Simulations of the whole lattice; growth of one cluster; and shape fluctuations for one cluster.

2.2.1. *Simulations of the whole lattice*

Table 1 gives the usual method of filling a lattice of $N = L^d$ sites in d dimensions randomly with pN occupied sites. In a thorough study one should vary the length L of the lattice and extrapolate the

results to $L = \infty$ [60, 61]. So far the largest systems studied seem to be $L = 4000$ in two and $L = 400$ in three dimensions [26, 61]; care with the computer memory is essential for such large systems. Each of these lattices can be simulated once or several times; ref. [62] simulated a 110×110 lattice forty thousand times. "Finite size" effects due to the limited size L can be annoying and might be reduced by employing periodic boundary conditions where layer number $L+1$ in a cube is identified with the first layer to give a quasi-infinite lattice. The really complicated programming problem is the counting of clusters; orders of magnitude in computer time can be saved by efficient algorithms. We refer the reader to refs. [7, 63, 64] for these details.

Monte Carlo simulation of percolation lattices were done already twenty years ago [65]; for the cluster numbers n_s the extensive tables of Dean and Bird [66] played, after a long time lag, an important role in the development and testing of scaling theories [67–70] and became obsolete only quite recently [62, 71, 72, 26]. The method has been used to calculate cluster numbers, perimeters, radii and energies. (The energy is the number of occupied–empty bonds for the cluster.)

2.2.2. *Growth of one cluster*

Leath's method [73] divides the lattice into concentric shells with the thickness of a nearest-neighbor distance. Starting with the innermost site occupied, all lattice sites in the next shell are randomly either occupied with probability p or left empty with probability $1-p$. It is tested which of these newly occupied sites are connected with the cluster in the inner shells. Then the next shell is filled randomly, and the process is repeated. It stops when in one new shell no sites were occupied which are connected with the cluster formed earlier in the inner shells. This method produces clusters of size s with a probability $s \cdot n_s$, i.e. with the probability that the origin belongs to an s-cluster. In the method of section 2.2.1 the formation probability is proportional to n_s instead. Thus Leath's method enhances the statistics for the large clusters needed for a scaling analysis. Also there are no "finite size" effects in Leath's method since L is infinite. But the method requires a cutoff s_{max} in the cluster size, taken as about 10^3, and thus could not give results like fig. 1 where s_{max} was near 10^6. And since this method is inefficient above p_c the results so far [71–73] were restricted to $p \leq p_c$. Detailed tables of cluster numbers were made available in ref. [72]. The method has been used to calculate cluster numbers, perimeters and radii.

2.2.3. *Shape fluctuations for one cluster*

If one is interested not in the number n_s of clusters but in other properties like cluster radii etc., one can start with a typical shape of a large cluster and try randomly any changes in the cluster shape which do not change the cluster size s and do not separate the cluster into several parts. If these attempted random changes are adopted with a probability $(1-p)^{\Delta t}$, where Δt is the change in the perimeter t produced by a given change of the cluster shape, then one approximates in this way the true distribution of cluster shapes according to eq. (7) at fixed s. (Here one has to wait for nonequilibrium effects due to the initial configuration to die out.) In this way, analogous to an early Ising model study [74], Stauffer [75] looked at the average perimeter and radii for s near 10^2; density profiles were analyzed in ref. [76]. No information on n_s can be gained in this way, but the method can be applied to large clusters far away from p_c where the other Monte Carlo methods fail. In particular, the "animal" limit $p = 0$ can also be treated with this algorithm.

2.3. Renormalization group

Only since 1975 has percolation been investigated [68] with Wilson's renormalization group technique which proved so useful for thermal phase transitions (vol. 6 of ref. [11]). Basically two variants of that method have been used for percolation: The epsilon expansion and the real space renormalization. Only the second method is explained here fully, and only a few papers are cited. Kirkpatrick [7] reviews renormalization technique in greater detail.

The basic idea behind renormalization is the assumption, eq. (6e), that near p_c the coherence length ξ diverges. If we look at any clusters of diameter l, with l much larger than the nearest-neighbor distance of the lattice, then we have in general to distinguish between $l < \xi$ and $l > \xi$. But right at p_c we have $\xi = \infty$, and all finite lengths like cluster diameter are much smaller than ξ. Thus it should not matter at p_c on what a length scale we are investigating the system; apart from simple scale factors the system looks similar whether we look at it with the eye, with a magnifying glass, or with an optical microscope (assuming the nearest-neighbor distance to be 1Ångstrom, visible in an electron microscope only). Thus we may "renormalize" the system by not looking at each lattice site separately but by averaging over regions $\ll \xi$ which have a diameter of b lattice constants. Then we may average again over these averaged regions, with the same length factor b, etc. At $p = p_c$ the averaged regions are still much smaller than the coherence length even after numerous such averaging iterations; and nothing drastic should have changed due to this renormalization. In this sense the critical point p_c is a mathematical fixed point of the renormalization transformation. If this transformation is done on the lattice itself it is called real space renormalization; if it is done in Fourier space it leads to the epsilon expansion. Scaling is built in both approaches; and the main sucesses have been with the calculation of critical exponents like ν.

2.3.1. Real space renormalization

The above ideas have been made quantitative in many papers [7]; our presentation here follows ref. [77] for the triangular lattice. (We thank P.J. Reynolds for his patience in explaining this section to us.) Imagine that all lattice sites are put together into triangles . ˙. in such a way that each site belongs to only one triangle. The center of each triangle is replaced by a new "supersite" ○ which represents the average (in the renormalization sense) over the three original sites. The whole lattice then looks like fig. 4, where the small triangular △ symbols show the "super-supersites", i.e. the averages over three supersites ○. We see that the supersites ○ and the super-supersites △ in that figure form each a new triangular lattice, similar to but larger than the original triangular lattice formed by the dots ·. We can continue by representing each separate triangle of △ by a new symbol ★, these stars would again form triangles, etc. For simplicity these higher orders of the renormalization transformation are not shown in fig 4. In every case the lattice constant of the new lattice equals the lattice constant of the old lattice multiplied with a factor $b = 3^{1/2}$.

If p is close to but not identical to p_c we have a large but finite correlation length ξ which, expressed in centimeters, is the same in the original lattice and the renormalized superlattices. In the original lattice we have $\xi = \xi_0 |p - p_c|^{-\nu}$ where ξ_0 is of the order of the nearest-neighbor distance. Thus in the superlattice after one renormalization step we have $\xi = \xi_0' |p' - p_c|^{-\nu}$, $\xi_0' = b \cdot \xi_0$, where ξ_0' is of the order of the enlarged nearest-neighbor distance in the superlattice. The difference between the renormalized p' and the original p takes into account that only at $p = p' = p_c$ the two lattices are completely similar to each other. Equating the two expressions for ξ we get $b|p' - p_c|^{-\nu} = |p - p_c|^{-\nu}$, or

$$\nu = \log(b)/\log[(p' - p_c)/(p - p_c)]. \tag{8}$$

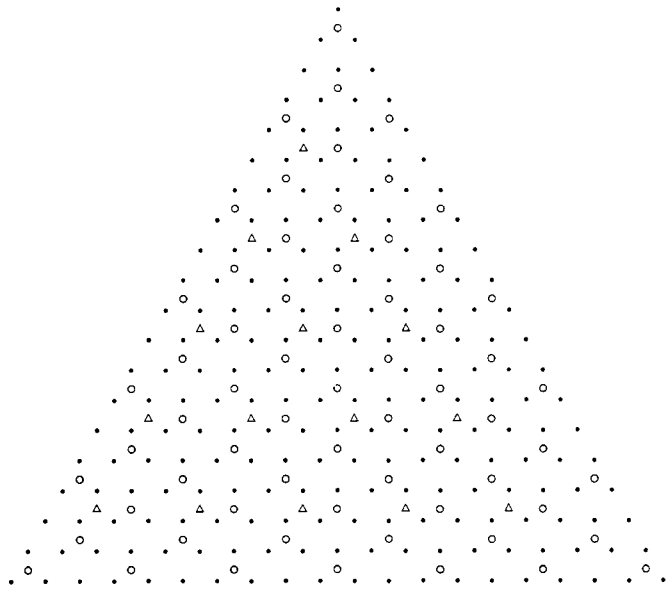

Fig. 4. Real space renormalization on a triangular lattice. At each iteration, three sites are combined into one supersite, denoted here by a different symbol. This picture was produced by S. Kirkpatrick on his computerized typewriter [7].

How do we define if the renormalized supersite in the triangle ȯ is occupied? If all three sites of the original triangle are occupied (empty) then also the supersite representing the average of the three sites is occupied (empty). If only two sites are occupied, we define the supers ite as occupied, but if only one original site is occupied, the supersite is defined as empty. Our diagrams show schematically the correspondence between occupied (·) and empty (×) sites in the original lattice and the superlattice:

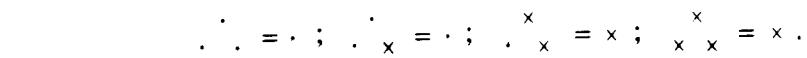

This correspondence gives the relation between the concentration p of occupied sites in the original lattice, and the probability p' that a supersite is occupied. For example, two occupied sites can produce an occupied supersite in three ways: 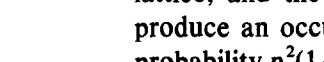 ; each possibility occurs with probability $p^2(1-p)$. Thus in total the probability p' for a supersite to be occupied is

$$p' = p^3 + 3p^2(1-p).$$

The fixed point p^* is determined by the nontrivial ($p \neq 0, p \neq 1$) condition $p = p' = p^*$ and agrees with the critical point p_c:

$$p_c = \tfrac{1}{2}$$

since then $p' = \frac{1}{8} + 3\,\frac{1}{4}\,\frac{1}{2} = \frac{1}{2} = p$. Expanding for small $p - p_c$ we get $p' - p_c = \frac{3}{2}(p - p_c)$. Thus eq. (8) with $b = 3^{1/2}$ gives

$$\nu = \log(3^{1/2})/\log(\tfrac{3}{2}) = 1.354\,755\,65. \tag{9}$$

This example showed rather easily how critical exponents are calculated by renormalization technique. Actually in this example not only is $p_c = \frac{1}{2}$ the desired exact result but also the exponent ν in eq. (9) is hoped to be exact [25]. This result of Klein et al. [25] (see also Reynolds et al. [22]) would be the

first exactly calculated percolation exponent, if their argument could be made rigorous. At least it agrees within a few percent or better with results derived from other methods, as cited in ref. [25].

Similar methods can be applied, although less successfully, to other lattices. One may also average over cells larger than the triangles with only 3 sites discussed above. Very accurate results were derived by calculations for very large cells (up to $b = 500$) of the renormalization transformation with the help of Monte Carlo methods by Reynolds et al. [78]. They checked if the cell contained one large cluster extending from one side to the opposite site, and then called the supersite for that cell occupied. Similar to the pure Monte Carlo results of the preceding subsection, these renormalization results were then extrapolated to $b \to \infty$, giving e.g. $\nu = 1.356 \pm 0.015$, in excellent agreement with eq. (9) and with an accuracy comparable with or better than series expansions [18]. Further work with this combination of Monte Carlo and renormalization methods is in progress.

These methods gave properties of the percolation lattice as a whole but not directly on clusters as a function of cluster size. A first attempt in that direction was made by Kunz and Payandeh [79] and, more quantitatively, by Kinzel [80]. Kinzel [80] calculated the cluster numbers for all p between zero and p_c and thus showed that real space renormalization works also far away from the phase transition.

2.3.2. *Epsilon expansion*

Another renormalization group method consists in expressing the fluctuations in a system by Fourier components. Then one sums them up over all wavevectors iteratively, just as we averaged iteratively over the real-space triangles above. An elementary review of that method was given by Wilson [81]. The summation over the wavevectors cannot be done exactly, and perturbation methods in terms of a small parameter ϵ are used, similar to diagram techniques in the field-theoretical approach to quantum many-body problems.

For percolation, the epsilon expansion [68] first transformed percolation into a thermal phase transition in the socalled Q-state Potts model [21] for $Q \to 1$. Kasteleyn and Fortuin [21], as reviewed already by Essam [2], derived for the partition function Z_{Potts} of this Potts model:

$$Z_{\text{Potts}} = \langle Q^{\Sigma m_s} \rangle$$

where each lattice site can be in one of Q different states. Here $\Sigma m_s = \Sigma_s m_s$ is the sum over the actual cluster numbers m_s in a given configuration, and $n_s = \langle m_s \rangle$ is the average cluster number. These averages $\langle \cdots \rangle$ are defined over all random (bond) percolation configurations, where temperature T and concentration p are related by $\log(1-p) \propto 1/T$. For $Q = 2$ the result corresponds to the spin $\frac{1}{2}$ Ising model of ferromagnets. We see easily that the limit $Q \to 1$ means percolation. For then we expand $Q^{\Sigma m_s} = \exp[\ln(Q)\Sigma_s m_s] \simeq 1 + \ln(Q)\Sigma_s m_s \simeq 1 + (Q-1)\Sigma_s m_s$; thus $-F_{\text{Potts}}/k_B T \equiv \ln(Z_{\text{Potts}}) = \ln\langle 1 + (Q-1)\Sigma_s m_s \rangle \simeq (Q-1)\Sigma_s \langle m_s \rangle$, where F_{Potts} is called the free energy:

$$F_{\text{Potts}} = -k_B T(Q-1)\sum_s n_s \quad \text{for } Q \to 1.$$

In this sense the sum over all cluster numbers in eq. (6a) corresponds to the limit of a Potts model free energy (suitably normalized). Thus a solution of the thermal phase transition in the Potts model also gives a solution for the probabilistic phase transition of percolation. (The limit $Q \to 0$ corresponds to trees percolating on a lattice [21, 82].)

With these methods the perturbation expansion to order ϵ and ϵ^2 with $\epsilon \equiv 6 - d > 0$ gives in d dimensions [83]:

$$\beta = 1 - \epsilon/7 - (61/12348)\epsilon^2 + \cdots \tag{10a}$$

$$\gamma = 1 + \epsilon/7 + (565/12348)\epsilon^2 + \cdots \tag{10b}$$

with the other exponents following from the scaling laws given later in section 3.1.

The crucial step was hidden before eq. (10a): Our perturbation parameter basically is the dimensionality d. What sense does it make to use in this way non-integral dimensionalities like $d = 5.9$ where eq. (10) should be a good approximation? (Later we will mention why six dimensions play a special role for percolation [84].) Obviously what we really need are results in three, and perhaps two, dimensions. But numerically already the rather short series in eq. (10) give reasonable results if applied to three dimensions ($\epsilon = 3$, $\beta = 0.53$, $\gamma = 1.84$), exponents which are wrong by 0.1 to 0.2 only. More importantly, later we will make scaling assumptions which are asserted to be valid for all dimensions (below 6). If one can prove such an assumption to be wrong in the epsilon expansion of eq. (10), then there is little reason to believe it is valid generally or in three dimensions. The introduction of non-integral dimensions by Wilson and Fisher [85] is a new mathematical tool to describe reality, just as the introduction of irrational and imaginary numbers was such a new concept many centuries or millenia ago. We simply have become accustomed to these "imaginations". Certainly, if L^d is the volume of hypercubes in d dimensions for all integer d, then L^d is a plausible definition for the volume in general nonintegral dimensionalities d. Only applications of that concept to real problems can show if it is useful; and now we give two examples of such applications:

(i) In polymer physics it was long assumed that excluded volume effects for self-avoiding walks were described by the Flory formula: average polymer radius $\propto$ (length)$^\nu$ for large polymers, with $\nu = 3/(d+2) = \frac{1}{2} + \frac{1}{6}(4-d) + \ldots$. But de Gennes [86] showed that the epsilon expansion gives $\nu = \frac{1}{2} + \frac{1}{4}(4-d) + \ldots$ proving that the Flory formula cannot be exact in general.

(ii) For percolation, in some expressions correction factors of the form $1 + O(s^{2\sigma-1})$ with $\sigma = 1/(\beta+\gamma)$ only slightly smaller than $\frac{1}{2}$ were derived, eq. (34). If for all cluster properties such correction factors with $s^{2\sigma-1}$ would exist as "corrections to scaling", then it would be nearly impossible to get accurate exponents from finite cluster sizes s, since the corrections would even for moderately large s not be negligible. These fears turned out to be not justified: Epsilon expansion showed [87] the exponent for s in the leading correction to be $\frac{1}{2}(6-d) + \cdots$, whereas $1 - 2\sigma$ varies as $(6-d)^2$. Thus the two exponents are not the same, and the extrapolation of the correction exponent to three dimensions gave a large value near unity [87].

Thus the concept of nonintegral dimensions and of epsilon expansions has been of practical use for our understanding of three-dimensional systems.

2.4. Inequalities

The latest method for the study of large percolation clusters are exact inequalities [88–91] introduced by Schwartz [88]. In particular the results of Kunz and Souillard [90] stimulated further research. We give here a simplified nonrigorous presentation of these rigorous results.

Assume that for sufficiently large s, at fixed p, the cluster numbers n_s decay as $\log(n_s) \propto -s^\zeta$ asymptotically [70]. This exponent $\zeta = \zeta(p)$ is not a critical exponent in the usual sense since it is defined for all p, not only close to p_c. Above p_c all available information suggests that the $n_s(p)$ decrease with increasing p at fixed s, as one can see already from the concentrations of single sites and pairs mentioned after eq. (7). For p near unity, only the most compact configurations [47] with the smallest perimeter $t_{\min}(s)$ survive in the sum of eq. (7). This minimum perimeter varies as $s^{1-1/d}$ for

large s; exact formulas for all s were given in ref. [92] for some two- and three-dimensional lattices. Eq. (7) gives for p near unity: $n_s = g_{st_{min}} p^s (1-p)^{t_{min}} = g_{st_{min}} (1-p)^{t_{min}}$, or $\log(n_s) \propto t_{min} \propto s^{1-1/d}$. Thus

$$\zeta(p \to 1) = 1 - 1/d. \tag{11a}$$

If for any p_1 between p_c and unity the exponent ζ would be larger than $1-1/d$ it would mean that cluster numbers n_s for such a p_1 would decay quicker with size than for p near unity. Thus for sufficiently large s we would have $n_s(p_1)$ to be smaller than n_s for p near unity; and such an effect was excluded by our initial statement. Thus we made plausible [90]

$$\zeta(p > p_c) \leqslant 1 - 1/d. \tag{11b}$$

In fact the equality holds in expression (11b) for a small interval near $p = 1$ according to ref. [90].

Below p_c we use the numerical result from series [42, 93] that the total number $\Sigma_t g_{st}$ of "animals" increases for large s as $s^{-\theta}\lambda^s$, with e.g. in the triangular lattice $\lambda \simeq 5.183$ and $\theta \simeq 1.00$. (See ref. [94] for inequalities on λ.) For p close to zero all animals in eq. [7] get equal weight since then $(1-p)^t$ can be approximated by unity: $n_s(p \to 0) = \Sigma_t g_{st} p^s (1-p)^t = p^s \Sigma_t g_{st} \propto s^{-\theta}(p\lambda)^s$, or

$$\zeta(p \to 0) = 1. \tag{12a}$$

For general p the same consideration gives an upper bound: $n_s(p) \leqslant \text{const} \cdot s^{-\theta}(p\lambda)^s$ for large s and all p. A lower bound is obtained also, since n_s is always larger than the average number of chains having the maximum perimeter t_{max}; for example, in the triangular lattice we have $t_{max}/s = 2$ for large s. With this asymptotic ratio of 2 (which may be replaced by any other constant) we find n_s to be larger than $p^s(1-p)^{t_{max}} = [p(1-p)^2]^s$. We thus have for large clusters [88]

$$p(1-p)^2 \leqslant (n_s)^{1/s} \leqslant p\lambda. \tag{12b}$$

Therefore, as long as $p\lambda < 1$, we need $\zeta = 1$ to agree with eq. (12b); otherwise either the upper bound or the lower bound would be violated:

$$\zeta(p < 1/\lambda) = 1. \tag{12c}$$

Furthermore refs. [88, 89, 91] derived

$$(g_{st})^{1/s} \leqslant (a+1)^{a+1}/a^a; \qquad a = t/s \tag{13a}$$

if t and s go to infinity at constant ratio a. [Proof: Eq. (7) gives for $t_a = as$ at arbitrary a: $n_s = \Sigma_t g_{st} p^s (1-p)^t \geqslant g_{st_a}[p(1-p)^a]^s$. This expression cannot increase exponentially with s, and thus we need $(g_{st_a})^{1/s} p(1-p)^a \leqslant 1$ for arbitrary a and p. If we use $p = 1/(1+a)$ or $a = (1-p)/p$ in that inequality we get $(g_{st_a})^{1/s} a^a/(1+a)^{1+a} \leqslant 1$, which gives eq. (13a).] Using this result, Reich and Leath [89] derived

$$\zeta(p < p_\lambda) = 1, \tag{13b}$$

where p_λ is determined by $a_\lambda = (1-p_\lambda)/p_\lambda$ and $(a_\lambda+1)^{a_\lambda+1}/a_\lambda^{a_\lambda} = \lambda$. In the triangular lattice the above data for λ give $a_\lambda = 1.429$ and thus $p_\lambda = 0.412$; for the square lattice $a_\lambda = 1.023$ and $p_\lambda = 0.494$. These values for p_λ are already quite close to $p_c = 0.50$ and 0.59, respectively, suggesting what we will find later, that $\zeta = 1$ for all p below p_c.

Thus the asymptotic "decay exponent" ζ equals $1-1/d$ above p_c and 1 below p_c, at least far away from the critical point. These inequalities do not yet exclude the possibility that there exists a second and third critical point p_2 and p_3 below and above p_c, respectively, such that $\zeta(p < p_2) = 1$, $\zeta(p > p_3) =$

$1-1/d$, but ζ different and unknown for p between p_2 and p_3. In that case no drastic changes are allowed in the cluster numbers at these additional critical points, if the "free energy" $\Sigma_s n_s(p)$ has only one critical point p_c where it is not analytic [95]. Our next section will show from Monte Carlo methods that at least in two dimensions no such complication seems to exist and that the decay exponent ζ equals unity for all p below p_c and equals $1-1/d$ for all p above p_c, even close to the critical point.

3. Cluster numbers

This section is the main part of our review and deals with a simple formula, eq. (15), to describe the average number of large s-clusters close to the percolation threshold p_c, as a function of s and $p-p_c$. Numerical tests are presented which confirm roughly that scaling formula. Except if stated otherwise our results here apply only to large s and small $p-p_c$.

3.1. Scaling theory

This subsection suggests a scaling assumption with two free exponents σ and τ, which are fitted on "experiment". All the other critical exponents then are derived from these two. In this sense a scaling theory is phenomenological, i.e. it merely relates different measurable quantities without calculating any of them directly. In contrast, the "microscopic" numerical techniques of section 2 predict such measurable quantities directly from first principles. The same distinction between phenomenological and microscopic approaches applies to thermal phase transitions [10, 11] and other problems. After we have explained exponents we also give a table summarizing the present numerical estimates for them as a function of dimensionality.

3.1.1. The basic assumption

The critical behavior near p_c is characterized by the fact that the typical cluster size becomes very large near the phase transition and diverges at p_c; otherwise the typical cluster radius ξ of eq. (6e) would not diverge. One may define the "typical cluster size" s_ξ as that size which gives the main contribution to the singular parts of $\Sigma_s s^2 n_s, \Sigma_s s^3 n_s$ or of any other sum appearing in eq. (6). (This typical cluster size is not identical to another expression which in the literature is unfortunately called the mean cluster size: $S \equiv \Sigma_s s^2 n_s / \Sigma_s s \cdot n_s$, a wording which we will avoid here.) We *assume* that all these definitions give the same typical size s_ξ apart from numerical constants, i.e. that the different s_ξ all diverge with the same power of $|p-p_c|$. This exponent of $p-p_c$ is sometimes called the gap exponent; we denote it here by $1/\sigma$. Thus our basic postulate is:

> We assume that the critical behavior of percolation is dominated by clusters of size $s_\xi \propto |p-p_c|^{-1/\sigma}$, where differently defined typical cluster sizes s_ξ all diverge with the same exponent. (14a)

In short, we assume an essentially unique typical cluster size. "Critical behavior" in assumption (14a) refers to the singular parts, as defined in section 1.2. For example, s_ξ is the size dominating in $[\Sigma_s s \cdot n_s]_{\text{sing}}$, but not in $\Sigma_s s \cdot n_s$; singularities come from typical clusters, analytic background terms arise from much smaller clusters.

How can we put eq. (14a) into a quantitative form? All singular cluster properties must depend

mainly on the single ratio s/s_ξ since the typical cluster size was assumed to be unique. If instead they would depend on two variables s/s_{ξ_1} and s/s_{ξ_2} we would have more than one typical cluster size s_ξ, in contradiction to eq. (14a). But the assumption $n_s(p) = f(s/s_\xi)$ would be too simple, since then at $p = p_c$, where $s_\xi = \infty$, the cluster numbers would be constant, in contradiction to fig. 3. It seems plausible, just as we expressed the cluster size by the ratio s/s_ξ, to calculate also the cluster numbers through the ratio n_s/n_{s_ξ} and to assume that this ratio depends only on the ratio s/s_ξ:

$$n_s/n_{s_\xi} = F(s/s_\xi). \tag{14b}$$

Since the typical cluster size is defined only up to numerical factors, this assumption (14b) is not very practical (except for one dimension: appendix 2) and we replace the ratio n_s/n_{s_ξ} by $n_s/n_s(p_c)$. (The final result (15) is the same.) Thus:

We assume that the ratio $v_s(p) = n_s(p)/n_s(p_c)$ and similar ratios of other cluster properties are a function of the ratio s/s_ξ only: $v_s(p) = \tilde{F}(s/s_\xi)$. (14c)

Equations (14b, c) explain why theories of this kind are called scaling theories: If we plot n_s versus s for different $p - p_c$ and if we scale the cluster size s by dividing through s_ξ and the cluster numbers $n_s(p)$ by dividing through $n_s(p_c)$ or n_{s_ξ}, then in these scaled variables the plots are independent of $p - p_c$.

We have already seen in fig. 3 that at $p = p_c$ the cluster numbers $n_s(p_c)$ decay with a simple power law: $n_s(p_c) \propto s^{-\tau}$. And now we understand why: Any more complicated decay law, like $n_s(p_c) \propto s^{-\tau} \exp(-s/s_0)$, would mean that at p_c there exists a finite typical cluster size s_0. Since $s_\xi(p = p_c)$ is infinite that result would mean that more than one typical cluster size exists, in contradiction to our basic assumption. Thus eq. (14c) reads: $n_s(p) \propto s^{-\tau}\tilde{F}(s/s_\xi)$. Since $s/s_\xi \propto |(p - p_c)s^\sigma|^{1/\sigma}$, we may summarize our assumption in its final form:

$$v_s(p) \equiv n_s(p)/n_s(p_c) = f(z), \text{ or } n_s(p) \propto s^{-\tau} f(z)$$
$$\text{with } z \equiv (p - p_c)s^\sigma \text{ and } f(0) = 1. \tag{15}$$

The normalization $f(0) = 1$ comes from the trivial requirement $v_s(p_c) = 1$. This assumption (15) is the basis of our interpretation of cluster numbers; we will determine the exponents σ and τ and the scaling function $f(z)$ from microscopic methods later, since they are not predicted by the present phenomenological scaling theory.

Eq. (15) was first mentioned by Stauffer [67] as a generalization of the Fisher droplet model [34]; for thermal phase transitions analogous generalizations were made earlier [96]. (See also refs. [18, 97, 98] for related assumptions.) This Fisher model [34] simply assumes $n_s \propto s^{-\tau} \exp(-\text{const} \cdot z)$ for p above p_c, which is clearly a special case of eq. (15). Although this Fisher formula finally turned out to be quantitatively inaccurate, as we will see later in fig. 7, it gives a rather good approximation for the "ferromagnetic" side of the phase transition and played an important role in the development of the scaling theory for percolation clusters. Many of the qualitative discussions of this section and of appendix 1 can be followed easier if the reader works with this simple Fisher formula instead of with the general scaling assumption (15). We may also regard eq. (15) as a generalization of the Bethe lattice result [30] where $n_s \propto s^{-5/2} \exp(-\text{const} \cdot z^2)$, $\sigma = \frac{1}{2}$, $\tau = \frac{5}{2}$.

[For finite s the cluster numbers n_s are a polynomial in p, eq. (7), without any singularities at $p = p_c$. Thus we expect also the limit function $f(z) = n_s/n_s(p_c)$ to remain regular at $p = p_c$, i.e. $z = 0$. The scaling function $f(z)$ is therefore assumed to be analytic in its argument z for all z including $z = 0$. For large z, the scaling function f must decay sufficiently rapidly to make all the sums in eq. (6) converge.]

3.1.2. Relation to critical exponents

Now we relate the cluster exponents σ and τ to the other critical exponents α, β, γ, δ defined in eq. (6). In order to evaluate the singular part of any moment $\Sigma_s s^k n_s$ qualitatively, i.e. in order to get its critical exponent correctly, we may replace in the sum each factor s by the typical size s_ξ and the cluster numbers n_s by the numbers of typical clusters $n_{s_\xi} \propto s^{-\tau} f(\text{const}) \propto s^{-\tau}$. Moreover the summation over all cluster sizes s gives an additional factor s_ξ: $[\Sigma_s s^k n_s]_{\text{sing}} \propto s_\xi^{1+k-\tau}$. Since $s_\xi \propto |p - p_c|^{-1/\sigma}$ by definition, we thus have [18]

$$\left[\sum_s s^k n_s(p)\right]_{\text{sing}} \propto |p - p_c|^{(\tau-1-k)/\sigma}. \tag{16}$$

A more rigorous derivation of this exponent, together with evaluations of the proportionality factor, is given in appendix 1. A reader who mistrusts our simple approximation above and does not want to go through the details of that appendix may check eq. (16) by simply using the Fisher formula, $n_s \propto s^{-\tau} \exp(-\text{const} \cdot z)$, and by evaluating the higher moments like $k = 2, 3, \ldots$ only. The integrals then can be expressed by gamma functions [99].

Eq. (16) gives us immediately the various exponents of eq. (6); we merely take $k = 0$ for the number of clusters (eq. (6a)), $k = 1$ for the percolation probability (eq. (6b)), $k = 2$ for the susceptibility (eq. (6c)) to get α, β, γ as [34]:

$$2 - \alpha = (\tau - 1)/\sigma, \qquad \beta = (\tau - 2)/\sigma, \qquad -\gamma = (\tau - 3)/\sigma. \tag{17a}$$

Right at $p = p_c$, the sum in eq. (6d) defining the exponent δ arises mainly from cluster sizes s near $1/h$. Thus the nonanalytic part of $\Sigma_s s \cdot n_s(p_c) e^{-hs}$ varies as $h^{-1} h^{-1} h^\tau = h^{\tau-2}$, as appendix 1 again will show in detail; and we therefore have

$$1/\delta = \tau - 2. \tag{17b}$$

We may solve these four equations to get the cluster exponents as a function of the other exponents and to derive two relations between the latter exponents:

$$\tau = 2 + 1/\delta; \qquad \sigma = 1/\beta\delta = 1/(\gamma + \beta) \tag{18a}$$

$$2 - \alpha = \gamma + 2\beta = \beta(\delta + 1) [= d\nu]. \tag{18b}$$

The last relation, where the dimensionality d enters, will be derived later in eq. (37c). These famous scaling laws (18b) are known since many years, also for other phase transitions [10, 11, 30]. If we would not have gotten them, we would have to change our scaling assumption (15), not the scaling laws. Again eq. (18) comes as no surprise since the same relations were known from the Fisher model [34]; in fact their first derivation for thermal phase transitions by Essam and Fisher [31] used this cluster model.

In this sense we fulfilled our promise to use percolation as a simple introduction to scaling laws: By a plausible assumption (15) on the cluster numbers we could derive the desired relations between critical exponents, eq. (18). Of course, it is no great revelation that we found four relations between six exponents, when we made an assumption which contains only two exponents as free parameters.

Our assumption (15) is completely analogous to experience made with other phase transitions. That experience has shown: Any "singular" function g depending on two "critical" variables $g(x, y)$ can, for small x and y, be written in general in the form $g(x, y) = x^c \cdot G(y/x^b)$ with two free exponents b and c. Our scaling assumption (15) is merely a special case of this general "scaling homogeneity" assumption [100]. (It is not easy to write down an explicit expression for $g(x, y)$ which does not reduce

to that simple homogeneous form for small x and small y.) For our percolation clusters we simply identified x with $1/s$ and y with $p-p_c$, and gave special names to the two exponents to get $n_s = s^{-\tau}G((p-p_c)s^{\sigma})$ in agreement with eq. (15). Percolation clusters follow what can be learned from other phase transitions and have no intention to learn new tricks. For some readers that might make assumption (15) more likable since it now has the form: "Percolation clusters are lazy and invent no new ways to deal with critical phenomena". For the reader who is also lazy and does not want to read about equation of state or universality we recommend to go directly to tables 2 and 3 at the end of this subsection 3.1.

3.1.3. Dilute ferromagnets and ghost fields

The equation of state of the dilute low-temperature ferromagnets mentioned in section 1.1 can also be brought into the scaling-homogeneity form mentioned above as customary for critical phenomena. The mathematics is simplified if we look at the susceptibility $\chi \equiv \partial M/\partial H$ since then the singular part is identical with the leading divergence, and the analytic background does not disturb us. At thermal phase transitions one has $\chi \propto |T_c - T|^{-\gamma} X(h/|T_c - T|^{\beta\delta})$ with the abbreviation $h \equiv \mu H/k_B T$ for the reduced magnetic field. The scaling function X must be a symmetric function of its argument, leading to $\chi(-h) = \chi(h)$, since the behavior of a magnet is independent of the direction which we choose for the coordinate axes. For the dilute magnet, eq. (5), we find by differentiation, using $\mathrm{d}(\tanh y)/\mathrm{d}y = \cosh^{-2}(y)$ and $z = (p-p_c)s^{\sigma}$

$$\chi \cdot pk_B T/\mu = p \cdot \partial M/\partial h = \sum_s s^2 n_s(p) \cosh^{-2}(sh) \propto \int_0^{\infty} s^{2-\tau} f[(p-p_c)s^{\sigma}] \cosh^{-2}(sh)\, \mathrm{d}s$$

$$= \frac{1}{\sigma} |p-p_c|^{(\tau-3)/\sigma} \int |z|^{-1+(3-\tau)/\sigma} f(z) \cosh^{-2}(|z|^{1/\sigma} h/|p-p_c|^{1/\sigma})\, |\mathrm{d}z|$$

$$\propto |p-p_c|^{-\gamma} \int |z|^{\gamma-1} f(z) \cosh^{-2}(|z|^{\beta\delta} \cdot h/|p-p_c|^{\beta\delta})\, \mathrm{d}z \tag{19a}$$

with the z-integration running from 0 to $+\infty$ for $p > p_c$ and from 0 to $-\infty$ for $p < p_c$. Thus our susceptibility obeys the simple homogeneity form postulated above, but with $p - p_c$ replacing $T_c - T$:

$$\chi = |p-p_c|^{-\gamma} \cdot X(h/|p-p_c|^{\beta\sigma}). \tag{19b}$$

Eq. (19) gives an explicit scaling expression, in terms of a cluster scaling function f to be determined later, for the susceptibility; it has the full symmetry, homogeneity and analyticity properties required generally near critical points. For thermal phase transitions that problem is much more complicated; the simple Fisher model, for example, violates the symmetry requirement [34]. No explicit formulas have to our knowledge been proposed for critical phenomena in other cases, which do fulfill all these requirements. As promised, percolation is a particularly simple phase transition; it merely requires substitution of integration variables as mathematical tool so far.

For the magnetization M in eq. (5) and the free energy $F = -\int M\, \mathrm{d}H$ analogous scaling-homogeneous expressions can be derived from eq. (15). The same is true for the generating function or ghost-field free energy $[\Sigma_s n_s(p) \mathrm{e}^{-hs}]_{\mathrm{sing}}$ and similar expressions for the higher moments. In fact, the result

$$\left[\sum_s n_s\, \mathrm{e}^{-hs}\right]_{\mathrm{sing}} = |p-p_c|^{\beta\delta+\beta} \cdot \hat{F}(h/|p-p_c|^{\beta\delta}) \tag{20}$$

has been postulated by Essam and Gwilym [30] in the first scaling theory of percolation, long before cluster scaling was suggested [67]. Nakanishi and Stanley [23] recently confirmed that assumption numerically by Monte Carlo computer simulations. It is rather obvious that a scaling assumption (15) with two free exponents for the cluster numbers n_s leads to a two-exponent scaling expression for the moments or generating functions, as in eq. (20). But the reverse is not true, see appendix 1: One can invent expressions for the cluster numbers n_s with three free exponents, which lead to only two free exponents in the scaling expression for these sums over cluster numbers. Thus the assumption (20) of Essam and Gwilym [30] is a consequence of our assumption (15) but is not equivalent to it; and more data than those of Nakanishi and Stanley [23] are needed to confirm eq. (15).

Therefore eq. (15) has to be tested directly since scaling laws alone do not prove it. In fact, also alternatives to eq. (15) have been proposed which do not employ just two free exponents but more or less. In the first scaling theory for cluster numbers $n_s(p)$, Domb [101] suggested to take $\sigma = \frac{1}{2}$ and to use only one free exponent τ. And later Leath [73] made an assumption which corresponds in many applications to a scaling ansatz with three free exponents τ, ϕ, ψ. But later work [54, 71, 83, 102] showed $\sigma < \frac{1}{2}$ and $\phi = \psi$, leaving us again with two free exponents. Very recently Kunz and Payandeh [79] showed how renormalization group makes assumption (15) plausible. Thus at the time of this writing eq. (15) seems to be the only viable scaling assumption still floating around, and we concentrate on that assumption when we present numerical tests in subsection 3.2.

3.1.4. The universality concept

The "universality" concept [11, 103] for thermal critical phenomena is a semi-empirical classification of different systems into few universality classes. It asserts that critical exponents and other qualitative properties like the shape of the scaling functions are independent of details like range of interaction or structure of the lattice. Only the dimension is important enough to change exponents. A precursor of this universality assumption is the law of corresponding states for fluids. Universality in this naive sense turns out to be valid in most but not all cases. Thus for the majority of thermal phase transitions one can predict rather reliably which different systems belong to the same universality class. Then one can predict critical exponents without having to solve in detail the critical behavior of these systems. This universality concept thus saves a lot of work if one can trust it; roughly speaking all three-dimensional systems then have the same exponents, etc.

For percolation, we postulate similarly [50] that exponents and the shape of the scaling function $f(z)$ in eq. (15) do not change if we change "minor" details like the lattice structure; only the dimensionality is important since, after all, it appears explicitely in the scaling laws (18). More quantitatively we may generalize the scaling assumption (15) for one lattice, $n_s \propto s^{-\tau} f[(p - p_c)s^{\sigma}]$, to a universality assumption for all lattices of the same dimensionality d [103] by introducing lattice-dependent scale factors q_0 and q_1 besides the lattice-independent exponents σ and τ. Also we denote a lattice-independent scaling function by f_u where u stands for universal, and require

$$n_s = q_0 s^{-\tau} f_u[(q_1(p - p_c)s^{\sigma}]; \qquad f_u(0) = 1. \tag{21}$$

This universality assumption (21) means that for a given p the shape of the size distribution n_s is the same for different lattices of the same dimensionality d; only the two scales for the n_s-axis and the s-axis are different. For example, if in the triangular lattice for large clusters the maximum value of $n_s(p)$ (as a function of p, at fixed s) is five times larger than $n_s(p_c)$, then also in the square lattice the maximum is five times higher than the critical value for the cluster numbers. But for three dimensions this ratio can be lower. Similarly, if one calculates the ratio of "susceptibilities" $\Sigma_s s^2 n_s(p <$

$p_c)/\Sigma_s s^2 n_s(p > p_c)$ for equal distances $|p - p_c|$ from the critical point, then *scaling* requires the ratio to be independent of $p - p_c$ for one lattice structure, and *universality* requires it to be the same for different lattices of the same dimensionality d. (How this ratio depends on d is not yet known in general [26].) More quantitatively, the ratio can be expressed by integrals involving only the universal f_u, where the lattice dependent factors q_0 and q_1 have cancelled out:

$$\sum_s s^2 n_s(p < p_c) \Big/ \sum_s s^2 n_s(p > p_c) = \int_0^\infty y^{\gamma-1} f_u(-y)\,dy \Big/ \int_0^\infty y^{\gamma-1} f_u(+y)\,dy$$

with $y = q_1(p - p_c)s^\sigma$, as can be checked easily with the methods used already in eq. (19). (One may also postulate relations between the coherence length ξ and the "free energy" $\Sigma_s n_s$ analogous to thermal phase transitions [104]; but little is known on that subject, which would be anyhow outside the scope of the present review.)

Marro [105] made several numerical tests involving similar ratios and found them indeed universal as desired. The critical exponents are universal, within small error bars, in two and three dimensions when various lattices are compared [54]. With larger error bars, exponents seem unchanged [24] if clusters in percolation are defined not just as nearest-neighbor connected groups but if also longer distances were allowed to connect the sites; but from now on we will again deal only with nearest-neighbor connected clusters. For the cluster size distributions, the universality assumption (21) was confirmed quite directly in both two and three dimensions for selected lattices [26, 71]. Thus it seems legitimate to regard critical exponents as a function of dimensionality d; our table 2, following Stanley [106] and more recent sources [107–110, 7, 26, 60, 71, 93], compiles averaged numerical estimates for many exponents as a function of dimensionality d.

We see that the scaling laws (18) are confirmed reasonably well in two and three dimensions, just as they are known to be valid in thermal problems. In the three-dimensional Ising magnet near its Curie temperature, there is a problem with the latest scaling law $d\nu = 2 - \alpha$; but according to ref. [111] the two error bars overlap. Similarly for two-dimensional percolation the estimate $2 - \alpha = 2.668 \pm 0.004$ of

Table 2

Numerical estimates of directly determined critical exponents. If one believes in scaling laws, eq. (18), one can fill in the empty spaces. The exponents θ and μ for animals and conductivity are defined later, eqs. (27–49). Our values are averages over different methods, if available; the error bar is seldomly more than one unit of the last decimal. Perhaps $\nu(d = 2) = 1.355$ is exact, eq. (9). References are given in Stanley's table [106]; see also refs. [7, 17, 60, 107]. Data for the exponents θ, μ, σ and τ from refs. [26, 71, 93, 108, 109]. One-dimensional percolation is discussed in appendix 1. Infinite dimensionality corresponds to "classical" results [27–30, 114, 149], they are expected to be valid already above six dimensions.

d	α	β	γ	δ	ν	σ	τ	θ	μ
1	1	0	1	∞	1	1	2	0	–
2	-0.6_7	0.14	2.43	18	1.3_5	0.39	2.0	1.00	1.2
3		0.4	1.7	5	0.8_4	0.4_5	2.1_5	1.5	1.7
4		0.5	1.5	$3._3$	0.7			1.9	2.4
5		0.7	1.2	$2._5$	0.6			2.2	2.7
6		1.0	1.0_6	2	0.5			2.4	3.0
7			1.0	2				2.4	
∞	-1	1	1	2	$\frac{1}{2}$	$\frac{1}{2}$	$\frac{5}{2}$	$\frac{5}{2}$	3

ref. [56] disagrees with $d\nu$ if $\nu = 1.355$ is exact, eq. (9). The estimate for $2-\alpha$ also does not agree well with other series estimates [107, 110] $\gamma = 2.425 \pm 0.005$ and $\beta = 0.139 \pm 0.003$ and the scaling law $2-\alpha = \gamma + 2\beta$. In the other cases no such problems occur at present.

One very important non-universal parameter, which moreover is not predicted by any of the above scaling theories, is the position p_c of the critical point. Scaling and universality tell us something about what is happening near p_c but tell us nothing about where p_c is. Table 3 lists numerical estimates and exact results for various lattices and various dimensions; no reliable connection exists at present between p_c and the critical exponents. In the triangular "site" percolation problem and the square "bond" percolation problem we have $p_c = \frac{1}{2}$, presumably exactly [24]; moreover $p_c = 2 \cdot \sin(\pi/18) = 0.34729$ for triangular bond percolation and $p_c = 1 - 2 \cdot \sin(\pi/18) = 0.65271$ for bond percolation in the honeycomb lattice. Clearly universality cannot assert that p_c is the same for all lattices.

Returning to the universal (?) exponents, we unfortunately have to mention the results of Klein et al. [112] that in one dimension the percolation exponents depend on the range of interaction, in contrast to higher dimensions [24]. This clear violation of law and order is discussed in detail in appendix 2; clearly the naive universality picture as suggested here is not valid in all cases. The special status of one-dimensional percolation is also evident from table 2, where $d = 1$ does not seem to follow for some exponents the trends evident from $d = 2, 3, \cdots$ [133] even when only nearest-neighbor connections are used. On the other hand the behavior for larger dimensionalities is rather smooth and agrees quite well with the epsilon expansion, eq. (10), even though only the first two terms of an expansion in $\epsilon \equiv 6 - d$ are used. This agreement is seen clearer in fig. 5 where β and γ are plotted for one to seven dimensions.

We conclude from the information presented here that the scaling laws for the critical exponents like β are confirmed rather well, that these scaling laws can be explained by a simple assumption on

Table 3
Numerical estimates (three digits) and (presumably) exact results (four digits) for the percolation threshold p_c. TR = triangular, SQ = square, HC = honeycomb, D = diamond, SC = simple cubic, BCC = body-centered cubic, FCC = face-centered cubic. Results for higher dimensions refer to hypercubic lattices. From refs. [7, 26, 44, 45, 54, 55, 60, 107].

Lattice	site	bond
HC	0.698	0.6527
SQ	0.593	0.5000
TR	0.5000	0.3473
D	0.428	0.388
SC	0.311	0.249
BCC	0.245	0.178_5
FCC	0.198	0.199
$d = 4$	0.197	0.161
$d = 5$	0.141	0.118
$d = 6$	0.108	0.094
$d = 7$	0.089	0.078
$d \to \infty$	$p_c = 1/(2d-1)$	

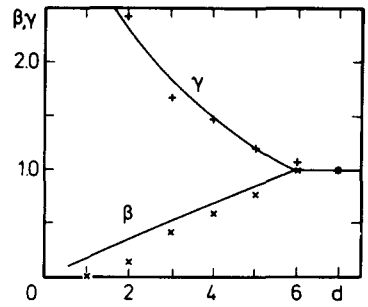

Fig. 5. Plot of the two independent exponents β and γ as a function of dimension d. The curves represent eq. (10), the epsilon expansion. Data for γ are directly from table 2; data for β also employ the scaling laws $\beta = \gamma/(\delta - 1) = \frac{1}{2}(d\nu - \gamma)$ and represent average estimates: $\beta = 0.41, 0.58, 0.76, 1.00$ in 3, 4, 5, 6 dimensions. In two dimensions, $\beta = 0.139 \pm 0.003$ [110].

the cluster numbers, and that we have to test this scaling assumption directly. This is done in the following subsection.

3.2. *Tests of scaling*

Only for two and three dimensions are cluster statistics known to us which have been analyzed in terms of scaling, eq. (15); the polynomials in refs. [45, 107] are still waiting for a "lover" to study n_s for general d. And Monte Carlo work in more than three dimensions has not yet been done on n_s. (In 5.99 dimensions, epsilon expansion results of Stephen [114] were consistent with eq. (15).) We restrict ourselves here mainly to recent Monte Carlo work of high accuracy by Stoll and Domb [62, 115], Leath and Reich [71, 72] and Hoshen et al. [26], each based on many millions of Monte Carlo step for each concentration. We mentioned already before that the Monte Carlo work of Nakanishi and Stanley [23] for the "equation of state" gives an indirect confirmation of the cluster scaling assumption (15).

The various regions to be investigated can be seen rather elementary if we look at the number $n_2(p)$ of pairs in the square lattice: Each pair consists of two occupied sites surrounded by six empty neighbors, and it can be oriented either horizontally or vertically. Thus we have $n_2 = 2p^2(1-p)^6$ exactly. This function has a maximum at $p = 0.25$, far below $p_c = 0.593$; for larger clusters the position of the maximum shifts closer to p_c, and the peak becomes more narrow. Thus generally we may look at what happens at p_c, above p_c, near the maximum below p_c, and asymptotically in the wings relatively far away from the maximum where n_s becomes extremely small. The latter questions will also be discussed outside the scaling region, i.e. with p not very close to p_c.

3.2.1. *At the percolation threshold*

Right at p_c the scaling assumption (15) asserts $n_s \propto s^{-\tau}$. We need $\tau > 2$ since the total number of occupied sites, $\Sigma_s s \cdot n_s = p_c$ from eq. (4), must remain finite even at the percolation threshold. Figure 3 in the introduction already showed two-dimensional results, right at the exact $p_c = \frac{1}{2}$ of the triangular lattice, giving such a simple power law. An analogous plot for three dimensions is given in fig. 6. These two computer simulations used the largest lattice known to us for Monte Carlo work, 4000×4000 sites in two and $400 \times 400 \times 400$ in three dimensions. The solid line in figs. 3 and 6 is not the best fit on the Monte Carlo data but the prediction from series expansions, $n_s \propto s^{-2-1/\delta}$, with both the exponent and the proportionality factor calculated from refs. [19, 55]. (If $n_s(p_c)$ varies as $s^{-\tau}$ for large s,

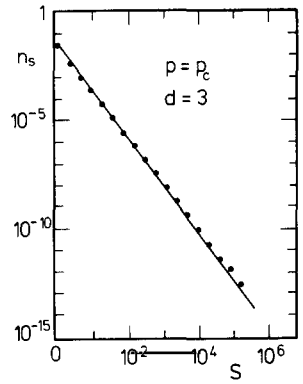

Fig. 6. Monte Carlo cluster numbers [26] at $p = p_c = 0.311$ in the simple cubic lattice, together with the series prediction [55].

then the relation $\tau = 2 + 1/\delta$ is exact and does not require the validity of eq. (15). Thus figs. 3 and 6 constitute only a weak test of the specific scaling assumption used here.) The agreement of Monte Carlo and series results is excellent on the scale of figs. 3 and 6.

Closer inspection, however, shows problems: The best fit for τ from large s in figs. 3 and 6 is $\tau(d = 2) = 2.02$ and $\tau(d = 3) = 2.13_5$, significantly lower than the series predictions [19, 55] $\tau = 2.055 \pm 0.002$ and 2.2 ± 0.03, respectively. (Monte Carlo data in ref. [71] give $\tau = 1.97 \pm 0.05$ in the triangular lattice at p_c, but $\tau = 2.05 \pm 0.02$ from scaling and all p.) There are two reasons [26] for these deviations, which we will discuss now: Neither the cluster size nor the lattice size are large enough for the asymptotic scaling behavior to be exact in the computer experiment; the true exponents should show up only for $s \to \infty$ in an extremely large lattice. Present computer technology unfortunately does not allow an infinite number of operations with an infinite computer memory during a finite time at small costs; thus Monte Carlo studies are always experiments with both systematic and statistical errors.

More precisely, already for the exact cluster numbers n_s for small s from series expansions [46] one can see that at p_c the measured n_s were below the extrapolated cluster numbers represented by the solid lines in figs. 3 and 6. If we assume $\tau \simeq 2.05$, as required in two dimensions, then a much better fit over nearly the whole range of s was obtained [26] for the triangular lattice by

$$n_s = 0.03\, s^{-2.05}(1 - 1.2\, s^{-2/3}) \tag{22}$$

where a first correction term to the simple asymptotic power law is used. This correction-to-scaling exponent 2/3 from Monte Carlo data agrees roughly with the analogous exponent 3/4 found for basically the same quantity from series expansions [19] and is consistent with the order-of-magnitude estimated [87] from the epsilon expansion [87]. If eq. (22) is correct, then the apparent slope $\tau_s \equiv -\mathrm{d}(\log n_s)/\mathrm{d}(\log s)$ in a log–log plot as in figs. 3 and 6 deviates from the true (asymptotic) slope τ as $\tau_s = \tau - 2.2 \cdot \frac{2}{3} \cdot s^{-2/3}$, and this deviation is, for $s \sim 10^2$, about as large as the difference between the Monte Carlo and the series value for τ. Quite generally, it is difficult to get from Monte Carlo method reliable values for the second decimal after the point in a critical exponent; and series extrapolations usually give more accurate exponents.

The influence of the finite lattice size can already be observed for very small clusters. E.g. in ref. [26] for isolated sites ($s = 1$) the actually observed cluster numbers in the Monte Carlo experiment were found to be larger by about 0.35 percent than the exact cluster numbers for infinite lattices. This

deviation increases with increasing cluster size s and is responsible for the deviations observed in fig. 3 for large s: the boundaries of the system break up some very large clusters into smaller clusters and isolated sites. The use of periodic boundary conditions (section 2.2.1) reduces these "finite size" effects [69, 62, 115]; in ref. [26] periodic boundary conditions made the numbers of small clusters agree within statistical errors with the exact results and shifted the fitted exponent τ upwards to 2.16, closer to the series prediction 2.2, inspite of the fact that the system used was smaller than the one used for fig. 6. (In Leath's method [71–73] there is no disturbing influence from the boundaries.) Thus we took $\tau = 2.15$ as the direct Monte Carlo estimate in table 2, although the true value is presumably slightly higher. Clearly a direct evaluation of $\tau = 2 + 1/\delta$ from Monte Carlo cluster numbers at p_c is not a very accurate way to determine the exponent δ; and series methods [19, 55] work better here. We now turn to the region $p \neq p_c$ where series methods gave only rather crude extrapolations [51] for the cluster numbers and their scaling function; here Monte Carlo methods can be more reliable than series extrapolations. (Also, in the following discussion we are satisfied with an accuracy of about 10 percent; all the above problems concern only the fine details of the second decimal.)

3.2.2. Above the percolation threshold

The cluster numbers above p_c decay monotonically with size. Figure 7 shows logarithmically the variation of the Monte Carlo ratio $v_s(p) = n_s(p)/n_s(p_c)$ with the scaling variable $z = (p - p_c)s^\sigma$ in the triangular lattice. Here the exponent σ was taken from the above results as $\sigma = 1/(\gamma + \beta) = 0.39$ [54]. If assumption (15) is correct then the values for different $p - p_c$ should all follow the same curve since z is used as a variable here. This is the basic result of scaling: By multiplying the original variables $p - p_c$ and n_s with suitable powers of s, or by similar rescaling of the axes, the original data are shifted such that different data (e.g. for different s) follow the same curve. We see that in fig. 7 different symbols, representing different $p - p_c$ in this case, follow the same curve within the "experimental" scattering. This figure thus confirms our basic assumption (15) for the cluster numbers. The curve through the points in fig. 7 is the extrapolation from series results [51] and agrees remarkably well with the Monte Carlo data. For three dimensions, similar confirmation of scaling by Monte Carlo results was obtained, too [26].

The tangent to the origin in fig. 7 arises from additional more accurate cluster numbers obtained very close to p_c. Taken together, fig. 7 shows convincingly that the data do not follow a straight line;

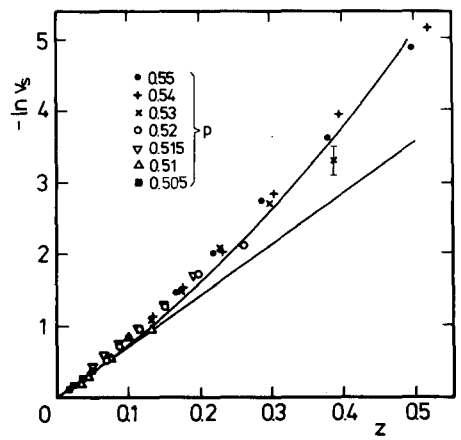

Fig. 7. Scaling plot above p_c. Variation with $z = (p - p_c)s^\sigma$ of the ratio $v_s = n_s(p)/n_s(p_c)$ on a logarithmic scale. Assumption (15) requires different symbols to follow the same curve. Monte Carlo data from 4000 × 4000 lattice. From Hoshen et al. [26].

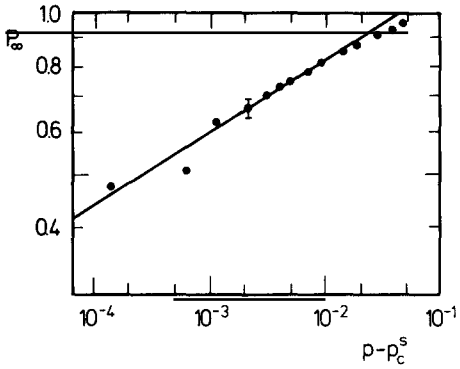

Fig. 8. Variation with p of the fraction P_∞ of occupied sites belonging to the "infinite" network in a 4000×4000 triangular lattice. p_c^s is shifted from p_c to $p_c + 0.00085$ to offset some of the boundary effects in the Monte Carlo calculation. From ref. [26].

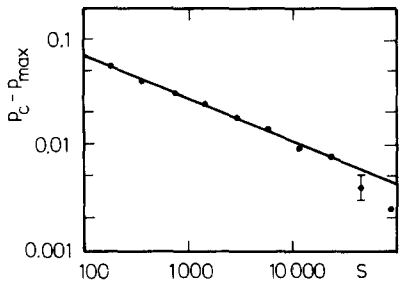

Fig. 9. Variation of p_{max} with cluster size s in the triangular lattice [26]. The cluster number $n_s(p)$ reaches at fixed s a maximum at $p = p_{max}$ below p_c. The fitted line has slope -0.40 in this log–log plot; scaling, eq. (15), requires the slope to be -0.39. Data for very large s are unreliable because of the finite size of the 4000×4000 triangular lattice.

the upward curvature proves that $\log v_s$ is not simply proportional to $-z = -(p - p_c)s^\sigma$. Therefore the simple Fisher droplet model above p_c, with $n_s \propto s^{-\tau} e^{-z \cdot \text{const}}$, is not exact since it would give a straight line in fig. 7. Instead, a straight line is obtained rather well [26, 62, 115] if the data for v_s are plotted against $z^{1/2\sigma}$ instead of z. Thus for not too small z we find $n_s \propto s^{-\tau} \exp(-\text{const} \cdot \sqrt{s})$ in two dimensions, for the triangular and square lattices [26, 62, 115] even when some correlations between occupied sites are taken into account [115] (see section 6.2.3).

If we define a decay exponent [70] $\zeta = \zeta(p)$ through

$$\log n_s \propto -s^\zeta \qquad (s \to \infty \text{ at fixed } p) \tag{23}$$

then these data suggest $\zeta \simeq \frac{1}{2}$ in two dimensions. Thus the scaling function $f(z)$ in eq. (15) seems to decay as $\log f \propto -z^{1/2\sigma}$ already for rather small z values above 0.1, and not merely for $z \gg 1$. Therefore the simple formula $n_s \propto s^{-\tau} \exp(-\text{const} \cdot \sqrt{s})$ fits most data quite accurately above the percolation threshold; according to assumption (15) this constant in the exponent vanishes as $(p - p_c)^{\beta\delta/2}$ at the threshold [115].

The percolation probability $P_\infty \propto (p - p_c)^\beta$ is particularly difficult to measure by Monte Carlo experiment, since in two dimensions $\beta = 0.14$ [110] is so small. In a finite lattice with free boundaries one may approximate P_∞ by the fraction of occupied sites belonging to the largest cluster; usually in a Monte Carlo experiment slightly above p_c the largest cluster is clearly larger than all the other clusters. The P_∞ determined in this way [26] obeys with surprising accuracy the desired power law; the slope of the line fitted in fig. 8 through the data is 0.133, very close to the series prediction of $\beta = 0.139 \pm 0.003$ [110]. Also the proportionality factor agrees well with the series prediction [26, 54]. In three dimensions the exponent for the percolation probability is $\beta \simeq 0.4$ [7, 60, 110].

Overall, above p_c no contradictions were observed between different Monte Carlo simulations, series extrapolations, and scaling assumptions; moreover we can fit the data with $\log v_s \propto -\sqrt{s}$, i.e. with $\zeta = \frac{1}{2}$ over most of the range for $d = 2$.

3.2.3. Below the percolation threshold

Below p_c the cluster numbers $n_s(p)$ as a function of p at fixed s show a maximum at $p = p_{max}$, as we discussed before in the simple case of $n_s = 2p^2(1-p)^6$, $p_{max} = 1/4$. If assumption (15) is correct,

this maximum corresponds to a maximum in the scaling function $f(z)$ at some negative argument $z = z_{max} = (p_{max} - p_c)s^\sigma$. (This quantity z_{max} is fixed for a given lattice, but depends on the lattice type.) Fig. 9 shows [26] how p_{max} approaches p_c for large cluster sizes: $p_{max} - p_c \propto -s^\sigma$, with an exponent $\sigma \simeq 0.40$ fitted on these data. Another scaling test [26] uses $d(n_s)/dp$ and gives $\sigma \simeq 0.38$. Leath and Reich [71], also from Monte Carlo studies, conclude $\sigma = 0.394 \pm 0.003$ for triangular and square lattice. Thus our table 2 gives $\sigma = 0.39$ as the directly determined cluster exponent. This value happens to agree with $\sigma = 1/(\gamma + \beta) = 0.390 \pm 0.001$ as predicted by scaling theory and the latest series estimates for γ [107] and β [110]. In three dimensions [26] direct Monte Carlo determinations of σ were less successful; values between 0.4 and 0.5 agreed with the data, leading to our estimate 0.45 in table 2; the scaling prediction is $\sigma \simeq 0.48$ from series expansions [54, 110].

Figure 10 shows that the scaling assumption is confirmed by two-dimensional Monte Carlo data [26, 72]: As required by eq. (15), different symbols representing different $p - p_c$ follow the same curve, just as they did in fig. 7. The short curve near the origin symbolizes numerous additional data [26] measured there for smaller values of the scaling variable z; they also agree with scaling, eq. (15). Again these data roughly agree with extrapolations [51] from series expansions.

Figure 10 gives a maximum of $v_s(p) = f(z)$ at $z = z_{max} = -0.41 \pm 0.03$, with a height $f_{max} = f(z_{max}) = 4.9$; universality asserts this f_{max} to be the same for all two-dimensional lattices. If the scaling assumption (15) is correct then this maximum in $n_s(p)$ or $v_s(p)$ as a function of p for fixed s must correspond to a maximum in $v_s(p)$ or $s^\tau n_s(p)$ as a function of s at fixed p below p_c, since $v_s(p)$ equals $f[(p - p_c)s^\sigma]$. The position of this maximum $s_{max}(p)$ is at $s_{max} = (z_{max}/(p - p_c))^{1/\sigma}$. Indeed, the insert in fig. 10 shows this maximum quite clearly, using data of Reich and Leath [72] for the triangular lattice. Similarly for the square lattice Stoll and Domb [115] also find such a maximum in v_s versus s, compatible with $z_{max} \simeq -0.4$. The height of the maximum, i.e. the value of f_{max}, found from the data of Reich and Leath [72] is compatible with the above estimate of about 4.9, as indicated by the error bars in the insert of fig. 10. Stoll and Domb [115] quote $f_{max} = 5.4$ taken from their data farther away from p_c. An earlier extrapolation of series results [50] gave $f_{max} = 4.5$ for triangular, square, and honeycomb lattices. Thus we conclude

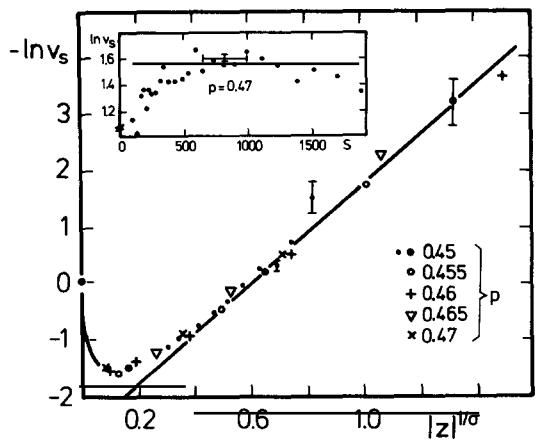

Fig. 10. Variation with $|z|^{1/\sigma} = (p_c - p)^{\beta\delta} \cdot s$ of the ratio $v_s(p)$ below p_c, analogous to fig. 7 above p_c, in the triangular lattice [26]. Scaling requires different symbols to follow the same curve. The small dots for $p = 0.45$ are from Reich and Leath [72]. The insert shows the variation of $v_s(p)$ with s at fixed p, with data from ref. [72], giving a maximum roughly where predicted by scaling [26] and fig. 9. (See also ref. [115].)

$$f_{max} \simeq 5 \qquad (d = 2)$$

as the combined estimate in two dimensions.

Leath and Reich [71] investigated scaling theory by Monte Carlo simulations of the triangular and square lattice and found eq. (15) to be valid for clusters containing more than 85 sites. For smaller clusters systematic deviations were observed which are larger than but in the same order-of-magnitude as those given here in eq. (22). It would be interesting to see in future research whether these deviations also follow a scaling form [116] like $v_s(p) = f(z) \cdot (1 + s^{-0.7} f_1(z) + \cdots)$ as a generalization of eq. (22). But such an analysis would require very accurate Monte Carlo data. (Refs. [71, 73] also determined the cluster perimeter distribution which in turn was used to get more information on cluster numbers. We refer to section 4.1 and ref. [71] for details.)

For large values of the scaling variable $z = (p - p_c)s^{\sigma}$ the cluster numbers decay rapidly with increasing $-z$; this wing on the left side of the maximum determines the exponent ζ of eq. (23). The straight line fitted in fig. 10 through the data suggests $\log v_s \propto -(-z)^{1/\sigma} = -(p_c - p)^{\beta\delta} s \propto -s$. Thus the exponent ζ is about unity below p_c and therefore different from its value $\frac{1}{2}$ in two dimensions above p_c. (The first indication of such an asymmetry came from Bakri [70].) Similarly, Müller-Krumbhaar and Stoll [37] concluded $\zeta = 1.1 \pm 0.1$ in the square lattice at $p = 0.50$, rather far below $p_c = 0.593$. Leath and Reich [71] found that the choice $\zeta = 1$ fits their Monte Carlo data better than the choice $\zeta = 2\sigma = 0.8$. And most recently, Kinzel [80] found $\zeta \simeq 1$ over sixty decades in n_s, using real space renormalization in the triangular lattice. Thus for sufficiently large values of $|z|$ we have in two dimensions rather reliably established for p below p_c:

$$\zeta(p > p_c) = \tfrac{1}{2}, \qquad \zeta(p < p_c) = 1. \tag{24}$$

When we combine data for the cluster numbers above, at and below p_c in one plot [26, 51] they follow roughly a Gaussian curve, as first suggested by Leath [73]:

$$v_s(p) = f(z) \propto \exp[-\text{const}(z - z_{max})^2]. \tag{25}$$

Of course, eqs. (24) and (25) contradict each other since eq. (25) gives $\zeta = 2\sigma \simeq 0.8$, violating the exact inequality $\zeta \leqslant 1 - 1/d$ of Kunz and Souillard [90] above p_c, eq. (11b). Thus the Gaussian fit is a reasonable approximation but not an exact solution for the scaling function $f(z)$. It may replace the Fisher model, $f(z) = \exp(-\text{const} \cdot z)$ above p_c, as a simple numerical approximation. Just as the Fisher model it does not work asymptotically for large z, but in contrast to the Fisher model it can be used on both sides of the phase transition.

In three dimensions, Monte Carlo data [26] for the simple cubic and the body centered cubic lattices [26] could be fitted well by a Gaussian approximation as in eq. (25), with $z_{max}/p_c = -0.8$. An example is shown in fig. 11, where again data for different $p - p_c$ follow the same curve since v_s is plotted logarithmically against z; thus the scaling assumption (15) again is confirmed. The solid line there is the parabola corresponding to the Gaussian approximation (25) and fits very well; ref. [26] does not determine the asymptotic decay exponent ζ. The maximum value of the scaling function was found to be [26]

$$f_{max} \simeq 1.6 \qquad (d = 3)$$

in these two lattices. In one dimension we will see in appendix 2 that $f_{max} = \infty$. For infinite dimensionality we expect the Bethe lattice solution $f_{max} = 1$ [30] to be valid [45, 84, 107, 114, 117]. Thus the above estimates $f_{max}(d = 2) = 5$ and $f_{max}(d = 3) = 1.6$ fit nicely into the general trend as a

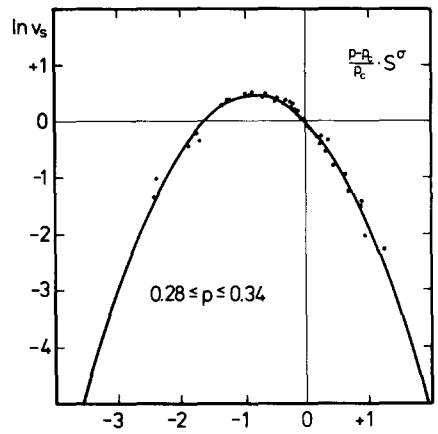

Fig. 11. Scaling plot in three dimensions on a simple cubic $100 \times 100 \times 100$ lattice. Data for different p follow the same curve, as required by eq. (15). The parabola follows eq. (25). From ref. [26].

function of dimensionality. It is not clear what to expect for f_{max} and more generally for the shape of the scaling function $f(z)$ for finite dimensionalities above six.

Universality for the cluster size distribution has also been tested in two [71] and three [26] dimensions. By adjusting the two lattice-dependent parameters q_0 and q_1 in eq. (21a) Leath and Reich [71] could confirm excellently the similarity of triangular and square lattices with respect to cluster numbers, for s above 85. And in three dimensions [26], bcc and sc lattice also seem to have the same shape of the scaling function f, as required by universality. Moreover, by using $(p - p_c)/p_c$ instead of $p - p_c$ in the definition of the scaling variable z, the two lattices even could be described [26] by the same parameter q_1, a particularly simple form of universality (also perhaps not exact).

In conclusion, scaling for the cluster numbers $n_s(p)$, eq. (15), seems to be confirmed well for sufficiently large clusters close to p_c in two and three dimensions. In two dimensions, different work by different authors using Monte Carlo and series techniques gives consistent results; deviations seldomly amount to more than ten percent. A comparison of two lattices in two and three dimensions confirmed well the universality concept. Very little is published on cluster numbers for more than three dimensions [45].

3.2.4. *Decay far away from p_c*

In eqs. (23, 24) we noticed already that for $p \neq p_c$ the cluster numbers decay exponentially for large s, with $\log n_s \propto -s^{1/2}$ above p_c and $\propto -s$ below p_c. That conclusion was based on Monte Carlo data with concentrations between $p_c - 0.05$ and $p_c + 0.05$ rather close to the critical point. Away from the critical point, the inequalities of section 2.4 give for this decay exponent: $\zeta(p \to 0) = 1$ and $\zeta(p \to 1) = 1 - 1/d$ in d dimensions [90]. How is the situation for intermediate concentrations, say at $p = \frac{1}{2}p_c$. And what about three dimensions?

Monte Carlo methods for the cluster numbers do not work well far away from p_c for large s since only close to p_c many large clusters appear. But since the typical cluster size $s_\xi \propto |p - p_c|^{-1/\sigma}$ is very large only close to p_c, we now perhaps are no longer forced to go to very large values of s to see the asymptotic behavior. Thus the exact cluster numbers of Sykes et al. [42, 44] can be used for an analysis. Far above p_c [46, 49, 50] the series data show, similarly to the Monte Carlo results of section 3.2.2, that a simple power law is quite good: $\log v_s \propto s^{1-1/d}$ fits for $d = 2$ and 3 dimensions the cluster

numbers from $s = 1$ to $s = s_{max} \sim 10$ within a factor 10 or better, even if the cluster numbers vary over twenty order-of-magnitude [49]. This result may have implications for nucleation theory [38, 118] if that experience can be generalized to thermal phase transitions. It means that in the cluster numbers n_s a "surface term" $\propto s^{1-1/d}$ can be extrapolated down to very small s, even pairs and single sites, without giving a wrong order-of-magnitude for n_s. One only has to fit the "microscopic surface tension", i.e. the factor in front of $s^{1-1/d}$ in $\log n_s$, on the true cluster numbers in the size range to be investigated [49, 118, 119]. Thus above p_c the result $\zeta = 1 - 1/d$ is established not only by the Kunz–Souillard theorem [90], eq. (11), but also by numerical data for rather small clusters in two and three dimensions [46, 49, 50] and for larger clusters in two dimensions [26, 62, 115].

Similarly below p_c, series data for p sufficiently far below p_c give $\log v_s \propto -s$ for not too small clusters, i.e. $\zeta = 1$ [46, 50, 70]. Since rigorous or reliable inequalities, section 2.4, cover the range from $p = 0$ to $p = p_\lambda$ with their prediction $\zeta = 1$, and since p_λ is rather close to p_c (e.g. $p_\lambda = 0.41$ in the triangular lattice where $p_c = \frac{1}{2}$) these older data were obtained in a region where later inequalities confirmed their result $\zeta = 1$ more reliably. But they show in addition that the asymptotic behavior can already be observed for cluster containing only ten sites.

Summarizing the information reviewed here on the asymptotic decay of cluster numbers we found from a variety of different methods that most probably

$$\zeta(0 < p < p_c) = 1 \text{ and } \zeta(p_c < p < 1) = 1 - 1/d. \tag{26}$$

(Right at p_c the clusters decay no longer exponentially but with a power law: $n_s \propto s^{-\tau}$.) This result for random percolation, eq. (26), agrees entirely with Binder's suggestion for (appropriately defined) clusters at thermal phase transitions [36, 120]. It is therefore a sign of hope that Stoll and Domb [115] observed similar behavior above p_c for correlated percolation, section 6.2.3 in two dimensions. Perhaps some better understanding of clustering for thermal phase transitions [25, 36, 155] at least in two dimensions is waiting in the near future.

These results for the decay exponent ζ have some implications which in the cluster literature are discussed under the heading "essential singularities" [34, 36, 121, 122]. If we look at the generating function or "free energy" $F(h) = \Sigma_s n_s e^{-hs}$, we may ask if $F(h)$ is analytic in h at $h = 0^+$. Or more precisely: Does a Taylor expansion of $F(h)$ work with $F(h) = \Sigma_k F_k h^k/k!$ for small positive fields h? (Here F_k is the kth derivative $d^k F/dh^k$ at $h = 0$.) Obviously all field derivatives F_k are finite for all $p \neq p_c$ since they are given by the moments $\Sigma_s s^k n_s$ and since the n_s decay exponentially according to eq. (26). But what is the radius R_{conv} of convergence for this Taylor series? If it is finite then $F(h)$ is analytic; but if $R_{conv} = 0$ we call this situation an essential singularity, similar to what happens with the function $F(h) = \exp(-1/h^2)$ at $h = 0$.

The general ratio criterion for power series gives R_{conv} as the limiting ratio of $|F_k/k!|/|F_{k+1}/(k+1)!|$. Thus in our case we have $R_{conv} = \lim_{k\to\infty}[\Sigma_s s^k n_s/\Sigma_s s^{k+1} n_s] \times (k+1)$. Evaluation of these moments for large k is easy [70] since then only very large cluster sizes s are relevant, where we may use the asymptotic form $\log n_s \propto -s^\zeta$. Thus we find $\Sigma_s s^k n_s \propto \int s^k \exp(-\text{const} \cdot s^\zeta)\, ds$, where all p-dependent factors are hidden in the constants. The maximum of $\log[s^k \exp(\ldots)]$ is located at $s = [k/(\zeta \cdot \text{const})]^{1/\zeta} \propto k^{1/\zeta}$; the value of $s^k \exp(\ldots)$ at this maximum is roughly $s^k \propto k^{k/\zeta}$ since the exponential term is then negligible. (Proof: $\log[s^k \exp(\ldots)] = k \cdot \ln(s) - \text{const} \cdot s^\zeta = k \cdot \ln(s) - k/\zeta \simeq \ln(s^k)$. The reader who mistrusts these tricks may evaluate the integrals by gamma functions.) Thus the kth moment $\Sigma_s s^k n_s$ varies for $k \to \infty$ as $k^{k/\zeta}$: The smaller the exponent ζ is the stronger is the increase of the higher derivatives with the order of the derivative. Thus R_{conv} equals the limit (for large k) of $(k+1)k^{k/\zeta}/(k+1)^{(k+1)/\zeta} = (k+1)^{1-1/\zeta}(1+1/k)^{-k/\zeta} \simeq (k+1)^{1-1/\zeta} e^{-1/\zeta} \propto k^{1-1/\zeta} (= 1/k^{1/(d-1)}$ for

$\zeta = 1 - 1/d$); thus [70]

$$R_{\text{conv}} = \lim_{k\to\infty} k^{1-1/\zeta}.$$

Thus below the percolation threshold, where $\zeta = 1$, the radius of convergence is finite. But above and at p_c where $\zeta < 1$ for all finite dimensionalities, the Taylor series has zero radius of convergence. This somewhat unusual behavior is called here an essential singularity and exists therefore above but not below p_c. (The reader may have guessed that result already by noticing that $F(h) = \Sigma_s n_s e^{-hs}$ may converge for negative h only if log n_s varies at least as $-s$ and not if it varies only as $-s^{1/2}$, for example.)

This extremely weak "essential" singularity has long been suggested [34, 36, 121, 122] from cluster models for thermal phase transitions (see ref. [123] for a renormalization group approach); the first rigorous proof came from Kunz and Souillard for percolation [90]. We see its physical significance [122] mainly in the implications it has for the exponent ζ, i.e. for the behavior of very large clusters. An essential singularity means that the cluster numbers cannot decay as a simple exponential. The behavior of these large and very rare clusters is relevant for nucleation theory [38]. (For dilute ferromagnets at finite temperatures, Schwartz [88] has shown the Griffiths singularity [124] to be an essential singularity in this sense as a function of the magnetic field, if all moments of the percolation cluster size distribution exist, as they do below p_c [125].)

The exponent ζ in log $n_s \propto -s^\zeta$ discussed so far describes only the leading term in log n_s for large s. More generally we make the ansatz: ln $n_s = -\text{const} \cdot s^\zeta - \theta \cdot \ln s$ that means [49, 42]

$$n_s \propto s^{-\theta} \exp(-\text{const} \cdot s^\zeta). \tag{27}$$

Here, just as ζ earlier, $\theta = \theta(p)$ is a new exponent to be fitted on the data. For $p \to 0$ we expect this exponent to agree with the exponent θ for "animals", section 5, whose value is listed in table 2. Of course, at $p = p_c$ we have $\theta = \tau$, $\zeta = 0$. Series analysis [49] by a modified ratio method gave in two dimensions for intermediate cluster sizes an effective exponent $\theta(p)$. It increased from $\theta(p \to 0) = 1$ to $\theta(p \to p_c) = \tau$, first slowly, then rapidly. Above p_c it decreased again with increasing p, but the extrapolation [49] became erratic for p close to unity. The trend in the extrapolation suggest possibly a simpler behavior of the true (asymptotic) exponent θ for very large cluster sizes: Then $\theta(p)$ stays fixed at its "animal" value of table 2 for all p between zero and p_c; and it jumps to $\theta = \tau$ at $p = p_c$. (In six and more dimensions we expect $\theta = \tau = \frac{5}{2}$ everywhere.) We know of no scaling laws relating this "prefactor exponent" θ to the other critical exponents or the dimensionality; neither is $\tau - \theta$ a constant nor is $\theta = \frac{1}{2}d$ in general. Apparently a new idea is needed here!

With this remark we conclude section 3 which we regard as the main section of this review. The results in sections 4 and 5 are at the time of this writing less reliable and more controversial than those in section 3.

4. Cluster structure

In the cluster numbers we saw in eq. (26) a clear asymmetry between n_s above p_c and n_s below p_c. Now we want to know if this asymmetry is reflected in the structure of clusters. We first discuss the cluster perimeter which can be derived directly from the cluster numbers, without any new assumptions. Then we look at other properties like cluster radii which require additional scaling assumptions beyond eq. (15).

4.1. Cluster perimeter and internal structure

The average perimeter t_s and the width Δ_s of the perimeter distribution are discussed here from the cluster numbers with the help of exact relations [71, 90, 126].

4.1.1. Exact relations

Let g_{st} be the number of different cluster configurations for s sites with perimeter t, where the "perimeter" (not necessarily a "surface" in the usual sense) is the number of empty neighbors of cluster sites, section 2.2. Then $n_{st} = g_{st}p^s(1-p)^t$ is the average number [39–41] of s-clusters with perimeter t, and $n_s = \Sigma_t n_{st}$ is the average total number of s-clusters. We define an average perimeter t_s and width Δ_s for the perimeter distribution function n_{st}/n_s by

$$t_s = \sum_t t \cdot n_{st}/n_s; \qquad \Delta_s = \left[\sum_t (t-t_s)^2 n_{st}/n_s\right]^{1/2}. \tag{28a}$$

(One could also define averages by summing over s at fixed t; but little work has been done in this direction so far [48].) The evaluation of the exact n_{st}/n_s shows a unique pronounced peak near $t = t_s$ [42].

The averages in eq. (28a) can be expressed by derivatives of the cluster numbers $n_s(p)$, just as in statistical thermodynamics one finds the average magnetization and its fluctuation from the first and second field derivative of the logarithm of the partition function. Let $Z_s = n_s p^{-s} = \Sigma_t g_{st} q^t$ with $q = 1-p$ be the partition function for s-clusters. Then the reader can check easily that the following two relations are exact in general, not only for large clusters near the critical point [90, 71]

$$t_s = (\partial/\partial \ln q) \ln Z_s; \qquad \Delta_s^2 = (\partial/\partial \ln q)^2 \ln Z_s. \tag{28b}$$

By differentiating n_s/p^s we can rewrite these results as

$$t_s = (q/p)s - q(\partial/\partial p) \ln n_s \tag{28c}$$

$$\Delta_s^2 = qp^{-2}s + q^2(\partial/\partial p)^2 \ln n_s - q(\partial/\partial p) \ln n_s. \tag{28d}$$

For large clusters and $p \neq p_c$ we have $\ln n_s \propto -s^\zeta$, with a proportionality factor depending on p and an exponent ζ given in eq. (26). Thus for all p except at p_c we get for $s \to \infty$:

$$t_s = (q/p)s + O(s^\zeta); \qquad \Delta_s^2 = qp^{-2}s + O(s^\zeta). \tag{29}$$

According to Kunz and Souillard [90] the exponent ζ is rigorously below unity for all p above p_c and all finite dimensionalities; hence

$$\lim_{s\to\infty} t_s/s = (1-p)/p \qquad (p \geqslant p_c). \tag{30a}$$

Moreover, if $\zeta = 1 - 1/d$ above p_c, then the "correction term" $\propto s^\zeta$ in eq. (29) varies as $s^{1-1/d}$ above p_c, i.e. as a cluster surface area. Since the perimeter t_s counts internal holes as well as external boundaries, its proportionality to s for large s is legitimate; see also section 4.3.2. (For $p = p_c$ the validity of eq. (30a) will be shown in eq. (33).)

This relation (30a) has a lively history since its simple derivation [90] was long overlooked: Domb [101] predicted t_s to be proportional to s for large s near p_c, and Stauffer [98] suggested the factor of proportionality to be $(1-p_c)/p_c$ at p_c. Leath [73] gave a much simpler but still not exact derivation of that relation; moreover he gave the first Monte Carlo confirmation, albeit somewhat below p_c. Series

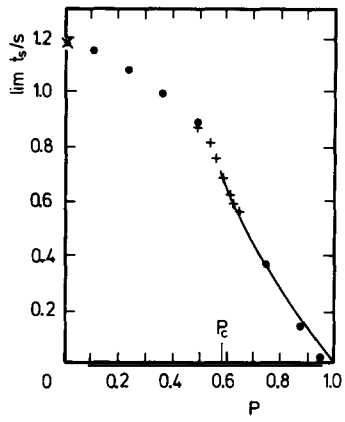

Fig. 12. Variation with concentration of the limiting perimeter-to-size ratio for large percolation clusters. The solid curve gives the exact result $(1-p)/p$ above p_c [90]. The Monte Carlo results of ref. [62], +, and of ref. [75], dots, and the series result from ref. [52], ×, refer to the square lattice.

extrapolations by Stauffer [50] and Domb [102] (but much more precise by Duarte [52]) agreed with eq. (30a) at p_c. For p slightly above p_c Stauffer [126] gave scaling arguments for eq. (30a); according to that work eq. (30a) is not valid below p_c. A *proof* of eq. (30a) at p_c was given by Reich and Leath [89], and for all p above p_c by Kunz and Souillard [90]. An independent different argument was presented by Hankey [91] for the analogous result in the infinite network for all p above p_c. Stoll and Domb [62] and Leath and Reich [71] confirmed eq. (30c) by Monte Carlo simulations for p at and near p_c (ref. [62] also for the infinite network), and Stauffer [75] added the Monte Carlo confirmation for p far above p_c. Below p_c deviations from eq. (30a) were observed by Monte Carlo [62, 75] and series work ([52] and Duarte, priv. comm.).

The corresponding result for the width of the perimeter distribution,

$$\lim_{s\to\infty} \Delta_s/s = (1/p)p^{-2} \qquad (p \geq p_c) \tag{30b}.$$

has a much simpler history: It was investigated theoretically and experimentally by the Rutgers University group [71–73, 89] whereas Stauffer's series extrapolations [50, also 46] turned out to be wrong [126]. All this numerical work was restricted so far to two dimensions; fig. 12 summarizes the variation of the limiting ratio of perimeter to size with s. See Note added in proof, Peters et al.

The partition function $Z_s = \Sigma_t g_{st} q^t$ for an s-cluster corresponds, in statistical mechanics, to the partition function $Z = \Sigma_E g_{sE} \exp(-E/k_B T)$. Here g_{sE} is the number of different quantum states for s particles with total energy E. We see that the perimeter t for percolation is the analog of the energy E for thermal phenomena; and if each broken bond between nearest neighbors contributes an energy $2J$ to the E, then we may identify in this analogy the quantity $q = 1-p$ with $\exp(-2J/k_B)$ and the perimeter t with the number of broken bonds, such that the energy E corresponds to the product $2tJ$. (Kasteleyn and Fortuin [21] give a more rigorous formulation of this analogy.) Apart from the trivial factor $2J$, the ratio $\lim(t_s/s) = (1-p)/p$ then corresponds to the thermal energy per particle, in the thermodynamical limit. Numerically this analogy is quite accurate [98]: For example, in percolation on the triangular lattice we have $p_c = \frac{1}{2}$, $\lim t_s/s = 1$ at p_c, i.e. to each critical cluster site belongs, in the average, one perimeter site. Analogously, for ferromagnets (spin $\frac{1}{2}$ Ising, interaction between nearest neighbors only) in the triangular lattice at the Curie point the average thermal energy tells us that each

spin has, in the average, one of its six neighbors antiparallel [98]. Thus the number of broken bonds per spin approaches at the Curie point the same limit as the number of perimeter neighbors per site at the percolation threshold, i.e. exactly one. Thus it is natural to expect [101] the perimeter t_s to be proportional to the clusters size s, just as the thermal energy is proportional to the system size for most problems in nature (provided surface effects are negligible). In particular also for the droplets used in classical nucleation theory [38] or in the Fisher droplet model [34] the thermal energy and similar quantities (like entropy) contain a bulk term proportional to the number of molecules in the liquid "raindrop". Broken bonds in the interior of the material are responsible for these proportionalities to the system size [50].

4.1.2. Scaling theory

Let us restrict ourselves now again to large clusters near p_c where scaling assumptions, eq. (15), can be applied to calculate the derivatives of n_s required in eq. (28). With $n_s \propto s^{-\tau} f(z)$ and $z = (p - p_c)s^{\sigma}$ we get

$$t_s = (q/p)s + s^{\sigma}\psi_1(z); \qquad \Delta_s^2 = qp^{-2}s - s^{2\sigma}\psi 2(z) \tag{31}$$

with

$$\psi_1 = -q \cdot \mathrm{d}(\ln f)/\mathrm{d}z; \qquad \psi_2 = -q^2 \mathrm{d}^2(\ln f)/\mathrm{d}z^2.$$

Thus the leading term $\propto s$ is very simple, but the higher order term contains a complicated scaling function. We now call the difference $t'_s = t_s - (q/p)s$ the "excess perimeter" [126] since above p_c this excess perimeter $t'_s \propto s^{1-1/d}$ seems to come from a surface area. On the other hand, the "bulk perimeter" $(q/p)s$ may be interpreted as a volume effect.

More quantitatively, above p_c with $\ln f \propto -z^{\zeta/\sigma} = z^{(1-1/d)/\sigma} = (p - p_c)^{\beta\delta(1-1/d)} \times s^{1-1/d}$, the excess perimeter is $t'_s = s^{\sigma}\psi_1 \propto s^{\sigma}\mathrm{d}(\ln f)/\mathrm{d}z = \mathrm{d}(\ln f)/\mathrm{d}p \propto (p - p_c)^{-1+\beta\delta(1-1/d)} s^{1-1/d}$. Eq. (37) will show us later that the volume V_s of a very large s-cluster varies as $(p - p_c)^{-\beta} s$ above p_c [50]; then the excess perimeter, expressed by the cluster volume, varies for very large s as $(p - p_c)^{(\beta\delta+\beta)(1-1/d)} \times V_s^{1-1/d}$, or

$$t'_s \propto (p - p_c)^{(d-1)\nu-1} V_s^{1-1/d} \qquad (p > p_c) \tag{32a}$$

where the scaling laws (18b) have been used. Again we see quantitatively the analogy between our perimeter and the energy for thermal critical phenomena: The excess perimeter has the same dependence on $p - p_c$ as the surface energy of a fluid or the domain wall energy of an Ising ferromagnet has on $T_c - T$. Thus we may identify

$$\text{excess perimeter} \triangleq \text{surface energy} \quad (p > p_c). \tag{32b}$$

(Disscussion of the exponent: The surface area of a homogeneous liquid sphere surrounded by its vapor varies as $(\text{volume})^{1-1/d}$ in d dimensions. Its surface free energy is the product of surface tension and surface area. The surface tension, as reviewed e.g. by B. Widom in vol. 2 of ref. [11] vanishes as $(T_c - T)^{(d-1)\nu}$ near the critical point; its temperature derivative gives the surface energy per unit area since $E = -T^2 \partial(F/T)/\partial T \propto -T \cdot \partial F/\partial T$. Thus the surface energy per unit area varies as $(T_c - T)^{(d-1)\nu-1}$, which is the same exponent as derived in eq. (32a) for the excess perimeter.)

Right at $p = p_c$, the derivative $\mathrm{d}(\ln f)/\mathrm{d}z$ is negative, as can be seen e.g. from the logarithmic plot in fig. 11. Its value at $z = 0$ is estimated [26] to be about -7.2 in the triangular lattice. Thus we have from eq. (31a) [98]:

$$t_s(p_c) = s(1 - p_c)/p_c + \text{const} \cdot s^{\sigma} \tag{33}$$

where the constant is about 3.6 and $\sigma \simeq 0.39$ in the triangular lattice. This relation is confirmed by both Monte Carlo and series results [52, 71]; e.g. the Monte Carlo work gave $t_s = s + 3.43\, s^{0.40\pm0.01}$, and the series work an exponent of 0.381 ± 0.003, for the triangular lattice.

Below p_c we have $\zeta = 1$ which means: No clear separation is possible between a surface term and a bulk term in the cluster perimeter, since both vary as s, as shown by eq. (29). Thus a surface in the usual sense of droplet surfaces seems not to exist below p_c but only above p_c. Only above p_c can we interpret the excess perimeter t'_s as a "measure" of the surface area in the usual sense. Already at $p = p_c$ this suggested proportionality of excess perimeter and surface area breaks down, as pointed out by Domb and Stoll [97] and in contrast to our first speculations [98]: Eq. (32b) indicates that the excess perimeter really is a surface energy, not a surface area. As long as the surface tension is independent of cluster size, both surface area and surface energy vary as $s^{1-1/d}$, eq. (32a). But right at p_c the powers of $(p - p_c)$ appearing in the surface tension above p_c are replaced by powers of s, and then surface area, surface free energy, and surface energy no longer vary with the same power of s. In this sense the exponent σ is not a true surface exponent, although the term $s^\sigma \psi_1(z)$ does give above p_c the analog of the surface energy, eq. (32).

Also the external perimeter, which ignores all holes in the interior of a cluster, has been suggested [50] as a measure of the surface area for large clusters. However, Leath and Reich [71] found for $p \leqslant p_c$ most of the perimeter sites to be external; fig. 13 shows one of their clusters with 4741 sites at $p = 0.48$ in the triangular lattice. Many fjords connect the perimeter sites with the outside world [71]. At $p = p_c$ ref. [71] found the external perimeter in the triangular lattice to increase as $s^{0.9}$ for cluster containing several hundred sites. This exponent 0.9 is clearly different from the exponent $\sigma = 0.4$ for the excess perimeter at p_c and also from the two-dimensional surface exponent $1 - 1/d = \frac{1}{2}$. Thus at least at p_c the external perimeter is not proportional to the excess perimeter, contrary to a hope in ref. [126]. Also far above p_c [75] most of the perimeter sites are external. (Perhaps in the square lattice [75] at $p = 0.75$ for s above 10^3 the internal perimeter roughly equals the bulk perimeter $(q/p)s$, and thus the external perimeter approaches the excess perimeter (surface energy) for very large clusters. But since clusters with more than 1000 sites are very difficult to produce this result would still mean that the external perimeter is not a practical tool to study cluster surfaces.) In three and more dimensions we have $p_c < \frac{1}{2}$ in general; thus near p_c an infinite network of holes percolates through the large clusters of occupied sites. Then the external perimeter completely loses its meaning as a surface measure.

Therefore at present the excess perimeter $t'_s = t_s - (q/p)s = s^\sigma \psi_1(z)$ seems to be above p_c the most promising measure of a surface area for large clusters, eq. (32b). Monte Carlo data have shown that t'_s/s^σ is indeed a function of $z = (p - p_c)s^\sigma$ alone; data for different $p - p_c$ follow the same curve [71], as in our scaling plots for the cluster numbers. The cluster size s had to be larger than 85 to agree with scaling [71]. Moreover, since eq. (28c) is exact, Monte Carlo data for the excess perimeter t'_s can be used to find cluster numbers n_s. In this way, and not directly from the n_s in fig. 10, Leath and Reich found their data [71] to support $\zeta = 1$ against $\zeta = 2\sigma$ for large clusters above p_c.

The width Δ_s of the perimeter distribution function is right at p_c given by eq. (31b):

$$\Delta_s^2 = (1 - p_c)p_c^{-2}s - \text{const}_1\, s^{2\sigma} + \text{const}_2\, s^\sigma. \tag{34}$$

The correction exponent 2σ here is about 0.8 in two dimensions and even closer to unity for higher dimensionalities. Thus even for rather large clusters the leading term is not much larger than the first correction term. For example, if $\sigma = 0.48$ in three dimensions, then only for s above 10^{25} sites per cluster would $s^{2\sigma}$ be less than ten percent of s. Even if every human being on earth would have its

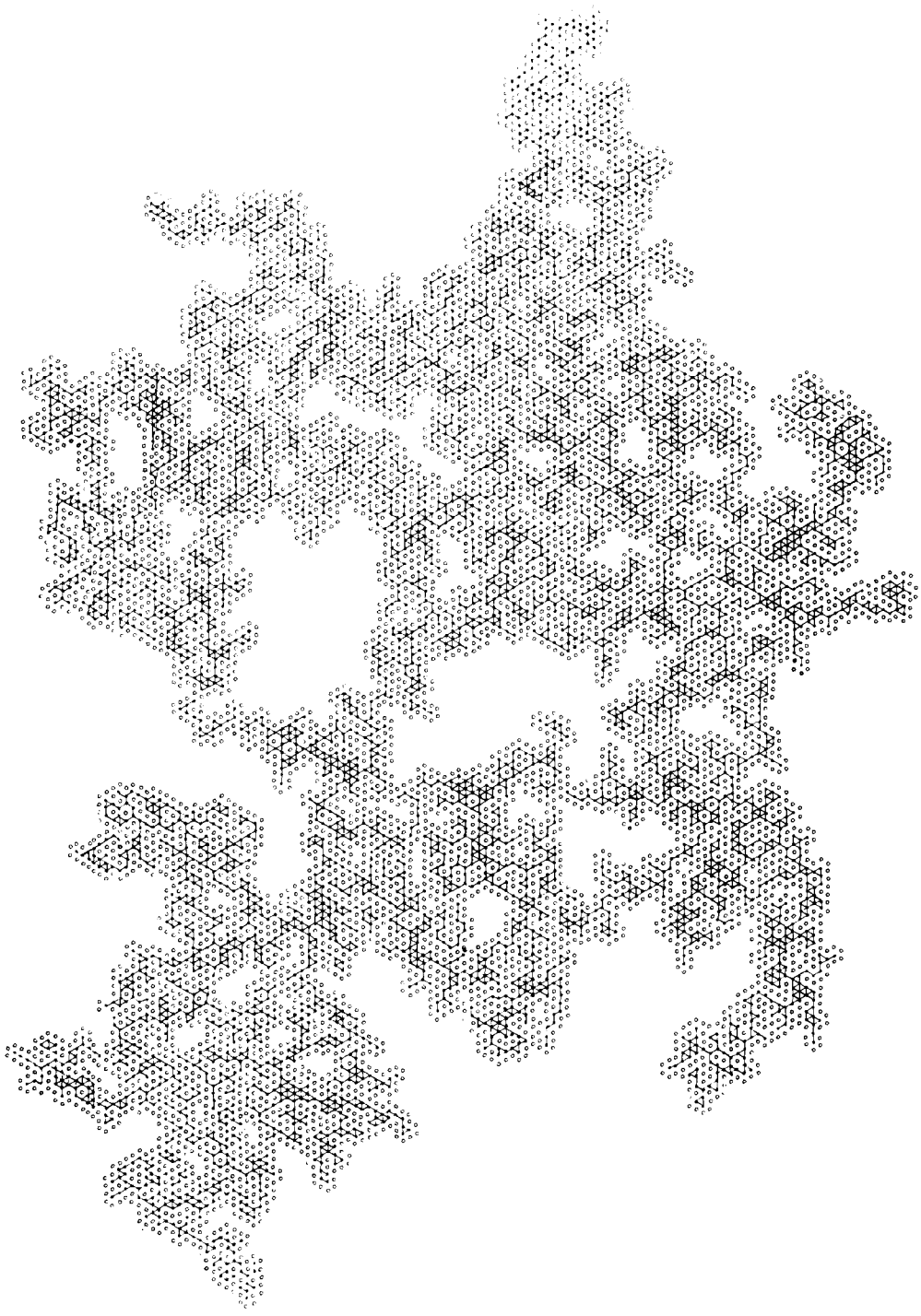

Fig. 13. Example of a large cluster slightly below p_c. The sites · are connected by lines and are surrounded by the perimeter sites ◦. From ref. [71].

own computer to store 10^8 sites [24] the combined memory would be too small by many orders of magnitude to handle such clusters. Therefore the correction terms in eq. (34) cannot be neglected. Series expansion analysis which neglected the correction term gave wrong exponents [46, 50]. Even in two dimensions, where the situation is better, Monte Carlo data [71] show a strong deviation from the asymptotic law, eq. (30b) even at $s = 2000$. However, with the two constants in eq. (34) determined from the cluster numbers in the triangular lattice [26] via eq. (28d), the Monte Carlo data of Leath and Reich for the width [71] fit nicely with eq. (34) for large s.

Thus the width Δ_s of the perimeter distribution function varies as $s^{1/2}$, the mean value t_s as s, and the excess perimeter t'_s as s^σ multiplied with a scaling function ψ_1. Because of these different exponents we have here an example where scaling assumptions do not hold. To describe the function $n_s(p)$ of two variables s and $p - p_c$ we assumed $n_s \propto s^{-\tau} f[(p - p_c)s^\sigma]$. The analogous assumption for the three variables s, $p - p_c$ and t entering the perimeter distribution would be

$$n_{st}(p) \propto s^{-\tau-\upsilon} f_1[(p - p_c)s^\sigma, ts^{-\upsilon}] \tag{35}$$

with a new phenomenological exponent υ. (υ = ypsilon; not to be confused with ν = nu for the correlation length, eq. (6e).) (The prefactor $s^{-\tau-\upsilon}$ is chosen such that summation over t gives the desired $n_s(p)$, eq. (15).) Such an assumption has in fact been made for the energy distribution of Ising model clusters [36] and the bond distribution of percolation clusters [114]. But it is *wrong* for the perimeter of percolation clusters. To accomodate $t_s \propto s$, we need $\upsilon = 1$; to allow $\Delta_s \propto s^{1/2}$ we need $\upsilon = \frac{1}{2}$: Contradiction. If instead we postulate eq. (35) to be valid for the excess perimeter $t'_s = t_s - (q/p)s \propto s^\sigma$, we would need $\upsilon = \sigma$ to accomodate this excess perimeter, but still $\upsilon = \frac{1}{2}$ for the width: The contradiction is not removed. Only close to six dimensions, or in the classical regime above six dimensions, the contradiction vanishes for the excess perimeter, since then $\sigma = \frac{1}{2}$ apart from a correction of order $(6 - d)^2$ below 6 dimensions. Thus we see, just as we will see with universality in appendix 2, that scaling is valid in most cases but not in all. The numerical tests of section 3.2 really were necessary and did not just prove a triviality.

4.1.3. Internal structure

Returning to bulk properties proportional to the cluster size s, we find besides the limit of t_s/s also other quantities characterizing the internal structure of large clusters. Trivially the concentration p is one of them. The "energy" e_s can be defined for s-clusters as the average number of nearest neighbor connections between an occupied cluster site and an empty perimeter site [48, 60, 127]. The bond number b_s in s-clusters is the average number of nearest neighbor connections between cluster sites [114]. The cyclomatic number c_s is the average number of cycles formed by the bonds in s-clusters (i.e. by its nearest-neighbor connections); e.g. in a Bethe lattice the cyclomatic number of trees is zero, for a polygon it is unity, and it is largest for fully compact configurations without internal holes [97, 115]. The genus g_s is the average number of topologically separated holes in the interior of s-clusters [128]. For every configuration, and thus also for the averages, one has [97] $c_s = b_s - s + 1$ and e_s = (coordination number) $\cdot\, s - 2b_s$. The compact 4-cluster □ for example has a perimeter of 8, an energy of 8, contains 4 bonds, has cyclomatic number one, and genus zero. For large clusters all these quantities vary as s; for example $\lim_{s\to\infty}(g_s/s) = 1/28$ in a bcc lattice [128] at p_c. Refs. [115, 97, 129] give the monotonic variation of $\lim(c_s/s)$ with p. Besides these Monte Carlo results also analytic results are available, as reviewed by Domb [129]. So far no scaling analysis in terms of exponents or functions of z were given for the leading terms or the first corrections; Sur et al. [60] remark that $e_s = \text{const}_1 \cdot s + \text{const}_2$ according to their Monte Carlo data. In that respect the perimeter is at present

better understood and investigated [71] than cyclomatic number, energy, bond number or genus in their scaling properties. (Refs. [97, 115, 129] also compare these bulk properties of percolation with those of ferro- and antiferromagnets at finite temperatures.)

In conclusion, the internal structure of large percolation clusters in terms of perimeter per site and analogous quantities seems well studied by now. For the perimeter also the leading correction term was studied in detail and found to agree with scaling theory. A cleary asymmetry about p_c was observed in this excess perimeter $t_s - (q/p)s$ and is related to the asymmetry in the cluster numbers.

4.2. Radius and density profile

4.2.1. The basic assumption

To describe parameters affecting the external shape of clusters, not their internal structure, new quantities like density or radius seem necessary. They are defined as statistical averages over a cluster (and, of course, also as averages over many clusters of the same size) and thus do not give us information on microscopic details like cyclomatic numbers etc. [115]. To describe their scaling behavior a new "hyper"-scaling assumption seems necessary. This assumption then will give us the scaling law $d\nu = 2 - \alpha$ postulated in eq. (18b) but not yet derived.

Eq. (14) gives us a hint how a scaling assumption similar to eq. (15) for n_s may be constructed for the cluster radius R_s: The ratio R_s/ξ might just have the same scaling property as $n_s(p)/n_{s_\xi}$ or $n_s(p)/n_s(p_c)$, i.e. it may depend on the ratio s/s_ξ only. Since $s/s_\xi \propto z^{1/\sigma}$ with $z = (p - p_c)s^\sigma$ we thus postulate

$$R_s = \xi \cdot \tilde{R}(z) \tag{36a}$$

where $\tilde{R}$ is a suitable scaling function to be fitted on experiment. We may rewrite this assumption as

$$R_s = s^{\sigma\nu}\tilde{R}_1(z) \tag{36b}$$

since $\xi \propto |p - p_c|^{-\nu} \propto s_\xi^{\sigma\nu}$. In this form our assumption [130] has the same structure as eq. (15).

We now assume in addition that the internal structure of a very large but finite cluster above p_c is the same as that of the infinite network. "Very large" means here: $s/s_\xi \gg 1$ or $z \gg 1$, that means radii much larger than the coherence length. "Internal structure" refers to average properties like density, visible over distances much smaller than the cluster radius. Thus we postulate:

> By looking at average cluster properties over distances much smaller than the cluster radius we cannot distinguish between very large but finite clusters and the infinite network, if p is above p_c. (36c)

An example for the validity of assumption (36c) is the ratio t_s/s for very large clusters, which is $(1-p)/p$ according to eq. (30a). In the infinite network, the corresponding ratio has the same value [62, 91]. Thus by looking only at a finite fraction of a sample we cannot tell if the large set of connected sites which we might observe there extends to infinity or belongs to a finite cluster. Similarly if a man and a woman get along well for one evening they still might not make it together through a long marriage. In that sense eq. (36c) is compatible with numerous experiments. But it is obviously constricted to concentrations p above p_c since below p_c there is no infinite network present with which very large but finite clusters could be compared.

4.2.2. Exponents for the radius

With this assumption we now get information on the limiting behavior of R_s above p_c, i.e. on the scaling function $\tilde{R}(z)$ or $\tilde{R}_1(z)$ for $z \to \infty$. In every unit volume of their interior the very large clusters thus should have the same fraction pP_∞ of sites connected to the cluster as has the infinite network. In short, the average "density" inside very large clusters is the same as the density of the infinite network. (The density is defined as the probability that a given lattice site belongs to a given cluster or network.) If surface effects are negligible for these very large clusters, we can calculate the cluster volume V_s from the "mass" s and the density pP_∞ through the well known relation: mass = volume times density:

$$s = V_s p P_\infty; \qquad p > p_c.$$

This argument was called the "Swiss cheese" picture in ref. [50], since in spite of its many internal holes a very large chunk of Swiss cheese still has a mass s proportional to its volume V_s. Close to p_c, where the percolation probability vanishes as $P_\infty \propto (p - p_c)^\beta$, we thus get

$$V_s \propto s \cdot (p - p_c)^{-\beta} \qquad (s \gg s_\xi, \quad p > p_c). \tag{37a}$$

Note that neither the cluster radius R_s nor the cluster volume V_s were defined here quantitatively; for example, one may use for R_s the radius of gyration: $R_s^2 = \Sigma_i r_i^2/s$ where the sum runs over all cluster sites, and r_i is the distance of a site from the center-of-mass of the cluster. We assume that this and all other "reasonable" definitions give the same critical exponents. We may define a cluster volume in three dimensions through $V_s = (4\pi/3)R_s^3$, and in d dimensions we have $V_s \propto R_s^d$. Thus eq. (37a) leads to

$$R_s \propto (p - p_c)^{-\beta/d} \cdot s^{1/d} \tag{37b}$$

for very large clusters above p_c.

If both eqs. (36) and (37b) are assumed to be correct, then the function $R(z)$ in eq. (36a) must vary as $z^{1/\sigma d} \propto s^{1/d}$ for $z \to \infty$, in order to make the radius proportional to $s^{1/d}$ in accord with eq. (37b). Now we get from eq. (36a), for p slightly above p_c:

$$R_s \propto \xi \cdot (p - p_c)^{1/\sigma d} \cdot s^{1/d} \propto (p - p_c)^{-\nu + 1/\sigma d} \cdot s^{1/d}.$$

If we compare this exponent of $p - p_c$ with the exponent appearing in eq. (37b) we conclude $\beta/d = \nu - 1/\sigma d$, or $d\nu = \beta + 1/\sigma = \beta(\delta + 1)$. This is the desired scaling law of eq. (18b) whose derivation was missing so far. Alternative derivations were given in refs. [18] and [109].

This scaling law $d\nu = \beta(\delta + 1) = 2 - \alpha$ is also known from other phase transitions [10, 11]. It is regarded as less reliable than the other scaling laws not involving d, but presumably [111] it is exact or a good approximation for not too high dimensionalities d. For $d \to \infty$, on the other hand, one expects classical exponents $\alpha = -1$, $\beta = 1$, $\gamma = 1$, $\delta = 2$, $\nu = \frac{1}{2}$, as in mean field theories [114] or Bethe lattices [27–30]. For all d above six, the above scaling law $d\nu = 2 - \alpha$ breaks down if these classical exponents are used. Therefore Toulouse [84] suggested, as confirmed by later results [45, 68, 117], that "hyperscaling", $d\nu = 2 - \alpha$, is valid only below six dimensions whereas classical exponents are valid above six dimensions. Only at the marginal dimensionality $d = 6$, where the two regimes coalesce, are both classical exponents and hyperscaling valid; but then logarithmic correction factors are important [17]. This special status of six dimensions as the transition from the classical to the hyperscaling regime is the reason why the epsilon expansion of renormalization group is a perturbation expansion about $6 - d$. For thermal phase transitions the classical exponents are usually $\beta = \frac{1}{2}$ and $\alpha = 0$ (and

$\delta = 3$); thus the same arguments as above give four dimensions as the marginal dimensionality above which classical exponents are valid. From now on we restrict ourselves to dimensionalities below six and assume that hyperscaling is valid, i.e. $2 - \alpha = d\nu$.

So far we dealt with p above p_c only; but the scaling assumption (35) should be valid for both sides of the phase transition. Right at p_c the average cluster radius R_s is finite and thus cannot be proportional to any power of $p - p_c$. Thus in eq. (36b) we have $\tilde{R}_1(z \to 0) \to$ const, or $R_s(p_c) \propto s^{\sigma\nu}$. Since $\sigma\nu = d\nu/d\beta\delta = (1 + 1/\delta)/d = 2/(d + \gamma/\nu)$ according to hyperscaling, eq. (18), we see that [50]

$$R_s(p_c) \propto s^{(1+1/\delta)/d}; \qquad V_s(p_c) \propto s^{1+1/\delta}. \tag{38}$$

A different derivation which does not use hyperscaling explicitely was given by Harrison et al. [109]. (De Gennes, private communication, pointed out that with the approximation $\gamma \simeq 2\nu$ the above relation reads $R_s \propto s^{2/(d+2)}$, similar to Flory's approximation $R_s \propto s^{3/(d+2)}$ for the radius of self-avoiding walks [131].)

Harrison et al. [109] also gave the first and so far best confirmation of eq. (38). They concluded $s \propto R_s^{2.66 \pm 0.13}$ from three-dimensional Monte Carlo simulations, this exponent 2.66 is roughly compatible with the predicted value $d/(1 + 1/\delta) = 2.50 \pm 0.07$, from eq. (38) and [55] $\delta = 5.0 \pm 0.8$. Clearly the exponent is not just equal to the dimensionality d. (For $d = 2$ the numerical evidence is less impressive since δ is much larger there [75].) For thermal phase transitions eq. (38) has been proposed much earlier [74, 132] but no direct confirmation seems to exist; again percolation turned out to be the best-understood cluster problem.

Below p_c, if R_s is assumed to vary for very large clusters as s^ρ with a new exponent ρ, the scaling assumption (36a) gives [130]

$$R_s \propto |p - p_c|^{\beta\delta\rho - \nu} \cdot s^\rho. \tag{39a}$$

This result describes also very large clusters above p_c and at p_c, if the above values for the exponent ρ, eqs. (37b, 38) are used. It seems likely that the exponent ρ below p_c is constant for all p between zero and p_c, just as the exponent ζ was. If we call this constant ν_0 we can summarize our results for the radius exponent as

$$R_s \propto s^\rho \quad (s \to \infty \text{ at fixed } p) \tag{39b}$$

$$\rho(0 < p < p_c) = \nu_0; \qquad \rho(p_c) = (1 + 1/\delta)/d; \qquad \rho(p_c < p < 1) = 1/d. \tag{39c}$$

Figure 14 summarizes Monte Carlo results for two-dimensional cluster radii. Above and at p_c the data are consistent with the predictions $\rho = \frac{1}{2}$ and $\rho = 0.53 = \frac{1}{2}(1 + 1/\delta)$, shown there as horizontal lines. Below p_c we find the new exponent ν_0 to be about 2/3, significantly lower than the "self-avoiding walk" prediction [130] of 3/4. It seems that a better theory [133] is needed since percolation clusters below p_c do not behave similar to self-avoiding walks.

The data of fig. 14 do not give exponent values which are constant in certain intervals and jump discontinuously at p_c; instead the numerically determined exponents vary continuously with p. But we see no real contradiction to the constant exponents predicted in eq. (39c). For these Monte Carlo data are taken for clusters containing ten to thousand sites, whereas eq. (39) refers to very large clusters only, $s \to \infty$. Only for clusters much larger in linear extension than the coherence length $\xi \propto |p - p_c|^{-\nu}$ can the simple power law (39a) be expected to hold. Thus particularly the data close to p_c should not be relied upon since there the scaling variable $|p - p_c| s^\sigma$ is not much larger than unity [130]. Therefore only the data for p close to zero or unity and for $p = p_c$ are reasonably reliable, whereas the exponents at other concentrations are effective exponents and not yet close to the true asymptotic

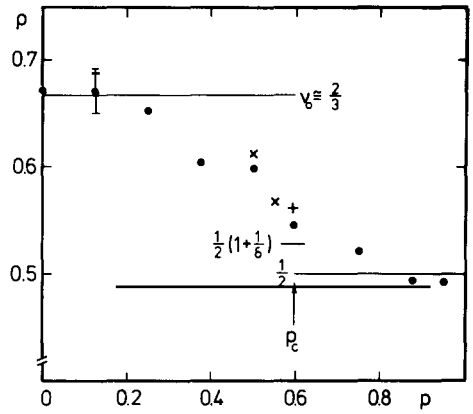

Fig. 14. Variation with p of the effective exponent ρ for the cluster radius $\propto s^{\rho}$. Monte Carlo data from ref. [75], ·, ref. [73], ×, ref. [109] and priv. comm., +. The horizontal lines symbolize the expected results, which are discontinuous at p_c.

exponents predicted in eq. (39). Similar variation of effective exponents are known from thermal phase transition; the analogy is particularly clear with self-avoiding walks with interaction [135].

Figure 15 tries to transform the above argument into a simple picture, analogous to dynamical critical phenomena near Curie points. The asymptotic exponents of eq. (39c) are valid only in the small sectors I, II and III of that figure. In between these sectors the cluster radius is described by the full scaling functions of eq. (35), which only in the asymptotic limits of the shadowed sectors become simple power laws. Similar effects are expected for other exponents like ζ and θ. Thus if we keep $s = 10^2$ constant and move continuously from $p = 0$ to $p = 1$, then we start in region III where $\rho = \nu_0$, $\zeta = 1$. With increasing p we leave region III and move along the dotted line of fig. 15. Here the cluster radii and cluster numbers are described by complicated scaling functions like eqs. (35, 15) or even more sophisticated expressions. Very close to p_c we reach sector I where $\rho = (1 + 1/\delta)/d$ and $n_s \propto s^{-\tau}$. Further increase of p along the dotted line brings us out of the sector I into the less understood intermediate region, until we reach safer ground again for $(p - p_c)s^{\sigma} \gg 1$ in region II, where $\rho = 1/d$, $\zeta = 1 - 1/d$ is valid. Nowhere along the dotted line is, for fixed finite cluster size s, a discontinuity in the cluster numbers or the cluster radii, since only the *asymptotic* exponents depend discontinuously

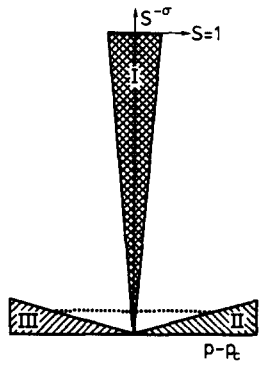

Fig. 15. Various sectors of the s–p-plane in percolation scaling theory. The shadowed regions correspond to $s \ll s_\xi$ (sector I), $s \gg s_\xi$ above p_c (sector II), and $s \gg s_\xi$ below p_c (sector III). Only in these narrow sectors are the asymptotic exponents ζ, θ and ρ directly observable for large clusters. (The three sectors were drawn with an enlarged angle to make them better visible.)

on p. A clear example of the similarity of *small* clusters above and below p_c is shown in ref. [115, fig. 10]; it contradicts in no way our fig. 15 and eq. (39c) here which try to describe the limit $s \to \infty$ only.

In conclusion it seems that the cluster radii behave roughly as they should. But higher accuracy and a better theory for $\nu_0 \simeq 2/3$ (for $d = 2$) are needed.

4.2.3. Density profiles

In order to understand better the difference in the cluster radii and cluster numbers above and below p_c it is useful to look at the density profile of clusters [75, 130, 134]. Let the density profile $D_s(r)$ of s-clusters be the probability that a lattice site at distance r from the cluster center-of-mass belongs to that s-cluster. (Contrary to ref. [130] we do not require the center-of-mass to belong to that cluster; that definition would be needed for correlation functions which are not discussed here.) This density thus is a "coarse-grained" average [115], similar to other statistical concepts in hydrodynamics (density, velocity, pressure). It does not give us microscopic details on the *structure* of clusters; instead the density profile describes the overall *shape* of a cluster.

As mentioned in the discussion after assumption (36) we take the density $D_s(r \ll R_s)$ inside very large clusters above p_c to be the same as the density pP_∞ of the infinite network, i.e.

$$\lim_{s\to\infty} D_s(r) = pP_\infty \tag{40a}$$

for fixed p above p_c and fixed r. If we are not in this simple asymptotic limit, the density profile $D_s(r)$ depends on three variables r, s and p. In the scaling regime of large clusters near p_c we may again postulate a scaling-homogeneous form [130] reducing the number of independent variables from three to two:

$$D_s(r) = P_\infty \tilde{D}(r/\xi, s/s_\xi) \tag{40b}$$

or equivalently,

$$D_s(r) = P_\infty \tilde{D}_2(rs^{-\sigma\nu}, (p - p_c)s^\sigma). \tag{40c}$$

The interested reader may invent many other forms [130] of this assumption. Trivially we have $\int D_s(r)\, \mathrm{d}r = s$ since the integral over the density gives the total mass s. (Discussions of correlation functions suggest for $r \gg R_s$ and $s \gg s_\xi$ the asymptotic decay laws $\log(D_s) \propto -r$ above p_c and $\log(D_s) \propto -r^{1/(1-\nu_0)}$ below p_c [130].) Thus if eq. (40c) is rewritten as $D_s(r) = s^{-x}\tilde{D}_1(r/s^{\sigma\nu}, (p - p_c)s^\sigma)$ then we must have $x = d\rho - 1$ in the three shadowed regions of fig. 15 [76].

This scaling assumption formulates more precisely the assumption made after eq. (37a) that all "reasonable" definitions of a cluster radius give the same exponent. Eq. (40) means that for a given s and a given p there is only one characteristic length $R_s \propto s^{\sigma\nu}$ for the cluster, and not several of them. Any reasonable definition, like $R_s^k = \int D_s(r)\, r^k\, \mathrm{d}r/s$, then will give the same length, apart from constant factors. Leath [73] used this definition with $k = 2$ in the first study of cluster radii, and was followed in ref. [75]. Harrison et al. [109] used instead of this "radius of gyration" the spanning length of the cluster, which corresponds, in some sense, to $k = \infty$. As we saw in fig. 14 these different definitions give roughly the same exponent in Monte Carlo simulations.

A complete test of the scaling assumption (40) is not yet known to us. Herrmann [76] looked at the density profiles [75] right at the percolation threshold $p = p_c$ (and also for the "animals" $p = 0$) where eq. (40c) reduces to the simpler form:

$$D_s(r) = s^{-1/\delta}\tilde{D}_3(r/R_s). \tag{41}$$

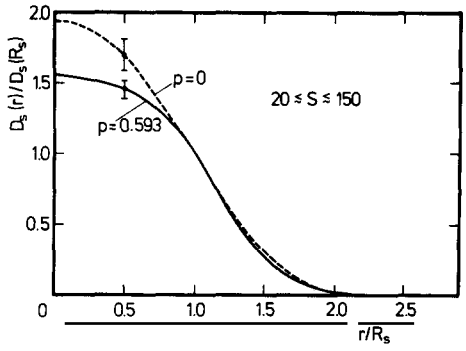

Fig. 16. Plot [76] of the scaled density profile $D_s(r)/D_s(R_s)$ as a function of the scaled distance r/R_s at the percolation threshold (solid line) and for "animals" ($p = 0$, dashed line). Error bars indicate statistical fluctuations as well as variations for different sizes s.

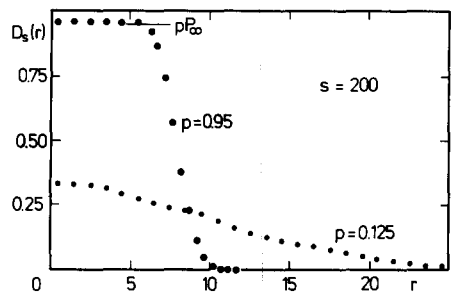

Fig. 17. Monte Carlo data [75] for the density profile far above and far below p_c (averages over more than 10^5 configurations at fixed s in the square lattice). These data suggest a droplet structure above but not below p_c.

He found this similarity law for the critical percolation clusters to be consistent with two-dimensional Monte Carlo data; in particular the prefactor was found [76] to vary as $s^{-0.055\pm0.025} = s^{-x}$, confirming well that $x = d\rho - 1 = 1/\delta \simeq 0.054$ according to eq. (38). Figure 16 summarizes the scaling form of the density profiles. For p away from p_c, fig. 17 shows the density profiles of two large clusters; again data far away from p_c give the asymptotic behavior better than data closer to p_c is s is fixed at some intermediate size. The cluster density profile above p_c has a plateau in the cluster interior, with the height near pP_∞, and decays rapidly to zero outside the cluster. The interior and exterior region are separated by a rather narrow interface. (Presumably the thickness of this interface is of the order of the coherence length ξ [126]; indeed already at $p = 0.75$ the transition is much smoother than at $p = 0.95$.) Below p_c the cluster shape is entirely different for very large clusters: The plateau is replaced by a bell-shaped curve [75, 76] where the transition layer separating interior from exterior parts now extends over the whole cluster. Thus a "surface" layer in the usual sense exists above p_c but not below p_c, if $s \to \infty$. We think that this difference is the reason for the asymmetries between above and below p_c discussed earlier in the cluster radii ($\rho = \frac{1}{2}$ versus $\rho = \frac{2}{3}$), the excess perimeter t_s' ($\propto s^{1/2}$ versus $\propto s$), and the cluster numbers ($\zeta = \frac{1}{2}$ versus $\zeta = 1$).

In this way a coherent scaling picture has been developed and partially tested. The cluster numbers n_s, eq. (15); the excess perimeter t_s', eq (31); the radius R_s, eq. (36b); and the density profile $D_s(r)$, eq. (40) are all expressed by "generalized homogeneous functions" [100], i.e. the number of independent variables is reduced by one:

$$n_s \propto s^{-\tau} f(z), \quad t_s' \propto s^{\sigma} \psi_1(z), \quad R_s \propto s^{\sigma\nu} \tilde{R}_1(z), \quad D_s(r) \propto s^{-1/\delta} \tilde{D}_1(r/s^{\sigma\nu}, z). \tag{42}$$

And in addition to this mathematical similarity, all four scaling functions in eq. (42) seem to exhibit a pronounced asymmetry in their asymptotic behavior for $z \to \pm\infty$, an asymmetry not restricted to p close to p_c but missing in classical theories (Bethe lattice).

4.3. Droplets, ramification, and fractal dimensionality

Headlines in newspapers try to inform the reader in a few words about the main content of the news; of course sometimes they are misleading and one needs to read the full text. Similarly concepts like ramification [101] etc. are simple catchwords trying to encompass as headlines what we have

described in greater detail in the preceding sections. And again these simple concepts may lead to a picture oversimplifying what we said before. (The contents of this subsection are not needed later.)

4.3.1. The raindrop or Swiss cheese model

Since the Fisher droplet model [34] of thermal critical phenomena and the raindrops of classical nucleation theory [38] long preceded the current interest in percolation clusters, it seems appropriate to start with the question: Are percolation clusters similar to raindrops, as assumed in the Fisher model above p_c?

How does a raindrop look before it is falling on your head? It consists of s "liquid" water molecules inside, and is surrounded by water vapor outside. The liquid interior is separated from the outside vapor by a narrow transition region or surface layer, with the ratio of layer thickness to droplet radius going to zero as the radius goes to infinity. In the interior, the density, entropy per molecule and thermal energy per molecule are the same as for bulk water if the droplet is large enough. More precisely, the density etc. of the raindrop interior is the same as that of bulk water at the same temperature and not the same as that of a (hypothetical)$T = 0$ groundstate. In particular, at any given moment the liquid water has density fluctuations which produce holes inside the raindrop just like holes in Swiss cheese. Only if we average over these holes we get a homogeneous density, for both raindrops and Swiss cheese.

Figure 17 and other results of the preceding section suggest that percolation clusters are like raindrops above p_c but not below p_c. Just like a Swiss cheese, they have on both sides of the phase transition an average density lower than the maximum possible density; above p_c their interior density approaches pP_∞ whereas it seems to go to zero for large clusters below p_c and at p_c [75, 76]. Only above p_c a relatively narrow interface region could be found. Of course, since a water droplet of 0.1 mm radius contains about 10^{17} molecules and the clusters in fig. 17 only 200 sites, the ratio of interface thickness to cluster radius is still quite large for our percolation clusters in comparison with raindrops. The reader should also keep in mind that the roughly spherical density profile of raindrops and percolation clusters arises only by averaging over many different configurations. For a single configuration, the holes and surface roughness of the Swiss cheese structure give a rather different picture which even above p_c is not dissimilar to fig. 13.

Instead of this definition of "droplet-like" by the density profile one may also call a cluster droplet-like if for $s \to \infty$ at fixed p its surface area (measured by R_s^{d-1} or t_s') varies as $s^{1-1/d}$, if its radius varies as $s^{1/d}$ or its volume as s, or finally if the logarithm of the cluster numbers varies as $-s^{1-1/d}$. With all these definitions we still find the same result: Very large percolation clusters ($R_s \gg \xi$) are droplet-like above p_c but not at and below p_c, as the reader can check himself by going through the preceding parts of this review. If one likes to use a word (different from "ramified") to describe the

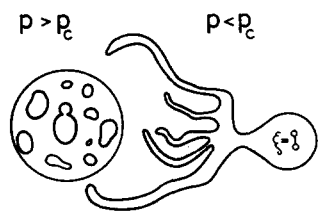

Fig. 18. Hungry hydra (clusters below p_c) eats Swiss cheese (clusters above p_c). The coherence length ξ is shown schematically. This review is based on the assumption apparent from the figure.

opposite of droplet-like one may try "hydra-like" [50]: The tentacles of this monster will engulf the scientist who tries to apply the simple droplet picture even below p_c.

In this sense, percolation clusters larger than the coherence length seem to be droplet-like, similar to a large sphere of Swiss cheese, for p above p_c but not at and below p_c, a conclusion summarized in fig. 18.

4.3.2. Ramification

Domb's suggestion [32, 101] that percolation clusters are "ramified" started the development of cluster scaling as presented in this review. Clusters were called ramified if their surface area increases with size $s \to \infty$ simply as s; they were called compact if they increased with a smaller power of s. What is the "surface area" for percolation clusters? If one takes the total perimeter as a measure of the surface area [101] then all clusters are ramified; internal "surfaces" are included in that definition. If the external perimeter only is identified with the surface area then the question of ramification is not yet entirely solved for two dimensions. With the excess perimeter t'_s as a measure of the surface the clusters are ramified below but not above p_c or at p_c. Finally, with R_s^{d-1} as the definition of surface area the clusters are never ramified in two dimensions. One may also use the density profile and thickness of the surface layer as criteria for ramifiedness; then one is likely to end up with ramified being identical to hydra-like and compact being the same as droplet-like. As discussed above, clusters are in this sense ramified below and at p_c but not above p_c. (If R_s^{d-1} is taken as a surface area, it may increase even faster than s with increasing s; e.g. in six dimensions we expect $R_s^{d-1} \propto s^{5(1+1/8)/6} = s^{5/4}$ at p_c. Such exponents larger than unity for the surface area are nothing unusual: The smallest sphere enclosing a random walk with s steps on a lattice has a surface area $\propto s^{(d-1)/2}$ in d dimensions.)

Later [97, 115, 129] Domb defined ramification more as a quantitative than a qualitative concept by regarding the cyclomatic number per site, $\lim_{s\to\infty}(c_s/s)$, as a measure of compactness for large clusters. More precisely, c_s was normalized [97] by the maximum cyclomatic number achieved in a fully compact cluster, without holes or surface roughness. The degree of ramification is then equal to unity minus the degree of compactness in this normalization. This ramifiedness decreases continuously with increasing p, as shown by Monte Carlo data [115], without any dramatic change at p_c. Ramifiedness in this sense therefore is drastically different from other criteria which may change from "yes" to "no" at p_c, as listed above. Clusters in the Ising model of ferromagnets at the Curie point were shown [129] to be less ramified than percolation clusters at p_c. If one uses the perimeter per site, $\lim_{s\to\infty}(t_s/s)$, as a measure of ramification one arrives at the same conclusion, fig. 12: Clusters below p_c are more ramified than above p_c, and at p_c they are more ramified than ferromagnetic Ising clusters at T_c [62, 75, 115]. (If the energy per site [32], $\lim(e_s/s)$, is taken as a measure of ramification for Ising ferromagnets, and the perimeter per site as measure of ramification for percolation, then Ising clusters are about as ramified as percolation clusters at their respective critical points [98].) Of course, ramification in this quantitative sense [97, 115, 129] is not a completely new concept but merely one of many quantities measuring internal structure and disorder, similar to the thermal energy per molecule or the entropy per cubic centimeter.

4.3.3. Fractal dimensions

Mandelbrot[136] introduced the word "fractals" to describe objects with fractal dimensions d' smaller than the Euclidean dimensionality d of the underlying lattice or space. This concept, which is an application of the Hausdorff–Besicovich dimension, was applied by Leath to percolation clusters [73]. Earlier, Reatto and Rastelli [134] in a discussion of the density profile of Ising clusters, used the

effective dimensionality $d' = 1/\sigma\nu$ but did not call it by any special name. For general background on fractals we refer to Mandelbrot's books [136]; percolation clusters are discussed more explicitely by Stanley [106] (see also recently Mandelbrot [137]). Roughly speaking, if the mass (or size s) of a system varies as (radius)$^{d'}$ then d' is the fractal or effective dimensionality and can be different from the Euclidean dimensionality d; in particular d' need not be an integer. We now review many different definitions, some of which giving the same result, and denote them consecutively by d_1', d_2', ...

Mandelbrot [136, p. 196] used a standard method for estimating the fractal dimension: He divided a large square lattice into G^2 equal squares, counted the number N of those that are intersected by the largest cluster, and determined d_1' through $N \propto G^{d_1'}$. (However, the value 1.78 that he found on p. 197 is presumably biased: B.B. Mandelbrot, private communication, November 1978.) A second standard method for estimating d' consists in taking circles or spheres of increasing size and measuring their contents or "mass". Forrest and Witten [138] estimated in this way the fractal dimension d_2' of two-dimensional electron-microscope pictures of large smoke particles consisting of many small iron spheres of uniform size. They counted the number N_l of small spheres in regions of linear extent l, and found $N_l \propto l^{1.6}$, giving a fractal dimension $d_2' \simeq 1.6$ which is clearly smaller than the Euclidean dimensionality $d = 2$. The latter would be found if the smoke particles would be spatially homogeneous and "compact". These dimensions d_1' [136] and perhaps also d_2' [138] are fractal dimensions, determined in a way close to the mathematical definition [136] of that concept. The other definitions listed below are less directly related to these mathematical procedures and are thus called "effective" dimensions in this review. Perhaps when this paper is published the relations between fractal and effective dimensions will already be clearer than at the time of this writing.

For percolation clusters at p_c the cluster density profiles $D_s(r)$ are all similar to each other according to eq. (41) and depend mainly on the ratio $r/s^{\sigma\nu}$, or equivalently on $s/r^{1/\sigma\nu}$. This similarity law suggests [134] to call $1/\sigma\nu$ an effective dimensionality d_3', since we may regard s as the "mass" of a cluster. Hyper-scaling, eq. (18), gives $1/\sigma\nu = d - \beta/\nu = d/(1 + 1/\delta)$. Thus

$$d_3'(p_c) = d/(1 + 1/\delta) \tag{42a}$$

is the effective dimensionality at $p = p_c$ as determined from the density profile. Also Harrison et al. [109], Kunz and Payandeh [79] and Mandelbrot [137] use this combination of critical exponent δ and lattice dimensionality d as the effective dimensionality or fractal dimension. More generally we may translate our definition $R_s \propto s^{\rho}$, eq. (39b), into $s \propto (R_s)^{d_3'}$ where this effective $d_3'(p) = 1/\rho$ is defined not only at or near the percolation threshold and differs in different regions for p:

$$d_3'(p > p_c) = d; \qquad d_3'(p = p_c) = d/(1 + 1/\delta); \qquad d_3'(p < p_c) = 1/\nu_0 \tag{42b}$$

according to eq. (39c); the last expression is about 3/2 in two dimensions [75].

In a different sense, Stanley [106] looks for a d' relating the *average* cluster size S with the *average* cluster radius R through $S \propto R^{d'}$ for $p \to p_c$. (The above definitions instead were based on $s \to \infty$ at fixed p.) How should one define these averages over all cluster sizes? (See also appendix 1.) If we use our "typical" cluster size s_ξ and typical cluster radius R_{s_ξ} for S and R we get an effective dimensionality identical to $d_3'(p_c)$, eq. (42a). If instead we define these averages through $S = \Sigma_s s^{k+1} n_s / \Sigma_s s^k n_s$, $R = \Sigma_s R_s s^{k+1} n_s / \Sigma_s s^k n_s$, we first have to distinguish whether we mean the full sums or only their nonanalytic parts. The singular parts give $S \propto s_\xi$ and $R \propto R_{s_\xi} = \xi$; and the resulting effective dimension d_4' with $s \propto R^{d_4'}$ is the same as $d_3'(p_c)$. If instead we do not subtract the analytic background from the sums, then we get again the same result for $k = 2, 3, 4, \cdots$ (provided d is smaller

than $\delta + 1$, which is the case for $d = 2$, 3 and 4). But for $k = 0$ and $k = 1$ different exponents result (details of how to evaluate such sums are explained in appendix 1): Close to the percolation threshold we have then $S = \text{const}$, $R = \text{const}$ for $k = 0$, and $S \propto |p - p_c|^{-\gamma}$, $R \propto |p - p_c|^{\beta-\nu}$ for $k = 1$. Thus with $k = 0$ we cannot define an effective dimensionality, and with $k = 1$ we get $d'_5 = \gamma/(\nu - \beta)$ which equals 2 for two dimensions and about 4 in three. Stanley [106] chooses $k = 1$ for the average cluster size s, which thus diverges with the exponent γ, but takes the typical cluster radius $R_{s_\xi} \simeq \xi$ for R, which thus diverges with exponent ν. Thus his effective dimension d'_6 is

$$d'_6 = \gamma/\nu = d \cdot \frac{1 - 1/\delta}{1 + 1/\delta}. \tag{43}$$

The same result is also obtained by Forrest and Witten [138] from the correlation function; it was also supported by Mandelbrot in his earlier papers [136] but rejected in his last work [137]. In two dimensions, eq. (42a) gives an effective dimension of about 1.9, whereas Stanley's eq. (43) gives about 1.8. The difference increases with increasing dimensionality d; e.g. in six dimensions we have $d'_3(p_c) = 4$ whereas $d'_6(p_c) = 2$.

Finally, Kirkpatrick [7] defines an effective dimension d'_7 by requiring that for $p \to p_c$ the mass within a region of linear extent ξ increases as $\xi^{d'_7}$. If one looks at the infinite network for p slightly above p_c, the number of network sites in such a region is about $P_\infty \xi^d \propto |p - p_c|^\beta \xi^d \propto \xi^{d-\beta/\nu}$; thus $d'_7 = d - \beta/\nu = d/(1 + 1/\delta)$ in this case, a result which agrees with $d'_3(p_c)$ in eq. (42a). But Kirkpatrick [7] also looks at other quantities X which vanish at the percolation threshold as $(p - p_c)^{\beta_x}$. Their effective dimension is $d'_8 = d - \beta_x/\nu$ and thus in general different from $d'_7 = d'_3(p_c)$. For example, his backbone of the infinite cluster has a β_x of about $\frac{1}{2}$ in two dimensions, giving an effective dimension of the backbone [7] as about 1.6.

We thus have seen that a variety of different definitions are possible, some of which lead to the same result for the effective or fractal dimension. The choice of eq. (42a), first suggested by Harrison et al. [109],

$$d' = d/(1 + 1/\delta)$$

seems to us particularly plausible for critical percolation clusters; moreover it is arrived at by the majority of definitions and authors [7, 79, 109, 134, 137]. The relations between some of these definitions are well understood in terms of percolation scaling and critical exponents. It seems likely [76] that similarity laws like eq. (41) will turn out to be relevant for a proof that the mathematically well defined [136] fractal dimension in the Hausdorff-Besicovich sense agrees with one of the effective dimensionalities d' discussed here.

In conclusion, concepts like the fractal dimension of droplet-like ramified clusters are useful catchwords if one knows what they mean in the given context. But they can also be misleading headlines when the real situation is somewhat complicated.

5. Lattice animals

So far we discussed properties of percolation clusters like the cluster numbers $n_s(p)$. These numbers then gave us other quantities like the moments $\chi \equiv \Sigma_s s^2 n_s \propto |p - p_c|^{-\gamma}$, involving sums over all cluster sizes s. In this sense the cluster numbers n_s of section 3 are more fundamental than the moments like χ derived from them. Now we go even one step further down to the basics and look at

eq. (7):

$$n_s(p) = \sum_t g_{st} p^s (1-p)^t .$$

Obviously the number g_{st} of geometrically different cluster configurations, which is independent of p, is more fundamental than the p-dependent number of percolation clusters, since the latter can be derived from the former according to the above equation. Moreover, the number g_{st} is simpler than the number $n_s(p)$ since it does not involve the concept of probability. Purely geometric counting is sufficient. In principle we thus reduced the whole percolation cluster problem to kindergarten mathematics: How can be put together s square pieces of a domino game?

The number g_{st} is also called the number of (lattice) animals since it refers to the question: How many different species of multicellular organisms can Nature form out of s single cells? (The word is due to Harary [139].) Domb [102] reviewed the mathematical background on these animals. The first scaling theory was attempted by Leath [73] whereas our scaling assumption here is taken from later papers [71, 89, 91, 126]. For animal numbers in subsection 5.1 we rely on refs. [42, 45, 48, 93]; most of the material in subsection 5.2 was not published before. We regret that in spite of the intrinsic simplicity of the problem our description is more mathematical here than in the other sections. Averages based on the g_{st} alone are "animal" properties, whereas percolation quantities use $g_{st}p^s(1-p)^t$ instead.

5.1. Scaling close to critical point

This part discusses the animal numbers g_{st} for perimeter-to-size ratios t/s near and below the critical point $(1-p_c)/p_c$; the following subsection 5.2 deals with those animals whose t/s-ratio is near the maximum of the perimeter distribution function for animals.

First one could think that g_{st} again equals, for large s and t near $t_c = s(1-p_c)/p_c$, a simple scaling expression analogous to our other assumptions like eq. (15):

$$g_{st} \propto s^{-\tau_1} \cdot f_1[(t-t_c)s^{\sigma_1}] .$$

But that assumption would be wrong as we will see now by deriving a presumably exact relation between g_{st} and $n_s(p)$, for all finite ratios t/s below $(1-p_c)/p_c$. That result (45b) will be different from the above speculation. Readers may proceed directly to that eq. (45b) if they dislike our formulas in between.

Throughout this section we denote the ratio t/s by a and the quantity $(1-p)/p$ by a_p. Thus percolation clusters at the threshold have an average a near a_c according to eq. (30a), and we may use our previous scaling results to get animal properties for a near $a_c \equiv a_{p_c}$. Let us define

$$g_{st} = \Lambda^s e^{sg} \Omega_{st} \tag{44a}$$

where

$$\Lambda = \Lambda(a) = (a+1)^{a+1}/a^a$$

is a function introduced by Leath [73], and

$$g = g(a) = \lim_{s\to\infty} \left[\frac{1}{s} \ln(g_{st}\Lambda^{-s})\right]$$

is the exponent for the leading exponential variation of the ratio g_{st}/Λ^s with size s, ref. [89]. Thus the

remaining factor Ω_{st} in eq. (44a) varies weaker with size s than the other factors: $\lim_{s\to\infty}[(1/s)\ln\Omega_{st}] = 0$ for all a. (These limits are taken at constant $a = t/s$ and are assumed to exist and to depend on a only.) For the numbers $n_s(p)$ of large percolation clusters we now get

$$n_s(p) = \sum_t \Lambda^s e^{sg}\Omega_{st} p^s (1-p)^t = \int \exp\{s[\ln\Lambda + \ln p + a\cdot\ln(1-p) + g(a)]\}\,\Omega_{st}\,dt. \tag{44b}$$

For large s the maximum of the integrand is determined by the brackets $[\cdots]$ since by definition the factor Ω_{st} is less important. The expression $\ln\Lambda(a) + \ln p + a\cdot\ln(1-p)$ has a maximum, as a function of a, at $\ln(a+1) - \ln(a) + \ln(1-p) = 0$, i.e. at $a = a_p \equiv (1-p)/p$, as required also by eq. (30a). The value of this expression at the maximum is zero, as the reader can easily check himself. Thus if the function $g(a)$ vanishes [89] we can calculate the above integral by expanding the bracket $[\cdots]$ quadratically in $a - a_p$:

$$\ln\Lambda + \ln p + a\cdot\ln(1-p) = \tfrac{1}{2}(a-a_p)^2\,[(a_p+1)^{-1} - a_p^{-1}] = -\tfrac{1}{2}(a-a_p)^2\cdot s/\Delta_s^2.$$

Our result $\Delta_s^2/s = a_p(a_p+1) = (1-p)/p^2$ again agrees with eq. (29) for the width of the perimeter distribution function. Eq. (44b) gives, with this assumption $g(a) = 0$,

$$n_s(p) = \int_0^\infty \exp[-\tfrac{1}{2}(a-a_p)^2\cdot s^2/\Delta_s^2]\,\Omega_{st}\,dt \simeq (2\pi)^{1/2}\Delta_s\Omega_{st}$$

with $t = a_p s$. From eq. (44a), with $e^{sg} = 1$, we thus find

$$g_{st} = n_s(p)\Lambda^s/(2\pi\Delta_s^2)^{1/2};$$
$$\Lambda = (a+1)^{a+1}/a^a; \qquad \Delta_s^2 = s(1-p)/p^2; \qquad a = t/s \tag{45a}$$

provided p is calculated through $t/s = (1-p)/p$ and the function $g(a)$ vanishes. Similar to a Laplace transform, we thus calculated g_{st} from $n_s(p)$.

When is this assumption $g(a) = 0$ correct on which eq. (45a) depends so much? We found above than $\ln\Lambda + \ln p + a\cdot\ln(1-p) + g(a)$ is zero at its maximum if g is zero. For nonzero g also this maximum will have a finite value M. Then the above evaluation of $n_s(p)$ will lead to a factor e^{sM} for n_s, apart from other factors varying weaker with s. Such a simple exponential decay of the cluster numbers for large cluster sizes s is possible only below p_c and not above p_c [90], as eq. (11b) shows. Thus M must vanish for p above p_c, corresponding to zero $g(a)$ for a below $a_c = (1-p_c)/p_c$. (See ref. [89] for more discussion of this point.) Thus we found eq. (45a) to be valid above p_c, i.e. for $a < a_c$, but not below p_c, i.e. not for $a > a_c$. For a below a_c we find $\lim_{s\to\infty}(g_{st})^{1/s} = \Lambda$ whereas in general we merely have the inequality $\lim_{s\to\infty}(g_{st})^{1/s} \leqslant \Lambda$ [88, 89]. More discussion of $\lim(g_{st})^{1/s}$ is found in ref. [91] which has been critized in ref. [140].

For a above a_c eq. (45a) cannot be valid exactly since fig. 12 has shown us already that for large clusters the ratio t/s no longer equals, in the average, $a_p = (1-p)/p$. But for p close to p_c, i.e. for a close to a_c, these deviations are quite small: $\lim_{s\to\infty}(t_s/s) - (1-p)/p \propto (p_c - p)^{\beta\delta-1}$ [126], as can be derived from eq. (31). Thus in the scaling regime of large clusters near the critical point we still may try eq. (45a) on both sides of a_c, at least for $\sigma < \frac{1}{2}$. With $n_s \propto s^{-\tau} f[(p-p_c)s^\sigma]$ and $\Delta_s \propto \sqrt{s}$ we get [71, 73, 126]

$$g_{st} \propto s^{-\tau-1/2}\cdot\Lambda^s\cdot f(z) \tag{45b}$$

where

$$z = (p-p_c)s^\sigma = (a_c - a)s^\sigma/(1+a)(1+a_c) \simeq (1+a_c)^{-2}(a_c-a)s^\sigma = p_c^2(a_c-a)s^\sigma.$$

Eq.(45b) is the scaling result for the animal numbers promised at the beginning. It differs by Leath's factor Λ^s from the speculation mentioned there. (Note that Λ^s can be rewritten in the symmetric form $(t+s)^{t+s}/t^t s^s$.) Direct numerical tests of eq. (45) are difficult [73] but it may look more reliable if one knows that it was first postulated [126] without this derivation and gave correct results for the perimeter distribution function of percolation clusters, section 4.1.

Thus we derived a presumably exact expression (45a) for large animals with $0 < t/s < a_c$ and a scaling assumption (45b) for t/s near a_c. Only an explicit result for t/s much larger than a_c is missing. Since in a triangular lattice $a = t/s$ can vary between zero and two for large clusters and since $a_c = 1$ there, one could first think that we solved more than half of the animal problem. But this is not so, as one can see from fig. 19: Most of the animals have a ratio $a = t/s$ near a_0 which is larger than a_c. (We can see this effect already from fig. 12 where $p = 0$ corresponds to animals.) For example, in the square lattice we have $a_0 = \lim_{s\to\infty}(t_s/s) = 1.2$ for animals [52, 75] but $a_c = \lim_{s\to\infty}(t_s/s) = 0.7$ for critical percolation clusters, eq. (30a). Thus for large s the difference between the average animal perimeter and the average percolation perimeter at p_c is about $0.5\,s$ in the square lattice (and about $0.6\,s$ in the triangular, $0.3\,s$ in the honeycomb lattices [52]). The width of the perimeter distribution function increases only as $s^{1/2}$. Thus for increasing s the region of t/s below a_c covers only an exponentially decreasing small fraction of the wings of the animal distribution. Therefore the next subsection 5.2 deals with the behavior near a_0 where most animals live, not with the few domesticated animals near a_c or below a_c which obey eq. (45).

Why is the animal problem a percolation problem at $p = 0$, as mentioned above [52, 75]? (Note that we keep s fixed and look at the average t_s over all perimeters.) The animal perimeter t_s is defined as $\Sigma_t\, t \cdot g_{st}/\Sigma_t\, g_{st}$, the percolation perimeter as

$$t_s = \sum_t t \cdot n_{st} \Big/ \sum_t n_{st} = \sum_t t \cdot g_{st} p^s (1-p)^t \Big/ \sum_t g_{st} p^s (1-p)^t = \sum_t t \cdot g_{st} (1-p)^t \Big/ \sum_t g_{st} (1-p)^t$$

according to eq. (28a). For p close to zero the factor $(1-p)^t$ cancels out, provided various limits can be interchanged. Indeed figs. 12 and 14 show that the limit $p \to 0$ agrees with the result at $p = 0$, as expected: At fixed size s the animals are the $p \to 0$ limit of percolation clusters. In the method of section 2.2.3 thus simply all "animal" configuration were taken as equally probable by putting $p = 0$ in the percolation computer simulation.

Figure 16 shows that the density profiles of large animals are similar to each other, $D_s(r) = s^{-0.334\pm0.010} \cdot \tilde{D}_4(r/s^{0.660\pm0.007})$, analogously to eq. (41) but with different exponents [76]. The perimeter t_s for animals obeys $t_s = a_0 s + \text{const}$ according to series [52] and Monte Carlo [75] results, compatible with the behavior expected for percolation clusters below p_c, eq. (29).

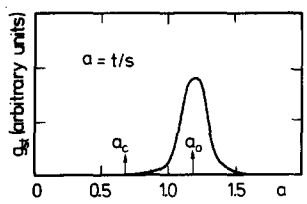

Fig. 19. Distribution of animal perimeters in the square lattice at $s \sim 10^2$. Critical percolation clusters have t/s near $a_c = (1-p_c)/p_c = 0.7$ whereas most animals have a larger perimeter with t/s near $a_0 = 1.2$, as can be seen from fig. 12. (Schematic.)

5.2. Exponents away from the critical point

To get the number of animals g_{st} in the region $t/s \simeq a_0$ above a_c we assume that the distributions are Gaussian peaks with a width increasing as $s^{1/2}$ for large s:

$$g_{st} = (c/2\pi s)^{1/2} \exp[-\tfrac{1}{2}c(a-a_0)^2 s] \cdot g_s \qquad (s \to \infty,\ a = t/s) \tag{46a}$$

$$g_s = \sum_t g_{st}. \tag{46b}$$

Here $a_0 = \lim_{s\to\infty}(t_s/s)$ and c are suitable constants to be determined later. First we will deal with the total number g_s of s-animals, eq. (46b).

Similar to our $g_{st} \propto s^{-\tau-1/2}\Lambda(a_c)^s$ at the critical point $a = a_c$, eq. (45b), Sykes et al. [42, 45] assume $g_s \propto s^{-\theta} \cdot \lambda^s$ with two free parameters θ and λ. Following a suggestion of Domb [102], Guttmann and Gaunt [93] fit the same series results more generally for large s by

$$g_s \propto s^{-\theta} \cdot \lambda^s \cdot \exp(-\text{const} \cdot s^{-\omega}) \tag{46c}$$

with a third exponent ω to be determined by "experiment" also. (ω is related but not identical to the exponent ω in correction-to-scaling theories [87].) If ω would be negative then the exponential factor in eq. (46c) would be more important, for large s, than the prefactor $s^{-\theta}$, casting doubt on the older analysis [42, 45] for θ as well as on analogous assumptions like eq. (27) for percolation cluster numbers. Fortunately ω turned out to be positive, whence we may expand $\exp(-\text{const} \cdot s^{-\omega}) = 1 - \text{const} \cdot s^{-\omega}$ in eq. (46c). This correction factor is entirely analogous to eq. (22) for $n_s(p_c)$. Even the numerical value obtained in two dimensions, $\omega = 0.75 \pm 0.1$, is consistent with the correction exponent of about 0.7 obtained for eq. (22) from Monte Carlo [26] and series [19] data. Thus there is at present no reason to doubt the validity of $g_s \propto s^{-\theta} \cdot \lambda^s$ for large enough s. The exponents θ and ω are supposed to be universal, i.e. to depend on the dimensionality d only. For example, $\theta(d=2) = 1.00 \pm 0.01$ [93]. For higher dimensions this exponent θ was listed already in ref. [45, table II]; for $d = 3$ we have [93] $\omega = 0.65 \pm 0.2$. The parameter λ depends on the lattice type; we have [93] $\lambda = 4.063 \pm 0.002$, 5.183 ± 0.001 and 8.34 ± 0.02 for the square, triangular, and simple cubic lattice, respectively.

In eq. (27) we have used the same exponent θ for percolation clusters below p_c as for the animal numbers in eq. (46c), since again the animal θ is the $p = 0$ limit of the percolation $\theta(p)$: If the limits $p \to 0$, $s \to \infty$ can be interchanged, then

$$n_s(p \to 0) = \sum_t g_{st} p^s (1-p)^t \simeq \sum_t g_{st} p^s \propto s^{-\theta}(\lambda p)^s.$$

Thus for sufficiently small p, the disturbing factor $(1-p)^t$ cancels out, and the numbers g_s of animals become identical to the cluster numbers n_s,

$$n_s(p \to 0) = g_s p^s [\propto s^{-\theta}(p\lambda)^s \text{ for } s \to \infty] \tag{46d},$$

apart from a simple factor p^s. Therefore, for g_s and $n_s(p \to 0)$, also the two exponents θ agree. Indeed, numerical analysis [49] of series data [42] gave $\theta(p \to 0) = 1.0$ from the cluster numbers $n_s(p)$, in full agreement with the exponent determined from the animal numbers for the same (triangular) lattice. (See also ref. [80].)

Now we explain the value $\lambda = 4.06$ in the square lattice, eq. (46c), by using our numerically determined percolation perimeters of fig. 12. Let $a_\infty = a_\infty(p)$ be the average perimeter-to-size ratio

$\lim(t_s/s)$ for large clusters below the percolation threshold, where $a_\infty = (1-p)/p$ no longer is valid. We abbreviate $\lim_{s\to\infty}((1/s)\ln n_s)$ by $g_1 = g_1(p)$; this function vanishes for all p above p_c according to eq. (11b). For large clusters, eq. (28c) gives $a_\infty = (1-p)/p - (1-p)\mathrm{d}g_1/\mathrm{d}p$, that means

$$g_1(p) = \ln(p/p_c) + \int_p^{p_c} \frac{a_\infty(p')}{1-p'}\,\mathrm{d}p'.$$

On the other hand for p near zero we have, as mentioned above, $n_s \propto s^{-\theta}(\lambda p)^s$, and thus $g_1(p\to 0) = \ln\lambda + \ln p + O(p)$. In the comparison of these two results for g_1 the diverging term $\log(p)$ cancels out, and we get

$$\ln\lambda = \ln(1/p_c) + \int_0^{p_c} \frac{a_\infty(p)}{1-p}\,\mathrm{d}p. \tag{47a}$$

With the known data for $a_\infty(p)$, fig. 12, and the numerical integration of eq. (47a) we get $\lambda = 4.1 \pm 0.1$ in the square lattice, only one percent larger than the true result 4.06 from series approximations [42].

With similar methods we may even improve on the simple approximation (46a) to get the leading s-dependence of g_{st} for most ratios t/s, not only near $t/s = a_0$ and $t/s = a_c$, the "animal" and "percolation" averages. (As before we assume the limit of s and t going to infinity at constant ratio a to exist and to be a smooth function of a.) Equation (44b) tells us that $a_\infty(p)$ is determined by the maximum of the function $\ln\Lambda + a\ln(1-p) + g(a)$, with p fixed and a as variable. Since the a-derivative vanishes at the maximum, we get $-\mathrm{d}g/\mathrm{d}a = \ln[(1+1/a_\infty)(1-p)]$ as the condition for $a = a_\infty$. Integration gives

$$-g(a) = \int_0^a \ln[(1+1/a_\infty)(1-p(a_\infty))]\,\mathrm{d}a_\infty \tag{47b}$$

where again the relation between a_∞ and p e.g. from fig. 12 can be used. (It does not matter whether the integration in eq. (47b) starts at zero or at a_c since for all a_∞ below a_c we have $a_\infty = (1-p)/p$, eq. (30a). Thus the logarithm in eq. (47) and $g(a)$ vanish there.) Figure 20 plots semiquantitatively this function $g(a)$ for the square lattice.

Equation (44a) gives $\lim_{s\to\infty}((1/s)\ln g_{st}) = \ln\Lambda + g(a)$ with $a = t/s$; and for $a \to a_0$ we have from eqs. (46, 47a) $\lim_{s\to\infty}((1/s)\ln g_{st}) = \ln\lambda$. Comparison gives, with the help of eq. (47b):

$$\lambda = \Lambda(a_0)\cdot \mathrm{e}^{g(a_0)}; \qquad g(a_0) = \int_0^{a_0} \ln[(1+1/a_\infty)\,(1-p(a_\infty))]\,\mathrm{d}a. \tag{47c}$$

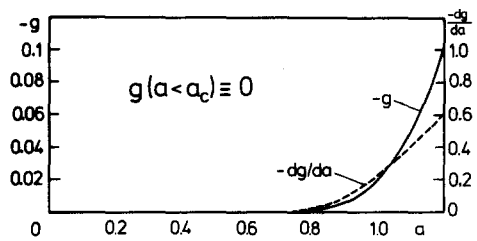

Fig. 20. Estimate of the (negative) function $g(a)$ and its derivative, eq. (44a).

Since $a_0 = 1.2$, fig. 12, and $g(a_0) = -0.1$, fig. 20, for the square lattice we thus have

$$\lambda = [(a_0+1)^{a_0+1}/a_0^{a_0}]e^{g(a_0)} = 4.1,$$

again in excellent agreement with the desired result [42]. We may also determine $g(a_0)$ from a_0 and λ, as given by Duarte [52] for the triangular and square lattice, and again find $g(a_0) = -0.1$. We see no reason, however, that this quantity should be exactly universal. The numerical agreement found for $\lambda \simeq 4.1$ in the square lattice seems to be the only test of this animal theory known at present.

(The constant c in eq. (46a) is given [89] by $c = a_0^{-1}(1+a_0)^{-1} - g''(a_0)$, which is about 2.4 in the square lattice. An unexplained exponent is the relation [48] $s_t \propto t^{3/2}$ for animals where the perimeter t is fixed and one looks at the average size of animals which have a given perimeter.)

Let us summarize our animal results here: For the leading s-dependence of the animal numbers g_{st} we have a general result (for $0 < t/s \leqslant a_0$)

$$g_{st} \sim \Lambda^s e^{sg} \qquad (\Lambda \equiv (a+1)^{a+1}/a^a) \tag{48a}$$

with $a = t/s$, and a function $g(a)$ given e.g. by fig. 20; g vanishes for a below $a_c = (1-p_c)/p_c$. Near $a = a_c$, the region relevant for percolation scaling, also the prefactors neglected in eq. (48a) are important and lead to eq. (45b):

$$g_{st} \propto s^{-\tau-1/2} \cdot \Lambda^s \cdot f[p_c^2(a_c - a)s^\sigma]. \tag{48b}$$

The scaling function here is the same as that for the percolation cluster numbers in eq. (15), since rather generally the cluster numbers and animal numbers are closely related by eq. (45a), for p above p_c. In this sense the problem of most animal numbers seems solved in the asymptotic limit: In genera! the function $g(a)$ in eq. (48a) describes the leading dependence on s; and the additional prefactors needed for percolation scaling are given in eq. (48b).

6. Other percolation problems

6.1. Random resistor networks

Already in subsection 1.1 we mentioned the question: how does an electric current flow through an inhomogeneous medium? Imagine than each elementary cell or small cube of a large simple-cubic lattice is randomly either a piece of electrically conducting copper (with probability p) or a piece of insulator (with probability $1-p$). An electric current is supposed to flow from one copper piece to its neighbor only if both cubes have one surface in common; no electrical connection is made by the edges or corners alone. Then an electric current flows through the whole lattice only if an infinite network of copper pieces is present, i.e. for p above p_c only. Let us for simplicity set the copper conductivity equal to unity and the length of the lattice also equal to the unit length. The size of the elementary cube and the coherence length are then much smaller than unity. A unit voltage is applied to two opposing faces (of unit area) of the lattice. The current now flowing through the lattice is called the conductivity $\Sigma = \Sigma(p)$. We review this property only shortly here since our review concentrates on percolation clusters. References [7, 13, 14, 15, 141–146] give real or computer experiments, and refs. [7, 146] review the scaling theory of conductivity.

Close to the percolation threshold p_c a positive exponent μ (also called t) can be defined through [3]

$$\Sigma \propto (p - p_c)^\mu; \tag{49}$$

the conductivity is zero below p_c. Table 2 already listed numerical estimates for this exponent, but they are in general less accurate than those for some other exponent. For example, two-dimensional Monte Carlo data [7] give $\mu = 1.10 \pm 0.05$ whereas a series prediction [108] is $\mu \simeq 1.43$. Our estimate $\mu \simeq 1.2$ in table 2 is therefore not very accurate. How can we relate this new exponent μ to our earlier exponents like σ and τ?

Following Skal et al. [5, 141, 147] we imagine the infinite network slightly above p_c to consist mainly of one-dimensional channels with a few crosslinks, fig. 21. The distance between two nodes is of the order of the coherence length $\xi \propto |p - p_c|^{-\nu}$ whereas the length of the chains connecting the nodes can be longer and is assumed to diverge as $(p - p_c)^{-\zeta'}$, with a new exponent ζ' (in the literature our prime is usually omitted). Of course this picture of one-dimensional channels is only an approximation [3] and requires that we remove all dead ends of chains which contribute to the percolation probability P_∞ but not to the conductivity Σ. Even then this "backbone" of the infinite network looks in reality [7, 148] quite different from the above picture, fig. 21. Since modifications make it more complicated without giving a simple generally accepted result [147] we still use here the simple picture of channels to calculate Σ, even though it may be wrong for $d = 2$.

Since the distance between two roughly parallel, current-carrying channels is of order ξ, the total number of such paths in our lattice is about $1/\xi^2$ in three and $1/\xi^{d-1}$ in d dimensions. Each path leads from the top to the bottom of the lattice and thus consists of about $1/\xi$ one-dimensional chains sections separated by nodes. Each section between two nodes has a length $\propto (p - p_c)^{-\zeta'}$; and thus a whole path leading from top to bottom has a length $\propto (p - p_c)^{\nu - \zeta'}$ and a conductivity $\propto (p - p_c)^{\zeta' - \nu}$. Taking together all $\xi^{1-d} \propto (p - p_c)^{(d-1)\nu}$ such paths we find their combined conductivity to vary as $\Sigma \propto (p - p_c)^{(d-1)\nu + \zeta' - \nu}$. Thus the conductivity exponent is [141]

$$\mu = \zeta' + (d - 2)\nu. \tag{50}$$

It is tempting to assume [141] $\zeta' = 1$, i.e. $\mu = 1 + (d - 2)\nu$. Then we have $\mu = 1$ exactly, apart from possible logarithmic correction factors [149], in two dimensions. This result may be compatible with the most recent computer simulations [7] and agrees with the epsilon expansion near six dimensions [108, 147]. (In six dimensions we have [149] $\mu = 3$ and $\zeta' = 1$.) But in two dimensions this assumption $\zeta' = 1$ together with $\nu \simeq 1.35$ makes the above picture internally inconsistent: Then the length of the chain segments connecting two nodes at distance ξ would have to be smaller, not larger, than this distance ξ if p is sufficiently close to p_c. Perhaps we have $\zeta'(d < 4) \neq 1$ but $\zeta'(d > 4) = 1$ [108, 149]. For example, $\zeta'(d = 2) = \nu$ has been suggested [150]. Or perhaps there is no simple relation between the conductivity exponent μ and the cluster exponents like σ and τ. Contrary to our understanding of

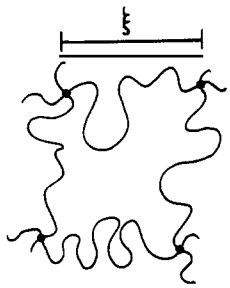

Fig. 21. Approximation for the structure of the infinite current-carrying network of resistors. The true distance between the nodes is of order $\xi \propto (p - p_c)^{-\nu}$, whereas the length of the chain segments connecting the nodes diverges as $(p - p_c)^{-\zeta'}$, $\zeta' = 1$, ref. [141].

cluster numbers and other cluster properties, no drastic improvement seems to have occured for the scaling theory of percolation conductivity since the older reviews [3] were written.

More fruitful were scaling ideas for relations between different conductivities if good and bad conductors are mixed, instead of conductors and insulators. Then the conductivity at $p = p_c$ is not zero; it increases smoothly with increasing concentration p of good conductors. Let R_{cond} be the ratio of the conductivity of "bad" conductors to "good" conductors (set equal to unity again). Now the total conductivity Σ depends on the two variables $p - p_c$ and R_{cond}. References [146, 150–152] make a scaling assumption of the same type as we have seen it repeatedly in this review:

$$\Sigma(p, R_{cond}) = (R_{cond})^{u} \cdot \phi[(p - p_c)(R_{cond})^{-u/\mu}]. \tag{51a}$$

In this assumption analogous e.g. to eq. (15) a new exponent u and a new scaling function $\phi = \phi(y)$ are introduced. For $R_{cond} = 0$ we have again a mixture of conductors and insulators and must recover eq. (49). Thus the scaling function $\phi(y)$ varies for large arguments y as y^{μ}, and then R_{cond} cancels out of the conductivity in eq. (51a). (More precisely we constructed eq. (51a) such that R_{cond} cancels out for $R_{cond} = 0$, as required by eq. (49).) Right at $p = p_c$ it is the difference $p - p_c$ which has to cancel out; thus $\phi(0)$ has to remain finite, giving $\Sigma \propto (R_{cond})^{u}$. Finally, below p_c for small R_{cond} the conductivity must be proportional to R_{cond} since then the bad conductors, not the good ones, give the main contribution to the resistivity. Thus $\phi(y \to -\infty) \propto (-y)^{\mu - \mu/u}$, or $\Sigma \propto R_{cond}(p_c - p)^{\mu - \mu/u}$. We now summarize these three cases $y \to +\infty$, $y \to 0$, and $y \to -\infty$:

$$\begin{aligned} &\Sigma \propto (p - p_c)^{\mu} && (R_{cond} \to 0 \text{ above } p_c) \\ &\Sigma \propto (R_{cond})^{u} && (p = p_c) \\ &\Sigma \propto (p_c - p)^{\mu - \mu/u} \cdot R_{cond} && (R_{cond} \to 0 \text{ below } p_c). \end{aligned} \tag{51b}$$

(The positive exponent $\mu/u - \mu$ is called s by Straley [146]; the exponent u is called s by Efros and Shklovskii [151]; and both papers denote our μ as t.) In the above discussion we took the "good" conductivity as unity and the bad one as R_{cond}; otherwise all results in eq. (51b) must be multiplied by the "good" conductivity. If we mix a superconductor (infinite conductivity) with a normal conductor, this latter formulation has to be used; below p_c the conductivity then diverges as $(p_c - p)^{\mu - \mu/u}$ multiplied with the normal ("bad") conductivity arising from the factor R_{cond} in eq. (51b).

In two dimensions duality arguments [151, 153] give $u = \frac{1}{2}$ exactly, and thus $\mu/u - \mu = \mu$: The conductivity of a metal-insulator mixture film vanishes above p_c with the same exponent as the resistivity of a superconductor-metal film vanishes below p_c (Levinshtein [128]). In three dimensions one has [146] $u \simeq 0.7$ and thus $\mu/u - \mu \simeq 0.7$ whereas $u = 1$ in six dimensions. Further exponents are listed by Straley [146] and, for μ only, by our table 2.

Experimentally we mention the possibility [145] of varying $p - p_c$ very finely by using the dependence of the volume fraction p on temperature, if the two materials mixed together have two different coefficients of thermal expansion; a reasonable exponent $\mu \simeq 1.8$ was found in this way for three dimensions. For more experiments see refs. [9, 143, 146]. Also the Hall effect in a resistor network and the influence of random capacitors have been discussed [3, 154, 155].

6.2. *Modifications of percolation*

6.2.1. *Miscellaneous*

BOND PERCOLATION: What we discussed so far was mainly the site percolation problem with nearest-neighbor bonds. One can also look at "bond percolation" where each lattice site is occupied

and where each bond connecting two neighbors is randomly in one of two states. This bond percolation problem seems to belong to the same universality class as site percolation, e.g. it is described by the same exponents [105, 107]. Also for the resistor network, the bond percolation problem refers to mixtures of conducting and insulating connections between lattice sites. Actually some of the numerical exponents quoted earlier refer to the bond problem, not to site percolation. For a combination of site and bond percolation we refer to ref. [156]. In special cases [2], bond percolation is transformed exactly into site percolation in a different lattice.

LONG-RANGE INTERACTION: Most percolation studies define a cluster as a group of occupied sites connected by nearest-neighbor distances. Again the universality concept asserts that the scaling behavior (critical exponents; shape of the scaling functions) does not change if also next-nearest neighbors are taken into account as parts of the same cluster, or if even longer ranges of interaction are used. Work on the bcc lattice with nearest and next-nearest neighbors showed no peculiarities [26, 69] compared with simpler lattices; and even longer ranges of interaction showed the same critical exponents [24].

In the opposite direction goes a recent attempt to describe dilute magnetics where the local magnetic moment is formed only if sufficiently many magnetic atoms are clustered together. Thus each site in a cluster is required [157] to have at least m occupied sites as nearest neighbors. It is not yet clear [157] if the scaling behavior of this model differs from the usual percolation problem (corresponding to $m = 1$).

POLYCHROMATIC PERCOLATION: If each lattice has not one but several states it can be in, the lattice now is no longer just black and white. Little is known [158] on cluster properties so far.

TREES ON A LATTICE: If in bond percolation on a lattice the clusters are restricted to be tree-like, with no cyclic bonds allowed (cyclomatic number = zero) then the scaling behavior is different from ordinary percolation. This problem corresponds [21, 82] to the zero-state Potts model of section 2.3.2; according to Wu [82] no phase transition occurs on the square lattice.

6.2.2. Continuous percolation

A major unsolved problem for percolation scaling is the question: How important is the existence of a lattice structure? Are the exponents the same if the sites are distributed randomly in a continuum instead of on a lattice? Computers like to have the sites on a square or simple cubic lattice, but many random processes in nature happen in a continuum, not on a periodic structure. The problem is analogous to a question in thermal phase transitions: Are the critical exponents calculated in a lattice gas (Ising) model of fluids the same as those observed at real liquid-gas critical points of, say, H_2O? In the lattice gas the molecules are restricted, similar to lattice percolation, to sites of a periodic lattice whereas in real water they can move more freely. Recent high-precision measurements and improvements in the theoretical lattice-gas predictions seem to allow the conclusion that in three dimensions the exponents are (nearly) independent of the lattice [159]. For percolation, the renormalization group approach also suggests the lattice to be unimportant. Monte Carlo cluster numbers of Fremlin [160] for continuum percolation seem not accurate enough to give critical exponents. We refer to Webman et al. [161; see also 145] for the exponent μ of random resistor networks in a continuum; earlier literature is cited there. More information on continuum percolation seems needed to arrive at clear conclusions.

6.2.3. *Interacting percolation*

What happens if the probability of one site to be occupied depends on whether or not its neighbors are occupied? A simple model to incorporate such correlations, which are ignored in random percolation discussed so far, is the Ising model of ferromagnets (or lattice gas model for fluids) at finite temperatures T. Here probabilities are proportional to $\exp(-E/k_B T)$ where E is the energy of a given configuration. In the Ising model we define

$$E = -J \sum_{i<j} \sum S_i S_j - H \sum_i S_i; \qquad S_i = \pm 1. \tag{52}$$

The double sum runs over all pairs of nearest neighbors on a lattice. If the "spin" S_i is positive we call the site i occupied; it is empty for negative S_i. The concentration $p = \frac{1}{2}(1 + \langle S_i \rangle)$ of occupied sites is varied by the "field" H (chemical potential); the larger H is the larger is p. ($\langle S_i \rangle$ is the average over many configurations for one site i or, equivalently, the average over all sites excluding those influenced by the boundaries of the system.) Clusters of occupied sites were investigated with this model in two and three dimensions, starting with refs. [33, 35]. In two dimensions one has $p_c = \frac{1}{2}$ [162 with earlier refs.], which agrees with the "Curie point" at T_c for magnetic properties. (For $H = 0$ the "magnetization" $\langle S_i \rangle$ is nonzero only for T below T_c.) The second moment $\Sigma_s s^2 n_s$ diverges for $H = 0$ as $(T - T_c)^{-\gamma}$, $\gamma \simeq 1.91$ in two dimensions [163]; this exponent is smaller than the corresponding $\gamma \simeq 2.43$ for random percolation, table 2, but larger than the exponent 1.75 for the magnetic susceptibility $\mathrm{d}\langle S_i \rangle / \mathrm{d}H$ at $H = 0$.

In three dimensions, unfortunately the percolative and the magnetic phase transition happen at different critical points, i.e. the threshold for interacting percolation is at a concentration $p_c(T)$ smaller than the concentration $\frac{1}{2}$ where the Curie point is located [35, 162]. Thus if one wants to describe the three-dimensional Curie point by a cluster model [34] one has to define "clusters" differently: No longer are they just groups of parallel spins with nearest-neighbor connections, as assumed in the Monte Carlo studies [35, 37]. Instead they may represent fluctuations in an averaged local magnetization [36, 96, 120, 127]. But little progress has been made in putting these ideas into a definition simple enough for computer handling.

Recent progress in two dimensions makes the situation more hopeful there [25, 115]. Since Curie point and percolation threshold agree in two dimensions [162] we may still define clusters as usual. At $H = 0$ near T_c the radius of typical percolation clusters diverges with the same exponent $\nu = 1$ as the spatial range of magnetic correlations, $\xi \propto (T - T_c)^{-\nu}$, ref. [25]. For fixed temperature T above T_c the typical cluster radius diverges as $(p_c - p)^{-\nu}$, with the same $\nu \simeq 1.35$ as for random percolation [25]. The cluster numbers at $T = 2T_c$ obey roughly a scaling relation like eq. (15); but the scaling function $f[(p - p_c)s^{\sigma}]$ seems to have a shape different from that observed in random percolation [115]. Thus, in spite of the results of Klein et al. [25] for the correlation exponent, the interacting percolation problem does not share the same universality class with the random percolation problem, not even in two dimensions.

Random percolation in this Ising model corresponds to infinite temperature T and infinite field H at finite ratio H/T. For then the interaction between neighboring sites, which influences the occupation probabilities through the ratio $J/k_B T$, is negligible. Thus percolation can be regarded as both the infinite-T and the zero-T limit of suitable magnets. (An even more complicated system [164], the magnetic alloy, has on each lattice site one of two sorts of atoms; and each atom has a magnetic moment which points either up or down.) Monte Carlo studies of these Ising clusters at finite temperatures are not only relevant for percolation but also for other questions, see ref. [165] for a recent paper with earlier references.

6.2.4. Dilute magnets at finite temperatures

The influence of finite temperatures is also a major problem for the dilute magnets of section 1.1, which were discussed there only at $T = 0$. At nonzero temperatures thermal motion can break the exchange interaction between two magnetic moments within one cluster and make them antiparallel. Then the methods of section 1.1 break down. Better theories have to distinguish between isotropic (Heisenberg) and anisotropic (Ising) magnets.

In the *isotropic* case one may look at "spin waves" as statistically independent thermal excitations; these "magnons" are harmonic waves in the direction of the local magnetization, just as sound waves are harmonic waves in the local mass density. It turns out [3, 166] that the frequency of these spin waves varies near p_c as $(p - p_c)^{\mu-\beta}/(\text{wavelength})^2$, with the exponents β and μ for percolation probability and conductivity, respectively. With this spin-wave approximation the variation of $T_c(p)$ near p_c and the dependence of thermodynamic properties on temperature for $T \to 0$ has been estimated. For example, $T_c(p)$ approaches $T_c(p_c) = 0$ roughly linearly in p. We refer to Shender [167] for details and earlier literature.

For *anisotropic* magnets the phase transition temperature $T_c(p)$ vanishes near p_c as $1/\log(p - p_c)$. The behavior near this transition is described by exponents which are in general neither those of the pure magnets nor those of percolation. We refer the reader to Lubensky's recent review [168].

7. Conclusions

This review centered on the scaling theory of percolation clusters: How do the properties of clusters depend on the cluster size s, and how does the phase transition at p_c enter these properties? The answers to these questions were described by several exponents σ, τ, θ, ζ, ρ. Of these five exponents, σ and τ (and the critical exponents α, β, γ, δ, ν derived from them) are defined only near the percolation phase transition $p = p_c$, whereas the asymptotic behavior of cluster numbers and radii for $s \to \infty$ defines ζ, θ, ρ both far away and near p_c through eqs. (23, 27, 39b). We saw that the latter exponents were different [70] above and below p_c; for example, $\zeta(p < p_c) = 1$ and $\zeta(p > p_c) = 1 - 1/d$ in d dimensions, eq. (26). On the other hand, the critical exponents σ and τ are the same on both sides of the phase transition and describe the cluster numbers there through eq. (15), a generalization of the Fisher droplet model [34]. Analogous expressions were proposed, as summarized in eq. (42), for the excess perimeter, the radius, and the density profile of clusters. Such simple scaling assumptions are familiar from thermal phase transitions. We also saw two examples where scaling expressions like eq. (42) are invalid: For the number of animals it is g_{st}/Λ^s, and not g_{st} itself, which follows a scaling form, eq. (45b). And for the perimeter distribution, no scaling assumption like eq. (35) is valid. The universality concept states that exponents and the shape of scaling functions do not depend on microscopic details like lattice structure. We saw this assumption confirmed in general, but an exception will be discussed in appendix 2.

In this sense the percolation clusters can serve as a simple introduction to scaling theory of critical phenomena at phase transitions [12]. For percolation the definition of the problem is particularly simple. It requires little background knowledge like thermodynamics, magnetism etc., for percolation merely combines geometry with probabilistic aspects. The more fundamental "animal" problem of section 5 even avoids the probabilistic concepts. Thus the animal problem, how to put together a given number of dominoe squares, is defined on a kindergarten level. In high school we may ask for the average number of percolation clusters obtained by flipping coins at concentration $p = \frac{1}{2}$. Different

quantities are related to each other by scaling theory, which requires sometimes college-level mathematics. More complicated "graduate" work is required to produce these quantities (like cluster numbers on a computer, or exponents in renormalization theory). Our review skipped over these complications but also pointed out unsolved problems.

In order to bring this review up-to-date we also covered problems, particularly in section 4, where no consensus is evident from the present literature. Only the cluster numbers of section 3 have been confirmed by different authors with a variety of methods. Thus future research may not only put more emphasis on points neglected here; it may also invalidate some conclusions particularly in section 4. Figure 1 suggested already quite clearly that percolation is not yet solved entirely. As mentioned at the beginning, the reader will get a more balanced view by reading other reviews, too [5–9]. We also refer to these reviews for a discussion of experiments, like the famous spread of disease in orchards [1–3]. Such experiments have seldomly given information on the cluster properties emphasized here.

Further research in the immediate future could center on testing scaling assumptions by Monte Carlo work. The majority of present Monte Carlo studies is restricted to two dimensions. But three dimensions are more relevant for applications, and higher dimensionalities are of theoretical interest to study the transition to classical behavior at the phase transition. Continuum percolation is more complicated but also more realistic than the lattice percolation emphasized here. A discussion of cluster properties by renormalization group techniques has barely started [79, 80, 114]. What cluster radii do series methods predict? Of course, should an exact solution [25] of percolation become available, such approximate methods would be only of historic and didactic value.

Even within the phenomenological scaling theory many questions are still open: Is the conductivity exponent μ related to the cluster exponents σ and τ? How can we explain the exponent θ of eq. (27) below p_c, and what is its true value above p_c? Why is the radius exponent ν_0 below p_c close to $\frac{2}{3}$ in two dimensions? What happens if clusters and animals are characterized by their perimeter t instead of their size s [48], particularly near $p = 1$? Which of the modifications of percolation mentioned shortly in section 6 form a new universality class?

This review was a snapshot of the situation in December 1978, as seen by the author. Thus we conclude, for the reader's amusement, with a historical remark. During the nineteen-thirties J.E. Mayer was one of the founders of cluster theory for collective phenomena, as developed here in detail for percolation near p_c. In a review of his "Statistical Mechanics" textbook it was asserted quite recently [169] that "the Mayer theory is no longer an active area of research in statistical mechanics". Mayer, in his reply [151], admits that the cluster development "certainly is obsolete in treatments of critical phenomena". Throughout most of this review we explained critical phenomena by clusters. Thus we hope to have convinced the reader that it is Mayer's recent remark and not his original ideas which are "obsolete". One merely has to select the right phase transition to study clusters: The percolation problem.

We thank numerous researchers in the field for helping us throughout many years with preprints, discussions and criticism. K. Binder, J.A.M.S. Duarte, H.J. Herrmann, W. Kinzel, S. Kirkpatrick, B.B. Mandelbrot, H. Müller-Krumbhaar, S. Redner, the referee, and in greatest detail P.J. Reynolds and H. Nakanishi helped to improve earlier versions of this paper.

Appendix 1. Evaluation of sums

A.1.1. Derivations

How do we calculate the nonanalytic part of sums over all cluster sizes s, like $[\Sigma_s s^k n_s]_{\text{crit}}$ in eq. (16), if we assume the scaling assumption $n_s = q_0 s^{-\tau} f(z)$, $z = (p - p_c)s^\sigma$ to be valid, eq. (15). Basically we replace the sum by an integral since only large clusters are responsible for singularities, and evaluate the integral apart from numerical factors by a substitution of variables. For this purpose we will often use $dz/ds = \sigma z/s$ at fixed p.

For example, we find for the kth moment of the cluster size distribution:

$$\sum_s s^k n_s = \int_0^\infty s^k n_s \, ds = q_0 \int_0^\infty s^{k-\tau} f[(p-p_c)s^\sigma] \, ds = (q_0/\sigma) \int_0^{\pm\infty} s^{1+k-\tau} z^{-1} f(z) \, dz$$

$$= q_0 \beta\delta |p-p_c|^{(\tau-1-k)/\sigma} \int |z|^{(1+k-\tau)/\sigma} \cdot z^{-1} f(z) \, dz$$

$$= |p-p_c|^{2-\alpha-k\beta\delta} \cdot q_0 \beta\delta \cdot \int |z|^{k\beta\delta+\alpha-3} \cdot f(z) \, |dz|. \tag{53}$$

(In this appendix all integrals over z run from 0 to $+\infty$ above p_c and to $-\infty$ below.) Thus eq. (16) is confirmed. (For the last equality we used the scaling laws (18).) Possible sign errors are easily corrected at the end since both n_s and $f(z)$ are always positive. Thus we found the critical exponent for the kth moment to be $2 - \alpha - k\beta\delta$ provided none of the following problems invalidates the above "derivation": By replacing n_s with $q_0 s^{-\tau} f(z)$ we made an error for small s, affecting additional correction terms which are part of the analytic background. This background is unimportant if the whole sum diverges or if only the "singular" part is investigated. Secondly, the prefactor q_0 may depend smoothly on p, giving correction factors of the type $1 + O(p - p_c)$. Again this error is not relevant for the leading nonanalytic part of the sum. Finally, of course, the integral on eq. (53) must exist, and here some caution is needed.

For large $\pm z$ the scaling function $f(z)$ decays exponentially, and thus for any finite k the integral in eq. (53) has no problems at $\pm\infty$. But for $z \to 0$ we normalized $f(0) = 1$, and the integral may diverge at $z = 0$, which simply means we were not allowed to replace the sum by an integral right at the beginning of eq. (53). In that case small clusters are more important than the typical clusters, $s \sim s_\xi$. For example, to evaluate $\Sigma_s s \cdot n_s$ we have $k = 1$ and $|z|^{k\beta\delta+\alpha-3} = |z|^{-\beta-1}$, whence the integral diverges at its lower boundary $z = 0$ for positive β. The reason is simple: In $\Sigma_s s \cdot n_s$ the main contribution comes from $s = 1, 2, 3, \ldots$, and the sum has to give $p(1 - B(p - p_c)^\beta + \cdots)$ according to eq. (4), if $P_\infty = B(p - p_c)^\beta$ near p_c. Thus the nonanalytic part we are interested in is only a small correction to the leading analytic background. Such problems occur whenever the sum in eq. (53) does not diverge, i.e. when $2 - \alpha - k\beta\delta$ is not negative.

But even in these more complicated cases eq. (53) is still correct if we look at the nonanalytic part $[\Sigma_s s^k n_s]_{\text{sing}}$ only. Why? In our above example, $\Sigma_s s \cdot n_s$, we may look at the derivative with respect to p. For β between zero and unity, as we assume from now on [50], this derivative equals $-\beta p B(p - p_c)^\beta + \cdots$, and the analytic background term $\Sigma_s s \cdot n_s(p_c) = p_c$ has cancelled out. On the other hand, with $dn_s/dp = q_0 s^{\sigma-\tau} f'(z)$, $f' = df/dz$, we get

$$\frac{\mathrm{d}}{\mathrm{d}p}\sum_s s\cdot n_s = q_0\int_0^\infty s^{1+\sigma-\tau}\cdot f'(z)\,\mathrm{d}s = (q_0/\sigma)\int |z|^{(2-\tau)/\sigma}\cdot f'(z)\,|\mathrm{d}z|$$

$$= q_0\beta\delta|p-p_c|^{\beta-1}\int |z|^{-\beta}\cdot f'(z)\,|\mathrm{d}z|.$$

($f'(0)$ is finite, and thus the integral converges at both boundaries.) The exponent thus agrees with the conclusion from eq. (53) with $k=1$. Moreover, a comparison of the two expressions for the derivative gives for the amplitude B above p_c:

$$B = -(q_0\delta/p_c)\int_0^\infty z^{-\beta}\cdot f'(z)\,\mathrm{d}z. \tag{54a}$$

Generally one may take the mth derivative $(\mathrm{d}/\mathrm{d}p)^m\,\Sigma_s s^k n_s$. If this sum contains a nonanalyticity $\propto|p-p_c|^x$ and one wants to determine the nonintegral positive exponent x, then with any m larger than x this mth derivative diverges as $|p-p_c|^{x-m}$ and can be evaluated as an integral:

$$(\mathrm{d}/\mathrm{d}p)^m\sum_s s^k n_s \propto q_0\beta\delta|p-p_c|^{(\tau-1-k-m\sigma)/\sigma}\int |z|^{m-1+(1+k-\tau)/\sigma}\cdot f^{(m)}(z)\,|\mathrm{d}z|$$

$$\propto |p-p_c|^{-m+(\tau-1-k)/\sigma}.$$

Thus we confirmed eq. (53) for the critical part of the sum: $x=(\tau-1-k)/\sigma = 2-\alpha-k\beta\delta$. For example, in the average number of clusters, $k=0$, the third derivative, $m=3$, finds out the nonanalytic part. (All derivatives $f^{(m)}=\mathrm{d}^m f/\mathrm{d}z^m$ exist if we assume as in section 3.1 that $f(z)$ is analytic in its argument.)

An alternative to this derivative trick is to subtract the disturbing background. Let us take again the sum $\Sigma_s s\cdot n_s$, i.e. $k=1$, and assume $0<\beta<1$. Right at the percolation threshold we have $\Sigma_s s\cdot n_s(p_c)=p_c$ from eq. (4). Now we look above p_c at

$$pP_\infty = p-\sum_s s\cdot n_s(p) \simeq p_c-\sum_s s\cdot n_s(p) = \sum_s s[n_s(p_c)-n_s(p)]$$

$$\simeq q_0\int_0^\infty s^{1-\tau}[f(0)-f(z)]\,\mathrm{d}s = q_0\beta\delta|p-p_c|^\beta\cdot\int |z|^{-\beta-1}[f(0)-f(z)]\,|\mathrm{d}z|. \tag{54b}$$

This expression equals $pB(p-p_c)^\beta+\cdots$, and thus we have found for the amplitude B of the percolation probability P_∞

$$B = (q_0\beta\delta/p_c)\int_0^\infty z^{-\beta-1}[f(0)-f(z)]\,\mathrm{d}z \tag{54c}$$

above p_c. The integral converges at the lower boundary since $f(0)-f(z)$ vanishes there as z. And, triumph of mathematics, partial integration of eq. (54c) recovers eq. (54a).

For p below p_c no infinite network is present, and $\Sigma_s s\cdot n_s(p)=p$ without the correction $pB(p-p_c)^\beta$. Thus the integral in eq. (54b) must vanish below p_c, as pointed out (in a similar context) by Reatto [134]:

$$\int_0^\infty z^{-\beta-1}[f(0)-f(-z)]\,dz = 0 \text{ or } \int_0^\infty z^{-\beta} f'(-z)\,dz = 0. \tag{54d}$$

(For clarity we replaced the integration variable z in eq. (54b) by $-z$ in eq. (54d).) This "sum rule" [50, 67] restricts the choice of the scaling function $f(z)$. In particular $f(z)$ cannot be symmetric about $z = 0$ since then the amplitude B would be the same on both sides of the phase transition. Equation (54d) also explains why there is a maximum in $f(z)$ at negative z: The derivative $f'(z)$ cannot have the same sign for all z below p_c since then the integrals in eq. (54d) cannot vanish. The simplest choice for $f(z)$ to obey the laws (54d) is to have a single maximum at negative z, and no maximum at positive z. And this behavior is exactly what we observed in section 3.2. The Bethe lattice solution, with $\log f(z) \propto -z^2$, is therefore a highly special case, incompatible with our assumption [50] $0 < \beta < 1$. (Equation (54d) was challenged in ref. [89] but confirmed numerically in two dimensions [51].)

A.1.2. Applications

With similar methods we evaluate the magnetization $M = M(H, T)$ in the low temperature limit of dilute magnets, eq. (5):

$$M_s \equiv M/|p-p_c|^\beta = \pm B + (q_0\beta\delta/p_c)\int |z|^{-\beta-1}\tanh(|z|^{\beta\delta}\cdot H_s)\cdot f(z)\,|dz| \tag{54e}$$

with $H_s \equiv H\mu/k_BT|p-p_c|^{\beta\delta}$. Thus the "scaled magnetization" is a function of the "scaled field" only: $M_s = M_s(H_s)$, and $p - p_c$ no longer appears in this relation explicitly. This scaling function $M_s(H_s)$ is given in eq. (54e) explicitly by an integral involving the cluster scaling function $f(z)$. The amplitude B for the spontaneous magnetization, $B = M_s(H_s = 0)$, is the same as in eq. (54a, c) and vanishes on the paramagnetic side, eq. (54d). As required, only the ferromagnet has a spontaneous magnetization $M(H = 0) \neq 0$. In the ferromagnetic state, i.e. above p_c, the $\pm B$ term in eq. (54e) gives $+B$ in the stable phase and $-B$ in the metastable phase, if $H > 0$. For negative H the signs are reversed. The $\pm B$ term in eq. (54e) arises from the infinite network whereas the integral is due to the many finite clusters. Of course, just as with nearly all other formulas in this review, eq. (54) is valid only for p close to p_c.

In eq. (6d) the evaluation of $\Sigma_s\, s\cdot n_s(p_c)\,e^{-hs}$ is even simpler mathematically: We merely substitute y for hs and get

$$p_c - \sum_s s\cdot n_s(p_c)\,e^{-hs} = \sum_s s\cdot n_s(p_c)\,(1-e^{-hs}) \simeq q_0\int_0^\infty s^{1-\tau}(1-e^{-hs})\,ds$$

$$= q_0 h^{\tau-2}\int_0^\infty y^{1-\tau}(1-e^{-y})\,dy = q_0 h^{1/\delta}\int_0^\infty y^{-1-1/\delta}\cdot(1-e^{-y})\,dy = p_c E\cdot h^{1/\delta}.$$

The amplitude E at $p = p_c$ is therefore, after partial integration, given by

$$E = (q_0\delta/p_c)\int_0^\infty y^{-1/\delta}\,e^{-y}\,dy = (q_0\delta/p_c)\Gamma(1-1/\delta) \tag{55}$$

where the gamma function of $1 - 1/\delta$ is about 1.04 in two and about 1.16 in three dimensions. In this

way we calculated the prefactor q_0 from the amplitude E [19, 55] in section 3.2.1. Since E is usually close to unity and δ is quite large one may also get a reasonable estimate for q_0 from $p_c = \Sigma_s s \cdot n_s(p_c) \sim q_0 \Sigma_s s^{1-\tau} = q_0 \zeta(1+1/\delta)$ with the Riemann zeta function [170].

So far we introduced the amplitudes B and E. Also A and C may be defined by the total number of clusters and the "susceptibility", respectively ($\Sigma \equiv \Sigma_s$):

$$\left[\sum n_s\right]_{\text{sing}} = pA|p-p_c|^{2-\alpha}; \qquad pP_\infty = -\left[\sum s \cdot n_s\right]_{\text{sing}} = pB(p-p_c)^\beta$$
$$\left[\sum s^2 n_s\right]_{\text{sing}} = pC|p-p_c|^{-\gamma}; \qquad -\left[\sum s \cdot n_s(p_c)\, e^{-hs}\right]_{\text{sing}} = pE \cdot h^{1/\delta}. \tag{56}$$

Table 4 presents estimates for these four amplitudes; if two of them are known the others might be calculated by universality assumptions [50, 55, 105].

All these complicated integrals are hiding somewhat the simple feature of our scaling theory: Only one characteristic cluster size enters the calculations. For $h = 0$ near p_c this size is $s_\xi \sim |p-p_c|^{-\beta\delta}$; and when we work with e^{-hs} at p_c then this characteristic cluster size can be taken as $1/h$. Therefore our sums can be evaluated by simple integrals. But even with more than one characteristic size, i.e. when assumption (15) is violated, we may recover the scaling laws (18b) and similar results based on sums over all cluster sizes. For example let us slightly modify an ansatz of Reatto [134] and use as an alternative to eq. (15) an ansatz with three free exponents σ, τ and x:

$$n_s(p) = q_0 s^{-\tau} e^{-z} \cdot F_s(z); \qquad z = (p-p_c)s^\sigma; \qquad F_s = [1 + \text{const} \cdot \exp(-(z+1)s^x)]^{-1}.$$

In the scaling limit of large clusters near p_c at fixed z we have $F_s(z) = 0$ for z below -1, and $F_s(z) = 1$ for z above -1, similar to the Fermi function in quantum-statistical physics. (x and the constant are positive.) Any sum over all cluster sizes can use, for its nonanalytic part, this approximation of $F_s(z)$ being either zero or unity, and thus the third exponent x cancels out from these sums. Neither the equation-of-state, eq. (20), not the scaling laws (18) depend on x. But this new exponent does enter the shape of the cluster size dstribution below p_c and is not merely a correction-to-scaling exponent in the

Table 4

Series estimates [19, 54–56] for the amplitudes A, B, C and E as defined in eq. (56), for various two- and three-dimensional lattices. (Abbreviations as in table 2). Both site percolation and bond percolation are listed. The dagger † warns that $\alpha = -2/3$ was assumed [56]; for the stars ★ Gaunt [55] gave estimates assuming universality to be valid. For C the value below p_c is listed; Monte Carlo results [26] give $C(p > p_c)/C(p > p_c) \simeq 180$ in two and $\simeq 11$ in three dimensions (but see also refs. [51, 54]). B refers to p above p_c, E to p at p_c, and A happens in the calculated cases to be symmetric about p_c [56].

Lattice:	HC	SQ	TR	FCC	BCC	SC	D
A (site)			8.7†				
A (bond)		8.5†					
B (site)	1.53	1.53	1.56	4.2	★	★	★
B (bond)	1.53	1.55	1.60	★	★	★	★
C (site)	0.140	0.147	0.128	0.101	0.142	0.185	0.26
C (bond)	0.145	0.134	0.084	0.041	0.074	0.122	0.222
E (site)	1.08	1.09	1.10	1.37	1.33	1.32	1.31
E (bond)	1.09	1.10	1.10	1.32	1.33	1.35	1.38

sense of eq. (22). If $s \to \infty$ below p_c, $-z$ becomes very large, and $\log F_s$ then varies as $(z+1)s^x \sim -|z|s^x \propto -s^{\sigma+x}$. Thus below p_c (but not above p_c) the new exponent x enters crucially into the decay exponent $\zeta = \sigma + x$ defined in eq. (23). In this sense two-exponent scaling, eq. (15), is violated for the cluster numbers n_s but it is still valid for the sums over the cluster numbers. Fortunately we have seen in section 3.2 that the additional assumption (15) is confirmed rather well: At present there is no need to introduce a third exponent for the cluster size distribution in the scaling limit.

So far we dealt only with the nonanalytic "singular" parts of the sums. If a sum diverges, its leading singularity is also the singular part, and we have no problems in the scaling regime. But e.g. $\Sigma_s n_s$ and $\Sigma_s s \cdot n_s$ remain finite at p_c, with the nonanalytic parts appearing only as corrections vanishing at p_c. These finite values at p_c cannot be calculated from the present scaling theory and are expected, contrary to critical exponents etc., to be different for every different lattice structure. Such non-diverging sums may lead to difficulties with *averages*. Let us assume that A_s is any cluster property (like radius R_s) increasing faster than $s^{1/\delta}$ and slower than $s^{1+1/\delta}$ for $1 \ll s \leqslant s_\xi$ and that it obeys a scaling assumption similar to eq. (42). The average $\langle A \rangle$ is defined by

$$\langle A \rangle \equiv \sum_s s^k n_s A_s \Big/ \sum_s s^k n_s, \tag{57}$$

with a suitable k. (Polymer scientists call $k = 0$ the number average, $k = 1$ the weight average, and $k = 2$ the z-average.) For $k = 2, 3, \ldots$ both sums in eq. (57) diverge and thus get their main contribution from $s \sim s_\xi$; then $\langle A \rangle = A_{s_\xi}$ apart from numerical constants, and the average has the properties which one would like it to have. But for $k = 1$ (and even worse for $k = 0$) there are surprises hidden in the innocent eq. (57). For the denominator there remains finite (and equal to p_c) in the scaling region, and only the numerator diverges. Thus $\langle A \rangle = p_c^{-1} \int_0^\infty s \cdot n_s A_s \, ds \propto \int s^{2-\tau} z^{-1} f(z) A_s \, dz \propto A_{s_\xi} |p - p_c|^\beta$. Thus a perhaps undesired factor $|p - p_c|^\beta$ is the result of this definition of averages with $k = 1$.

The differences in the effective dimensionality of percolation clusters, section 4.3.3, are due to such differences in definitions [106]. Another example is provided by the labyrinthine ant [5, 171]. Assume an ant is parachuting into a two-dimensional lattice, filled randomly with sites below the percolation threshold. (Experimental details on ant training were missing in ref. [171].) After landing the ant runs away randomly but is restricted to the single cluster it has jumped into. After a long time one measures how far the ant has run away from its landing site, and repeats the experiment many times. What is the average distance $\langle R^2 \rangle$ it has run away? Clearly that distance is connected with the average cluster radius. We leave it as an exercise to the reader to check which of the two expressions in ref. [171], $\langle R^2 \rangle \propto (p_c - p)^{-2\nu}$ and $\propto (p_c - p)^{\beta - 2\nu}$ is the correct one for the type of average defined by the jumping ant. In general we recommend to define averages through eq. (57) with $k = 2$, not with $k = 1$, since then they have nicer properties in the scaling region. For example, with $A_s = s$ we do not recommend to call $\langle s \rangle$ with $k = 1$ a "mean cluster size", as is often done. But with $k = 2$ eq. (57) simply gives our typical cluster size s_ξ for that average.

Appendix 2. One-dimensional percolation

In order to have at least one exactly solved problem in this review, which otherwise made no attempt to be rigorous in its "proofs", we now look at the special case of one dimension [112, 113].

Percolation clusters in one dimension are chains of s occupied places; the two ends of the chain

border on empty sites. Thus the perimeter t is always 2, independent of cluster size. Therefore the cluster numbers are

$$n_s(p) = p^s(1-p)^2. \tag{58}$$

For no p below unity can an infinite cluster exist, since already a single gap in the chain breaks it up into two parts. At $p = 1$, of course, the whole lattice is one infinite cluster, in all dimensions. Thus we have $p_c = 1$ for one dimension, and only the "paramagnetic" region below p_c is accessible. For $p \to p_c$ we rewrite eq. (58) with $p = \exp(\ln p) = \exp(p-1) = \exp(p-p_c)$ as

$$n_s(p) = p^s(p_c-p)^2 = s^{-2}[(p-p_c)s]^2 \exp[(p-p_c)s] = s^{-2} f(z);$$
$$z = (p-p_c)s; \qquad f(z) = z^2 e^z.$$

Comparison with our basic assumption (15) shows that scaling is valid, with $\sigma = 1$ and $\tau = 2$ exactly. Equations (17, 18) then lead to the other exponents [113] $\alpha = 1$, $\beta = 0$, $\gamma = 1$, $\delta = \infty$, $\nu = 1$, as already listed in table 2. Unfortunately these exponents for $d = 1$ are not the limits for $d \to 1$, as table 2 shows, particularly for γ and ν: The limits $p \to p_c$ and $d \to 1$ cannot be interchanged.

A surprise is waiting [112] if the range of interaction is changed. Naive universality assumptions, section 6.2.1, assert that then the exponents remain unchanged. But this is not so in one dimension [112]. Let us define a cluster as a group of occupied sites connected by nearest or next-nearest neighbor distances; thus our range of interaction is two lattice constants instead of one. Again we have $p_c = 1$. Each cluster now has four empty neighbors as external perimeter: $t_{ext} = 4$. But in addition it may have t_{int} internal perimeter sites, i.e. single holes of one empty site surrounded on both sides by at least one occupied site. We have $g_{st} = \binom{s-1}{t_{int}}$ possibilities to distribute t_{int} holes among the $s-1$ bonds of an s-cluster. With a total perimeter of $t = t_{ext} + t_{int} = 4 + t_{int}$ we thus get for the cluster numbers:

$$n_s = \sum_t g_{st} p^s (1-p)^t = p^s \sum_{t_{int}=0}^{s-1} \binom{s-1}{t_{int}} (1-p)^{t_{int}+4} = p^s (2-p)^{s-1} (1-p)^4$$
$$\simeq (p_c-p)^4 \exp[-(p_c-p)^2 s] = s^{-2} z^4 \exp(-z^2) \tag{59a}$$

where $z = (p-p_c)s^{1/2}$. (We used the binomial law and $\ln[(2-p)p] = \ln[1-(1-p)^2] \simeq -(1-p)^2 = -(p_c-p)^2$.) Thus scaling is valid again, with $\tau = 2$, but now with $\sigma = \frac{1}{2}$ instead of unity: The universality assumption is violated because one of the exponents has changed. More generally, if occupied sites separated by l lattice distances are still regarded as part of one cluster, one has [112] $\sigma = 1/l$, $\tau = 2$, leading to $\alpha = 2-l$, $\beta = 0$, $\gamma = l$, $\delta = \infty$, $\nu = l$.

This failure of universality in one-dimensional percolation can be hidden if instead of the scaling variable $-z = (p_c-p)s^\sigma$ we use the scaling variable $z_l \equiv (p_c-p)^l s^\sigma$. For the usual case $l = 1$ we now get near p_c:

$$n_s(p) = s^{-\tau} f(z_l); \qquad \tau = 2; \qquad f(z_l) = z_l^2 e^{-z_l} \tag{59b}$$

with $\sigma = 1$. But in this form (59b) the scaling result obeys universality for general l and no longer depends on the range of interaction, as one can see from eq. (59a) for $l = 2$, and from the results of Klein et al. [112] in general.

One-dimensional Ising ferromagnets are similar to one-dimensional percolation in that they have a phase transition, at $T = T_c = 0$, where only the paramagnetic side $T > T_c$ is accessible. Wiethege [172] looked at the specific heat of this magnet to find out if universality is violated also there, if longer

ranges of interaction are taken into account. If the energy needed to break up a bond between two magnetic moments at distance l is J_l, and if we define $K_1 \equiv \Sigma_l 2J_l/k_B T$, $K_2 \equiv \Sigma_l l \cdot J_l/k_B T$, we can expect the specific heat to depend exponentially on K_1 and K_2 for $T \to T_c = 0$. The calculation [172] showed that for T near $T_c = 0$ the specific heat varied as e^{-K_1} or e^{-K_2}, whatever was larger. Thus the temperature enters the specific heat in a complicated way, depending strongly on the choice for the interaction energy. Universality is violated much stronger than for percolation, where a simple modification, eq. (59b), was sufficient to save the universality concept.

These two one-dimensional examples showed that simple and plausible concepts like universality of critical phenomena need not always be true, even if they were confirmed for numerous other examples. This conclusion is regrettable but true.

References

[1] V.K.S. Shante and S. Kirkpatrick, Adv. Phys. 20 (1971) 325.
[2] J.W. Essam, in: Phase Transitions and Critical Phenomena, eds. C. Domb and M.S. Green (Academic, London 1972), vol. 2, p. 192.
[3] S. Kirkpatrick, Rev. Mod. Phys. 45 (1973) 574.
[4] D.J.A. Welsh, Sci. Progr. (Oxford) 64 (1977) 65.
[5] P.G. de Gennes, La Recherche 7 (1976) 919.
[6] D.J. Thouless, lecture notes, Les Houches Summer School on III Condensed Matter, 1978 (North-Holland).
[7] S. Kirkpatrick, Les Houches lecture notes [6].
[8] J.W. Essam, private communication.
[9] P. Pfeuty and E. Guyon, private communication.
[10] H.E. Stanley, Introduction to Phase Transitions and Critical Phenomena (Clarendon, Oxford, 1971) (2nd edition is in preparation).
[11] Phase Transition and Critical Phenomena, vols. 1 to 6, eds. C. Domb and M.S. Green (Academic, London, 1972–1976).
[12] D. Stauffer, Am. J. Phys. 45 (1977) 1001;
D. Stauffer and P. Heiss, Mathem. Naturwiss. Unterricht, to be published.
[13] H. Ottavi, J. Clerc, G. Giraud, J. Roussenq, E. Guyon and C.D. Mitescu, J. Phys. C 11 (1978) 1311.
[14] B.J. Last and D.J. Thouless, Phys. Rev. Lett. 27 (1971) 1719.
[15] B.P. Watson and P.L. Leath, Phys. Rev. B 9 (1974) 4893.
[16] R.J. Birgeneau, R.A. Cowley, G. Shirane and H.J. Guggenheim, Phys. Rev. Lett. 37 (1976) 940;
R.A. Cowley, G. Shirane, R.J. Birgeneau and E.C. Swensson, Phys. Rev. Lett. 39 (1977) 894.
[17] J.W. Essam, D.S. Gaunt and A.J. Guttmann, J. Phys. A 11 (1978) 1983.
[18] A.D. Dunn, J.W. Essam and J.M. Loveluck, J. Phys. C 8 (1975) 743 and 4219.
[19] D.S. Gaunt and M.F. Sykes, J. Phys. A 9 (1976) 1109.
[20] R.B. Griffiths, J. Math. Phys. 8 (1967) 484.
[21] P.W. Kasteleyn and C.M. Fortuin, J. Phys. Soc. Japan Suppl. 26 (1969) 11, and Physica 57 (1974) 536.
[22] P.J. Reynolds, H.E. Stanley and W. Klein, J. Phys. A 10 (1977) L 203.
[23] H. Nakanishi and H.E. Stanley, J. Phys. A 11 (1978) L 189.
[24] J. Hoshen, R. Kopelman and E.M. Monberg, J. Statist. Phys. 19 (1978) 219.
[25] W. Klein, H.E. Stanley, P.J. Reynolds and A. Coniglio, Phys. Rev. Lett. 41 (1978) 1145.
For an alternative suggestion for ν see M.P.M. den Nijs, preprint.
[26] J. Hoshen, D. Stauffer, G.H. Bishop, R.J. Harrison and G.P. Quinn, J. Phys. A 12 (1979), to be published.
[27] P.J. Flory, J. Am. Chem. Soc. 63 (1941) 3083, 3091 and 3096.
[28] W.H. Stockmayer, J. Chem. Phys. 11 (1943) 45.
[29] M.E. Fisher and J.W. Essam, J. Math. Phys. 2 (1961) 609.
[30] J.W. Essam and K.M. Gwilym, J. Phys. C 4 (1971) L 228 and C 9 (1976) 365.
[31] J.W. Essam and M.E. Fisher, J. Chem. Phys. 38 (1963) 802.
[32] C. Domb, J. Phys. A 9 (1976) 283.
[33] E. Stoll, K. Binder and T. Schneider, Phys. Rev. B 6 (1972) 2777.
[34] M.E. Fisher, Physics 3 (1967) 255.
[35] H. Müller-Krumbhaar, Phys. Lett. 50 A (1974) 27.
[36] K. Binder, Ann. Phys. 98 (1976) 390.
[37] H. Müller-Krumbhaar and E.P. Stoll, J. Chem. Phys. 65 (1976) 4294.

[38] A.C. Zettlemoyer (ed.), Nucleation Phenomena, Advances in Colloid and Interface Sciences, vol. 7 (Elsevier, Amsterdam, 1977).
[39] R.E. Behringer, J. Chem. Phys. 29 (1958) 537.
[40] P.G. de Gennes, P. Lafore and J. Millot, J. Phys. Chem. Sol 11 (1959) 105.
[41] C. Domb, Nature 184 (1959) 509.
[42] M.F. Sykes and M. Glen, J. Phys. A 9 (1976) 87.
[43] J.L. Martin, in: ref. [11, vol. 3 (1974) p. 97].
[44] M.F. Sykes, D.S. Gaunt and M. Glen, J. Phys. A 9 (1976) 1705.
[45] M.F. Sykes, D.S. Gaunt and H. Ruskin, J. Phys. A 9 (1976) 1899.
[46] A. Flammang, Z. Physik B 28 (1977) 47.
[47] M.F. Sykes, D.S. Gaunt and M. Glen, J. Phys. A 9 (1976) 715.
[48] J.A.M.S. Duarte, Z. Physik B 33 (1979) 97 and Z. Naturf. 33a (1978) 1404.
[49] K.R. Bauchspiess and D. Stauffer, J. Aerosol Sci. 9 (1978) 567.
[50] D. Stauffer, Z. Physik B 25 (1976) 391.
[51] W.F. Wolff and D. Stauffer, Z. Physik B 29 (1978) 67.
[52] J.A.M.S. Duarte, Lett. Nuovo Cim. 22 (1978) 707.
[53] Fig. 12 and ref. [75].
[54] M.F. Sykes, D.S. Gaunt and M. Glen, J. Phys. A 9 (1976) 97 and 725; see also ref. [110].
[55] D.S. Gaunt, J. Phys. A 10 (1977) 807.
[56] C. Domb and C.J. Pearce, J. Phys. A 9 (1976) L 137.
[57] D.S. Gaunt, J. Phys. A 11 (1978) 1191.
[58] A. Coniglio, H.E. Stanley and D. Stauffer, in preparation; see also ref. [146].
[59] K. Binder (ed.), Monte Carlo Methods in Statistical Physics; Topics in Current Physics, vol. 7 (Springer, Heidelberg, 1979).
[60] A. Sur, J.L. Lebowitz, J. Marro, M.H. Kalos and S. Kirkpatrick, J. Statist. Phys. 15 (1976) 345.
[61] Hoshen et al. [24]; Levinshtein et al. [142]; J. Roussenq, J. Clerc, G. Giraud, E. Guyon and H. Ottavi, J. Physique (Paris) 37 (1976) L 99. For a review see Kirkpatrick [7].
[62] E. Stoll and C. Domb, J. Phys. A 11 (1978) L 57.
[63] J. Hoshen and R. Kopelman, Phys. Rev. B 14 (1976) 3438.
[64] H. Müller-Krumbhaar, in: ref. [59] chapter 5.
[65] V.A. Vyssotsky, S.B. Gordon, H.L. Frisch and J.M. Hammersley, Phys. Rev. 123 (1961) 1566.
[66] P. Dean and N.F. Bird, National Physical Laboratory Report Ma 61, Teddington, England 1966, unpublished.
[67] D. Stauffer, Phys. Rev. Lett. 35 (1975) 394.
[68] A.B. Harris, T.C. Lubensky, W.K. Holcomb and C. Dasgupta, Phys. Rev. Lett. 35 (1975) 327.
[69] G.P. Quinn, G.H. Bishop and R.J. Harrison, J. Phys. A 9 (1976) L 9.
[70] M.M. Bakri and D. Stauffer, Phys. Rev. B 14 (1976) 4215.
[71] P.L. Leath and G.R. Reich, J. Phys. C 11 (1978) 4017.
[72] G.R. Reich and P.L. Leath, Tables of cluster size and perimeter distributions on the square and triangular lattices just below percolation threshold, unpublished (Jan. 1978).
[73] P.L. Leath, Phys. Rev. Lett. 36 (1976) 921 and Phys. Rev. B 14 (1976) 5046.
[74] K. Binder and D. Stauffer, J. Statist. Phys. 6 (1972) 49.
[75] D. Stauffer, Phys. Rev. Lett. 41 (1978) 1333.
[76] H.J. Herrmann, Z. Physik B 32 (1979) 335.
[77] P.J. Reynolds, W. Klein and H.E. Stanley, J. Phys. C 10 (1977) L 167;
See also C. Tsallis and G. Schwachheim, J. Phys. C 12 (1979) 9.
[78] P.J. Reynolds, H.E. Stanley and W. Klein, J. Phys. A 11 (1978) L 199.
[79] H. Kunz and B. Payandeh, preprint Ecole Polytechnique Federale de Lausanne (May 1978).
[80] W. Kinzel, Z. Physik B, to be published.
[81] K.G. Wilson, Physica 73 (1974) 119.
[82] M.J. Stephen, Phys. Lett. 56 A (1976) 149;
F.Y. Wu, Phys. Rev. B 18 (1978) 516.
[83] R.G. Priest and T.C. Lubensky, Phys. Rev. B 13 (1976) 4159 and 14 (1977) 5125 (erratum);
D.J. Amit, J. Phys. A 9 (1976) 1441.
[84] G. Toulouse, Nuovo Cimento B 23 (1974) 234.
[85] K.G. Wilson and M.E. Fisher, Phys. Rev. Lett. 28 (1972) 240.
[86] P.G. de Gennes, Phys. Lett. 38 A (1972) 338; see also ref. [131].
[87] A. Houghton, J.S. Reeve and D.J. Wallace, Phys. Rev. B 17 (1978) 2956;
G.S. Grest, priv. comm.; see also ref. [17].
[88] M. Schwartz, Phys. Rev. B 18 (1978) 2364.
[89] G.R. Reich and P.L. Leath, J. Phys. C 11 (1978) 1155.
[90] H. Kunz and B. Souillard, Phys. Rev. Lett. 40 (1978) 133 and J. Statist. Phys. 19 (1978) 77.

[91] A. Hankey, J. Phys. A 11 (1978) L 49; see also ref. [140].
[92] K.P. Mühlberg, preprint Cologne University (1978).
[93] A.J. Guttmann and D.S. Gaunt, J. Phys. A 11 (1978) 949.
[94] S.G. Whittington and D.S. Gaunt, J. Phys. A 11 (1978) 1452.
[95] A. Hintermann, H. Kunz and F.Y. Wu, J. Statist. Phys. 19 (1978) 623.
[96] K. Binder, D. Stauffer and H. Müller-Krumbhaar, Phys. Rev. B 10 (1974) 3853 and 12 (1975) 5261.
[97] C. Domb and E. Stoll, J. Phys. A 10 (1977) 1141.
[98] D. Stauffer, J. Phys. C 8 (1975) L 172.
[99] C.S. Kiang and D. Stauffer, Z. Physik 235 (1970) 130.
[100] A. Hankey and H.E. Stanley, Phys. Rev. B 6 (1972) 3515.
[101] C. Domb, J. Phys. C 7 (1974) 2677.
[102] C. Domb, J. Phys. A 9 (1976) L 141.
[103] D.D. Betts, A.J. Guttmann and G.S. Joyce, J. Phys. C 4 (1971) 1994.
[104] P.C. Hohenberg, A. Aharony, B.I. Halperin and E.D. Siggia, Phys. Rev. B 13 (1976) 2986, with earlier literature.
[105] J. Marro, Phys. Lett. 59 A (1976) 180.
[106] H.E. Stanley, J. Phys. A 10 (1977) L 211;
see also H.E. Stanley, R.J. Birgeneau, P.J. Reynolds and J.F. Nicoll, J. Phys. C 9 (1976) L 553.
[107] D.S. Gaunt and H. Ruskin, J. Phys. A 11 (1978) 1369.
[108] R. Fisch and A.B. Harris, Phys. Rev. B 18 (1978) 416.
[109] R.J. Harrison, G.H. Bishop and G.D. Quinn, J. Statist. Phys. 19 (1978) 53.
[110] J. Blease, J.W. Essam and C. M. Place, J. Phys. C 11 (1978) 4009;
see also M.F. Sykes, D.S. Gaunt and J.W. Essam, J. Phys. A 9 (1978) L 43.
[111] W.J. Camp, D.M. Saul, J.P. van Dyke and M. Wortis, Phys. Rev. B 14 (1976) 3990.
[112] W. Klein, H.E. Stanley, S. Redner and P.J. Reynolds, J. Phys. A 11 (1978) L 17.
[113] M. Wortis, Phys. Rev. B 10 (1974) 4665;
D. Stauffer and C. Jayaprakash, Phys. Lett. 64 A (1978) 433;
Reynolds et al. [22].
[114] M. Stephen, Phys. Rev. B 15 (1977) 5674;
M.R. Giri, M. Stephen and G.S. Grest, Phys. Rev. B 16 (1978) 4971.
[115] E. Stoll and C. Domb, J. Phys. A 12 (1979).
[116] F.J. Wegner, Phys. Rev. B 5 (1972) 4529.
[117] S. Kirkpatrick, Phys. Rev. Lett. 36 (1976) 69.
[118] K. Binder and M.H. Kalos, preprint IFF-KFA, 5170 Jülich 1, West Germany.
[119] C.S. Kiang, D. Stauffer, G.H. Walker, O.P. Puri, E.M. Patterson and J.D. Wise Jr., J. Atmospheric Sci. 28 (1971) 1222;
D. Stauffer and C.S. Kiang, in: ref. [38, p. 103].
[120] R. Kretschmer, K. Binder and D. Stauffer, J. Statist. Phys. 15 (1976) 267.
[121] A.F. Andreev, Sov. Phys. JETP 18 (1964) 1415.
[122] Y. Imry, Phys. Rev. B 15 (1977) 4448.
[123] W. Klein, D.J. Wallace and R.K.P. Zia, Phys. Rev. Lett. 37 (1976) 639.
[124] R.B. Griffiths, Phys. Rev. Lett. 23 (1968) 17.
[125] J.C. Wiermann, J. Math. Phys. 19 (1978) 1979.
[126] D. Stauffer, J. Statist. Phys. 18 (1978) 125.
[127] C. Domb, T. Schneider and E. Stoll, J. Phys. A 8 (1975) L 90.
[128] G.D. Quinn, G.H. Bishop and R.J. Harrison, Nuclear Metallurgy 20 (1977) 1213.
[129] C. Domb, Ann. Israel Physical Society 2 (1978) 61.
[130] D. Stauffer, Z. Physik B 30 (1978) 173.
[131] For a recent paper with earlier literature see e.g. M.K. Kosmas and K.F. Freed, J. Chem. Phys. 69 (1978) 3647.
[132] D. Stauffer, C.S. Kiang and G.H. Walker, J. Statist. Phys. 3 (1971) 323.
[133] T.C. Lubensky and J. Isaacson, Phys. Rev. Lett. 41 (1978) 829; 42 (1979) 410, and private communication.
[134] L. Reatto and E. Rastelli, J. Phys. C 5 (1972) 2785;
L. Reatto, Phys. Lett. 33 A (1970) 519.
[135] F.L. McCrackin, J. Mazur and A.J. Guttmann, Macromolecules 6 (1973) 859;
M. Lax, A.J. Barrett and C. Domb, J. Phys. A 11 (1978) 361.
[136] B.B. Mandelbrot, Fractals: Form, Chance and Dimension (W.H. Freeman, San Francisco, 1977).
See also B.B. Mandelbrot, Les Objets fractals: forme, hasard et dimension (Flammarion, Paris and Montreal, 1975) and Ann. Israel Physical Society 2 (1978) 226.
[137] B.B Mandelbrot, preprint IBM Yorktown Heights, N.Y.
[138] S.R. Forrest and T.A. Witten, J. Phys. A 12 (1979) L 109.

[139] F. Harary, Graph Theory and Theoretical Physics (Academic, London, 1967).
[140] J.A.M.S. Duarte and R.J. Cherry, preprint King's College, London.
[141] A.S. Skal and B.I. Shklovskii, Sov. Phys. Semicond. 8 (1975) 1029.
[142] M.E. Levinshtein, B.I. Shklovskii, M.S. Shur and A.L. Efros, Sov. Phys. JEPT 42 (1976) 197.
[143] T.J. Coutts, This Solid Films 38 (1976) 313;
B.A. Abeles, H.L. Pinsh and J.I. Gittleman, Phys. Rev. Lett. 35 (1975) 247;
N.T. Liang, Y. Sham and S.Y. Wang, Phys. Rev. Lett. 37 (1976) 526.
[144] M.E. Levinshtein, J. Phys. C 10 (1977) 1895;
M.E. Levinshtein, M.S. Shur and A.L. Efros, Sov. Phys. JETP 42 (1975) 1120;
K. Onizuka, J. Phys. Soc. Japan 39 (1975) 527;
Y. Yuge, J. Statist. Phys. 16 (1977) 339 and Phys. Rev. B 18 (1978) 1415;
Y. Yuge and K. Onizuka, J. Phys. C 11 (1978) L 763.
[145] G. Fug, R. Canet and P. Delhaes, Comptes Rendus Acad. Sc. Paris 287 B (1978) 5.
[146] J.P. Straley, AIP Conf. Proc. 40 (1978) 118. See also other articles in this volume and
J. Bernasconi, Phys. Rev. B 18 (1978) 2185,
P.M. Kogut and J.P. Straley, J. Phys. C 12 (1979) 1.
[147] C. Dasgupta, A.B. Harris and T.C. Lubensky, Phys. Rev. B 17 (1978) 1375.
[148] S. Kirkpatrick, AIP Conf. Proc. 40 (1978) 99.
[149] P.G. de Gennes, J. Physique 37 (1976) L 1.
For an alternative to eq. (50) see T.A.L. Ziman, preprint.
[150] J.P. Straley, J. Phys. C 9 (1976) 783, and Levinshtein et al. [144].
[151] A.L. Efros and B.I. Shklovskii, Phys. Stat. Sol. b 76 (1976) 475.
[152] M.J. Stephen, Phys. Rev. B 17 (1978) 4444.
[153] J.P. Straley, Phys. Rev. B 15 (1977) 5733.
[154] B.I. Shklovskii and A.L. Efros, Sov. Phys. Uspekhi 18 (1976) 945 and Levinshtein et al. [144].
[155] B.E. Dubrov, M.E. Levinshtein and M.S. Shur, Sov. Phys. JEPT 43 (1976) 1050;
T. Geszti, preprint, Central Research Institute for Technical Physics, Budapest;
B.I. Shklovskii, Sov. Phys. JEPT 45 (1977) 152.
[156] H. Ottavi, in ref. [13];
H.J. Wintle and P.H. Puhach, J. Statist. Phys. 18 (1978) 557;
A. Coniglio, H.E. Stanley and W. Klein, Phys. Rev. Lett. 42 (1979) 518;
P. Agrawal, S. Redner, P.J. Reynolds and H.E. Stanley, J. Phys. 12 (1979);
J. Hoshen, P. Klymko and R. Kopelman, J. Statist. Phys., to be published.
[157] G.R. Reich and P.L. Leath, J. Statist. Phys. 19 (1978) 611.
J. Chalupa, P.L. Leath and G.R. Reich, J. Phys. C 12 (1979) L 31.
See also D.S. Gaunt, M.F. Sykes and S.G. Whittington, J. Phys. A 12 (1979) 75.
[158] R. Zallen, Phys. Rev. B 16 (1977) 1426;
J.W. Halley and W.K. Holcomb, Phys. Rev. Lett. 40 (1978) 1670.
[159] J.M.H. Levelt Sengers, R. Hocken and J.V. Sengers, Physics Today 30 (Dec. 1977) 42;
but see O.T. Valls and J.A. Hertz, Phys. Rev. B 18 (1978) 2367.
[160] D.H. Fremlin, J. Physique 37 (1976) 813.
[161] I. Webman, J. Jortner and M.H. Cohen, Phys. Rev. B 16 (1977) 2593.
[162] A. Coniglio, C.R. Nappi, F. Peruggi and L. Russo, J. Phys. A 10 (1977) 205.
[163] M.F. Sykes and D.S. Gaunt, J. Phys. A 9 (1976) 2131.
[164] T. Kawasaki, Prog. Theor. Phys. 59 (1978) 1812 and 61 (1979) 384.
[165] O. Penrose, J.L. Lebowitz, J. Marro, M.H. Kalos and A. Sur, J. Statist. Phys. 19 (1978) 243; see also ref. [118].
[166] A.B. Harris and S. Kirkpatrick, AIP Conf. Proc. 24 (1976) 99.
[167] E.F. Shender, Zh. Eksp. Teor. Fiz. 75 (1978) 352 and preprint Leningrad Nuclear Physics Institute.
See also I. Ya. Korenblit and E.F. Shender, Usp. Fiz. Nauk 126 (1978) 233.
[168] T.C. Lubensky, Les Houches lecture notes [6].
[169] J.R. Dorfman, J. Statist. Phys. 18 (1978) 415;
J.E. Mayer, J. Statist. Phys. 18 (1978) 529.
[170] C.S. Kiang, Phys. Rev. Lett. 24 (1970) 47.
[171] C.D. Mitescu, H. Ottavi and J. Roussenq, AIP Conf. Proc. 40 (1978) 377.
[172] C. Wiethege, unpublished, Cologne University.

Note added in proof. After completion of this review we learned of additional work of interest for the scaling theory of percolation. Some of these papers are listed below together with the section or reference for which they are most relevant:

J. Roussenq, C. Mitescu and H. Ottavi, Comptes Rendus Acad. Sc. Paris 288 B (1979) 49, on section 3.2 and ref. [23].
H.P. Peters, D. Stauffer, H.P. Hölters and K. Loewenich, Z. Physik B, to be published, on ref. [75] in 3 dimensions, section 4.
S. Redner, preprint, on radius of branching polymers [75, 133], section 4.2.2.
B. Rocksloh and D. Stauffer, preprint, on number of animals [48], section 5.2.
G. Shlifer, W. Klein, P.J. Reynolds and H.E. Stanley, preprint, on backbone exponents [7, 148], section 4.3.3.
J.P. Straley, preprints, on ref. [82] and section 6.1.
P.G. De Gennes, J. Physique (Paris) 40 (1979) L 197 on ref. [149] and section 6.1 and 4.2.2.
S. Redner and H.E. Stanley, preprint, on theory for anisotropic percolation, section 6.2.1.
L.N. Smith and C.J. Lobb, Bull. Am. Phys. Soc. 24 (1979) 360 and preprint, on experiment for anisotropic percolation, section 6.2.1.
L. Turban, J. Phys. C 12 (1979) L 191, on percolation with voids, section 6.2.1.
L. Turban and P. Guilmin, J. Phys. C 12 (1979) 961, on Reich and Leath [157], section 6.2.1.
H. Nakanishi and P.J. Reynolds, preprint, on site-bond percolation [156], section 6.2.1.
S.G. Whittington, G.M. Torrie and D.S. Gaunt, J. Phys. A 12 (1979) L 119, on Gaunt et al. [157], section 6.2.1.

Completed 9 May 1979.